



THE UNIVERSITY OF  
**WAIKATO**  
*Te Whare Wānanga o Waikato*

Research Commons

<http://researchcommons.waikato.ac.nz/>

## Research Commons at the University of Waikato

### Copyright Statement:

The digital copy of this thesis is protected by the Copyright Act 1994 (New Zealand).

The thesis may be consulted by you, provided you comply with the provisions of the Act and the following conditions of use:

- Any use you make of these documents or images must be for research or private study purposes only, and you may not make them available to any other person.
- Authors control the copyright of their thesis. You will recognise the author's right to be identified as the author of the thesis, and due acknowledgement will be made to the author where appropriate.
- You will obtain the author's permission before publishing any material from the thesis.

# **Methane emission hotspots from a drained peat soil under dairy grazing**

A thesis  
submitted in partial fulfilment  
of the requirements for the degree  
of  
**Master of Environmental Science in Earth Sciences**  
at  
**The University of Waikato**  
by  
**Jacob Peter Hamill**



THE UNIVERSITY OF  
**WAIKATO**  
*Te Whare Wānanga o Waikato*

2019



# Abstract

---

Methane (CH<sub>4</sub>) is a greenhouse gas that is emitted from natural peatland ecosystems due to their high water tables. However, large areas of natural peatlands have been drained for agricultural purposes, resulting in a reduction in overall methane emissions. However, where soil is saturated, such as within or adjacent to drainage ditches, methane emission can remain high. The aim of this research was to determine the magnitude of soil- and drainage ditch-derived methane emissions from a drained Waikato peatland under dairy grazing and where and when these emissions occur.

Gamma Farm is a pastoral dairy farm located on the remnants of the Moanatuatua peatland and drained by shallow surface “spinner” drains that discharge into deeper field-border drains. The paddocks were classified into four different landforms based on the location and hydrology of the drainage features. These landforms are crown, slope, ditch edge and drainage ditch. To adequately determine the spatial and temporal variation in methane fluxes chamber measurements of methane fluxes were undertaken along a transect across the width of the study site, approximately perpendicular to the border drains. A campaign approach was used, with chamber measurements being undertaken from autumn through to winter to capture methane fluxes under different environmental conditions. To measure seasonal and annual-scale methane emissions an eddy covariance flux tower was used.

Based on chamber measurements drainage ditches were shown to have average methane emissions of  $0.071 \pm 0.005$  mg CH<sub>4</sub> m<sup>-2</sup> h<sup>-1</sup>. Conversely, the soil of the crown, slope and ditch edges were shown to be a net methane sink, with average net methane oxidation of  $-0.019 \pm 0.006$ ,  $-0.01 \pm 0.008$  and  $-0.023 \pm 0.006$  mg CH<sub>4</sub> m<sup>-2</sup> h<sup>-1</sup> respectively. Weighting the chamber measurements by landform area it was concluded that the study site was primarily a minor net methane sink. However, eddy covariance measurements indicated that the study site was a net source of methane with annual emissions of 44.72 kg CH<sub>4</sub> ha<sup>-1</sup> yr<sup>-1</sup>. This large discrepancy between the chamber and eddy covariance measurements is likely

caused by the large spatial and temporal scale differences between the two measurement techniques.

In addition, it was found that there was no relationship between soil methane fluxes and the soil temperature, Olsen-P, and nitrate concentration. However, methane fluxes were shown to decrease as the ammonium concentration and depth to the water table increased. In addition, methane fluxes decreased as volumetric moisture content (VMC) decreased, but at low VMCs (<40%) methane fluxes tended towards zero. For the water-borne methane fluxes there was no relationship found between methane fluxes and any measured variable (pH, dissolved oxygen, electrical conductivity, water temperature, water depth, nitrate concentration or dissolved phosphorus). However, at longer time scales such as monthly averages of eddy covariance measurements, methane fluxes were positively correlated with soil temperature and air temperature. Additionally, both seasonal and diurnal cycles in the eddy covariance methane fluxes were observed.

# Acknowledgements

---

This thesis would not have been possible without the support of a number of people. Firstly, I would like to thank my supervisor, Dave Campbell. Dave, you have been immensely helpful throughout this process and I have enjoyed working with you.

A big thank you to Chris Morcom for all your help with my fieldwork and to Noel Bates for all of your help in the laboratory. Thanks to Anne Wecking for all of your help with the chamber and QCL methodology. I would also like to thank Jordan Goodrich, especially for reviewing thesis drafts. Thanks to Annie Barker and Dorisel Torres-Rojas for all of your help running my samples through the ion chromatograph. Additionally, I would like to thank Dean Sandwell. Thank you to everyone in the WaiBER group, it has been an enjoyable experience working with all of you

I would also like to thank J.D. & R.D. Wallace Ltd for allowing us to conduct research on Gamma Farm. Additionally, thanks to Stuart Lindsay at AgResearch for loaning me the chambers that were used in this study.

I am thankful to have received funding from both PEATWISE and DairyNZ.

Finally, I would like to thank my family for all of your support.



# Table of Contents

---

Abstract .....	i
Acknowledgements .....	iii
Table of Contents .....	v
List of Figures.....	ix
List of Tables.....	xiii
Chapter One .....	1
Introduction.....	1
1.1    Global methane emissions .....	1
1.2    Drained peatlands .....	3
1.3    New Zealand drained peatlands .....	4
1.4    Aims and objectives.....	6
1.5    Thesis outline.....	7
Chapter Two .....	9
Literature review .....	9
2.1    Methane production and consumption in soil .....	9
2.1.1    Methanogenesis .....	11
2.1.2    Methane oxidation (methanotrophy).....	12
2.1.3    Methane transport .....	14
2.2    Soil Methane emissions .....	15
2.3    Methane production and consumption in water .....	15
2.4    Methane production and consumption in drained peat soils .....	16
2.4.1    Methane emissions from drained peat soils .....	18
2.5    Controls of methane emissions from drained peat soils .....	21
2.5.1    Substrate availability .....	21
2.5.2    Water .....	21
2.5.3    Temperature.....	22
2.5.4    Vegetation .....	23
2.5.5    Soil pH.....	23



2.5.6	Electron acceptors .....	24
2.5.7	Fertiliser / nutrient addition .....	25
2.6	Climate change and methane emissions from drained peatlands .....	26
2.7	Methane measurement methods .....	28
2.7.1	Incubation .....	29
2.7.2	Chambers .....	29
2.7.3	Eddy Covariance.....	33
Chapter Three .....		37
Site description .....		37
Chapter Four .....		41
Methane emissions from a drained peatland under dairy grazing.....		41
4.1	Introduction .....	41
4.2	Methods.....	42
4.2.1	Chamber measurements of methane fluxes.....	42
4.2.2	Soil physical properties .....	46
4.2.3	Soil chemical properties.....	46
4.2.4	Water analysis.....	47
4.2.5	Spatially integrated methane fluxes .....	47
4.2.6	Eddy covariance .....	48
4.3	Results.....	49
4.3.1	Climate / hydrological setting .....	49
4.3.2	Soil characteristics.....	51
4.3.3	Temporal variation in the methane flux .....	52
4.3.4	Spatial variation in the methane flux .....	54
4.3.5	Soil physical properties .....	58
4.3.6	Soil chemical properties.....	60
4.3.7	Drainage ditch chemical and physical properties .....	62
4.3.8	Eddy covariance .....	63

4.3.8.1	Eddy covariance footprint analysis .....	66
4.3.8.2	Environmental variables .....	69
4.3.9	Eddy covariance versus chamber measurements .....	70
4.4	Discussion .....	72
4.4.1	Methane emission hotspots .....	72
4.4.1.1	Spatial variation in the methane flux.....	72
4.4.1.2	Temporal variation in the methane flux .....	74
4.4.1.3	Methane fluxes from cow dung patches .....	77
4.4.2	Controls on methane emissions .....	77
4.4.2.1	Soil physical properties.....	77
4.4.2.2	Soil chemical properties .....	80
4.4.2.3	Drainage ditch physical and chemical properties .....	81
4.4.3	Annual and seasonal methane fluxes .....	83
4.4.3.1	Eddy covariance .....	83
4.4.3.2	Eddy covariance versus chamber measurements.....	88
4.4.4	Impact of drained peatlands on New Zealand’s greenhouse gas inventory.....	93
Chapter Five.....		95
Summary and conclusions.....		95
5.1	Review of thesis aims and objectives .....	95
5.2	Summary.....	95
5.3	Recommendations for future research .....	97
References.....		99



# List of Figures

---

<b>Figure 1.1</b> Global long-term trend in atmospheric methane concentration, 1010 – 2018 [Source: Loulergue et al., 2008; Etheridge et al., 2002; Etheridge et al., 1998 and Dlugokencky, NOAA/ESRI., 2018 as cited in (2 Degrees Institute, n.d.)].	1
<b>Figure 2.1</b> The classical strata model of methane dynamics versus the emerging heterogenous model [Source: (Yang et al., 2017)].	10
<b>Figure 2.2</b> Anaerobic decomposition of organic matter [Adapted from: (Boone, 1993)].	11
<b>Figure 2.3</b> Mean methane emissions from peatland drainage ditches under different land uses. Error bars show 95% confidence interval for the per study means only [Adapted from: (Evans et al., 2016)].	19
<b>Figure 2.4</b> Map of regional climate change impacts in New Zealand [Adapted from: Ministry for the Environment (2017a)].	28
<b>Figure 3.1</b> Location of Gamma Farm: (a) in relation to the North Island of New Zealand and; (b) showing the location of the study site, a pair of paddocks within Gamma Farm [Source: Google Earth (2019)].	37
<b>Figure 3.2</b> Features of the study site, showing the location of the shallow “spinner” drains and deeper “border” drains. Arrows indicate flow direction. Also shown is the location of the chamber and hydrological dip-well transect and eddy covariance flux tower [Adapted from: Google Earth (2019)].	38
<b>Figure 4.1</b> Diagram of the dominant landforms at the study site	42
<b>Figure 4.2</b> Chambers installed on collars for methane flux measurements in (a) soil (b) shallow standing water and (c) a floating chamber.	44
<b>Figure 4.3</b> Soil cores: (a) large volumetric soil core used for soil physical property analysis and (b) small soil core used for soil chemical property analysis.	47
<b>Figure 4.4</b> Monthly average air temperature from October 2018 to September 2019. Also shown are the monthly temperature normal, measured in Hamilton over the period 1981 – 2010 [Source: NIWA (n.d.)].	49
<b>Figure 4.5</b> Monthly total rainfall from October 2018 to September 2019. Also shown is the monthly rainfall normal, measured in Cambridge over the period 1981 – 2010 [Source: NIWA (n.d.)].	50
<b>Figure 4.6</b> Water table depth (a), daily rainfall (b) and soil volumetric moisture content (c) at 10 cm depth. Vertical lines represent the chamber sampling dates.	51

**Figure 4.7** Temporal variation in net methane fluxes from (a) crown (b) slope (c) ditch edge and (d) drainage ditch landforms. Error bars show the standard error of the mean, which was calculated where  $n \geq 2$ . Red points indicate values where  $n=1$ . Note that (d) has a different y-axis scale. ....53

**Figure 4.8** Variation in the measured methane fluxes from the different landforms (crown, slope, ditch edge and drainage ditch). The \* shows the mean methane flux and the + shows the outliers. ....54

**Figure 4.9** Spatial variation in methane fluxes from the drainage ditches. The drainage ditch landform is comprised of two different drainage ditch types, the shallow “spinner drain” and the deeper main / border drain. ....56

**Figure 4.10** Methane fluxes measured from cow dung, (a) boxplot showing the distribution of methane fluxes and (b) methane fluxes from cow dung vs days since the last grazing. The \* in (a) shows the mean methane flux. ....57

**Figure 4.11** Relationship between methane fluxes and (a) soil temperature (b) water table depth (c) volumetric moisture content and (d) water filled pore space. The dashed line (b) shows the linear regression between methane fluxes and water table depths for all three landforms. ....59

**Figure 4.12** Effect of water table depth on the volumetric moisture content. Note that the VMC has a different range than shown previously (Figure 4.11c) due to no water table depth measurements occurring during the 14 March 2019 sampling date when the lowest VMC values were measured. ....60

**Figure 4.13** Effect of (a) pH (b) Olsen-P (c) ammonium concentration and (d) nitrate concentration on methane fluxes. ....61

**Figure 4.14** Effect of (a) pH (b) dissolved oxygen (c) electrical conductivity (d) water temperature (e) water depth (f) nitrate concentration (g) dissolved phosphorus and (h) volumetric moisture content and water filled pore space on methane fluxes in the drainage ditch landform. The soil moisture content and water filled pore space measurements were made when there was no standing water in the drainage ditch landforms. The rest of the measurements were from water samples.63

**Figure 4.15** Half-hourly methane fluxes as measured by eddy covariance (a) methane fluxes before filtering of grazing events (b) methane fluxes after filtering out grazing events (October 2018 – September 2019)..64

**Figure 4.16** Mean daily methane fluxes measured by eddy covariance. Fluxes were filtered to remove grazing events any peaks above an arbitrary set threshold of  $10 \text{ mg CH}_4 \text{ m}^{-2} \text{ h}^{-1}$  (October 2018 – September 2019). ....65

<b>Figure 4.17</b> Average methane fluxes recorded for each hour of the day. Error bars show the standard error of the mean (October 2018 – September 2019).....	66
<b>Figure 4.18</b> Eddy covariance methane fluxes versus footprint distance. The footprint distance is shown as both footprint peak distance ( $X_{peak}$ ) and footprint distance from which 70% of the measured flux is sourced ( $X_{70}$ ).....	67
<b>Figure 4.19</b> 30-minute eddy covariance methane fluxes versus wind direction. Note that the gap observed around 86 - 130° is due to the filtering of fluxes measured when the wind is blowing over the QCL enclosure at the study site. ....	68
<b>Figure 4.20</b> Eddy covariance footprint peak distance ( $X_{peak}$ ) versus wind direction. Note that the gap observed around 86 - 130° is due to the filtering of fluxes measured when the wind is blowing over the QCL enclosure at the study site. ....	68
<b>Figure 4.21</b> Methane fluxes vs (a) soil temperature (b) volumetric water content (c) water table depth and (d) air temperature. Methane fluxes were measured with eddy covariance and are mean half-hourly fluxes. Air temperature was measured at the EC flux tower and soil temperature, volumetric moisture content and water table depth were measured in close proximity to the flux tower. The soil temperature was measured at 20 cm depth.....	69
<b>Figure 4.22</b> (a) Mean monthly air temperature and (b) mean monthly soil temperature at 20 cm depth vs methane fluxes measured by eddy covariance. Error bars show the standard error of the mean. ....	70
<b>Figure 4.23</b> Area coverage of the different landforms.....	70
<b>Figure 4.24</b> Net methane emissions. The black bars show the upscaled chamber measurements for each sampling date. The grey bars show the range of EC flux measurements, where they were available on the chamber sampling date and the * shows the mean EC flux. Shown in (a) is the full extent of the data; (b) is a zoomed in view of (a).....	71
<b>Figure 4.25</b> Conceptual model showing the relative contribution to the measured flux of the footprint area of an eddy covariance flux tower. The eddy covariance flux tower is at an upwind distance of zero [Adapted from: Schmid (2002)].....	90



## List of Tables

---

<b>Table 2.1</b> Comparison between the CH <sub>4</sub> emission rates reported in studies on drained peatland ecosystems. Mean CH <sub>4</sub> emission rates are in mgCH <sub>4</sub> m <sup>-2</sup> h <sup>-1</sup> and the three middle columns represent the landscape elements [Source: Schrier-Uijl et al. (2010)].....	20
<b>Table 2.2</b> Advantages and disadvantages for measuring soil gas fluxes [Adapted from Denmead (2008); Topp and Pattey (1997)]. .....	33
<b>Table 4.1</b> Soil bulk density of the different landforms. Sampling depth was 8cm. ....	52
<b>Table 4.2</b> Methane fluxes (± standard error of the mean) by landform. Values are reported in mg CH <sub>4</sub> m <sup>-2</sup> h <sup>-1</sup> . ....	55
<b>Table 4.3</b> Methane fluxes from cow dung (mg CH <sub>4</sub> m <sup>-2</sup> h <sup>-1</sup> ).....	58
<b>Table 4.4</b> Seasonal mean methane fluxes (± standard error of the mean) as measured by eddy covariance from October 2018 to September 2019. ....	66
<b>Table 4.5</b> Comparison between net methane emissions from drainage ditches reported in studies on drained peatland ecosystems. Mean CH <sub>4</sub> emission rates are in mg CH <sub>4</sub> m <sup>-2</sup> h <sup>-1</sup> [Adapted from: Schrier-Uijl et al. (2010)]. .....	74





# Chapter One

## Introduction

---

### 1.1 Global methane emissions

Methane (CH<sub>4</sub>) is a greenhouse gas that has a global warming potential 28 times higher than carbon dioxide (CO<sub>2</sub>) and is the second most important anthropogenic greenhouse gas behind CO<sub>2</sub> (IPCC, 2014b). Since the beginning of the industrial era, atmospheric methane concentrations have risen from approximately 720 ppb to over 1858.6 ppb today (Dlugokencky, 2019; Prather & Holmes, 2017). Changes in the atmospheric methane concentration for the last 1000 years is shown in Figure 1.1.

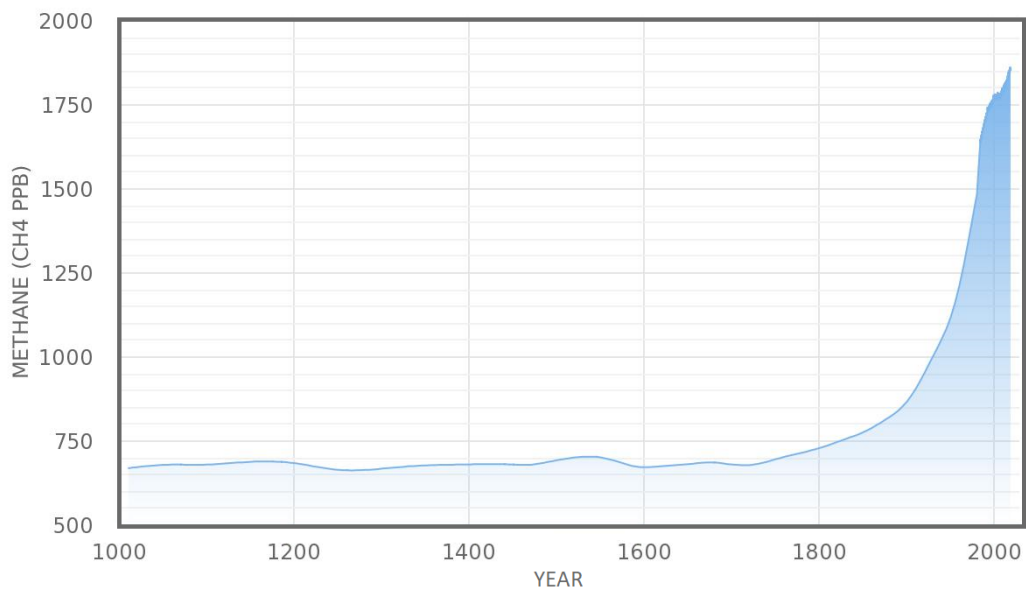


**Figure 1.1** Global long-term trend in atmospheric methane concentration, 1010 – 2018 [Source: Louergue et al., 2008; Etheridge et al., 2002; Etheridge et al., 1998 and Dlugokencky, NOAA/ESRI., 2018 as cited in (2 Degrees Institute, n.d.)].

This increase in atmospheric methane concentration is largely as a result of anthropogenic methane emissions from agriculture, wastes and fossil fuel emissions (Prather & Holmes, 2017). However, there was a brief plateau in atmospheric methane concentrations over the late 1990's and early 2000's (Reay et al., 2010). Although a definitive cause is unknown and atmospheric methane

concentrations are increasing once again, both Turner et al. (2017) and Rigby et al. (2017) suggested that the cause was an increase in the rate of destruction of methane by OH radicals in the troposphere. Methane is responsible for approximately 18% of human-induced radiative forcing and although most research and policy for climate change tends to focus on reducing/mitigating CO<sub>2</sub> emissions, it is becoming increasingly apparent that reducing/mitigating methane emissions may be a more efficient and cost effective strategy to mitigate anthropogenic climate change (Bridgham et al., 2013; Reay et al., 2010).

The global methane budget is composed of a wide variety of anthropogenic and natural sources which are balanced by a small number of sinks (Reay et al., 2010). Methane sources can be broadly classified into three types; biogenic, thermogenic and pyrogenic (Kirschke et al., 2013). Biogenic methane is sourced from anaerobic methanogenic bacteria and sources include wetlands, ruminant animals, rice agriculture, and organic waste deposits (Kirschke et al., 2013). Thermogenic methane is methane that was formed through geological processes and it can be released through exploitation of fossil fuels and natural features such as volcanoes, and terrestrial/marine seeps (Kirschke et al., 2013). Pyrogenic methane is produced by the incomplete burning of biomass and soil carbon during wildfires as well as the incomplete combustion of fossil fuels (Kirschke et al., 2013). Anthropogenic methane emissions are largely sourced from agriculture (ruminant livestock / rice production), fossil fuels, waste management, and from climate change affected natural sources / sinks (Ciais, 2013). The total methane emission for all sources is estimated to be 574 Tg CH<sub>4</sub> yr<sup>-1</sup> and anthropogenic methane emissions account for 54 – 72% of the total global methane flux (Bridgham et al., 2013; Reay et al., 2010).

There are three main sinks for atmospheric methane, which are oxidation of methane in aerobic soils, stratospheric loss and the destruction of atmospheric methane by hydroxyl (OH<sup>•</sup>) radicals in the troposphere (Reay et al., 2010). Tropospheric OH<sup>•</sup> radicals are the dominant methane sink, accounting for an estimated -467 Tg CH<sub>4</sub> yr<sup>-1</sup>, and although aerobic soils only account for -30 Tg CH<sub>4</sub> yr<sup>-1</sup>, they are still a significant control on atmospheric methane concentrations

(Dlugokencky et al., 2011; Reay et al., 2010). The total methane flux for methane sinks is estimated to be  $-536 \text{ Tg CH}_4 \text{ yr}^{-1}$  (Reay et al., 2010). This results in an estimated annual net flux of  $38 \text{ Tg CH}_4 \text{ yr}^{-1}$  into the atmosphere.

## 1.2 Drained peatlands

Wetlands are the largest natural source of atmospheric methane and are defined as areas that are covered by, or saturated by water for all or part of the year and includes peatlands, wet soils, swamps, bogs and waterways (Ciais, 2013; IPCC, 2013; Ministry for the Environment, 2016). Global annual wetland methane emissions have been estimated to be  $177 - 284 \text{ Tg CH}_4 \text{ yr}^{-1}$  (Ciais, 2013). Peatlands are a subsection of wetland types that are characterised by water saturated soil and the accumulation of organic matter as peat due to incomplete decomposition (Hahn et al., 2018).

Within soils, methane is produced and consumed by two competing processes; methanogenesis and methanotrophy (methane oxidation) whereby methane is primarily produced in the anaerobic soils below the water table and methane is consumed in the aerobic soil above the water table (Le Mer & Roger, 2001). However, methanogenesis can still occur within anaerobic microsites above the water table and methane oxidation can still occur with other electron acceptors (e.g. nitrate, sulphate, organic matter etc.) in the absence of oxygen (Yang et al., 2017). Methane can then be transported through the soil via three processes; diffusion, transport through aerenchymous plant tissue and ebullition (Le Mer & Roger, 2001). Hence, the primary controls on the net methane flux are the ratio of methane produced to methane consumed and the type/rate of methane transport (Männistö et al., 2019). This ratio of methane produced to methane consumed is primarily driven by the water table level which changes the ratio of aerobic soil to anaerobic soil.

Natural peatlands are characterised by their high water tables and saturated soils which results in primarily anaerobic conditions within the soil (Hahn et al., 2018). However, close to the peat surface aerobic conditions still persist. This results in natural peatlands being large sources of atmospheric methane (Bridgham et al.,

2006). However, large areas of peatlands have been drained for agriculture and forestry, which lowers the water table and greatly increases the aerobic zone within the peatland soil (Evans et al., 2016). It is typically assumed that methane emissions from drained peatlands are negligible with the methane that is produced below the water table being consumed before it reaches the soil surface (Evans et al., 2016; IPCC, 2014a).

Drained peatlands are complex ecosystems with methane emitting “hot and cold” spots, due to the variable water table depth as a result of flooded drainage ditches (Baldocchi et al., 2012). Even though methane emissions from drained peat soils are significantly reduced, methane fluxes from drainage ditches can remain high (Schrier-Uijl et al., 2010; Teh et al., 2011). In addition, methane can be emitted from anaerobic microsites located above the water table in the aerobic zone (Yang et al., 2017). It has also been shown that the methane emissions from drainage ditches within peatlands tends to increase with increasing land use intensity (Evans et al., 2016). This has been largely attributed to the higher soil fertility together with increased amounts of labile organic matter transported into the drainage ditches (Evans et al., 2016). However, water flow rates and vegetation inside the drainage ditches also play a role in influencing the methane emissions from drainage ditches (Evans et al., 2016). Lastly, spatial variation in methane fluxes across drained peatlands can be caused by agricultural management practices and vegetation composition (Peltola et al., 2015).

### **1.3 New Zealand drained peatlands**

Methane is of significant importance to New Zealand as greenhouse gas emissions are dominated by methane and nitrous oxide rather than the global norm of carbon dioxide as the dominant greenhouse gas (Ministry for the Environment, 2016). Methane and nitrous oxide account for 42% and 11% of New Zealand’s annual greenhouse gas emissions respectively (Ministry for the Environment, 2019b). This is due to the dominance of the agricultural sector (48% of total emissions) and relatively low levels of heavy industry CO<sub>2</sub> emissions in New Zealand (Ministry for the Environment, 2019b; Saggart et al., 2008). With methane emissions in New Zealand being so high it significantly changes how New Zealand

can implement policies to reduce or mitigate anthropogenic climate change compared with the rest of the world, which is focused on reducing CO<sub>2</sub> emissions.

There are a limited number of studies that have investigated methane emissions from drained peatlands and many emission reports assume that drained peatlands have zero methane emissions. For example, the New Zealand Greenhouse Gas Inventory follows the methodologies set out in the 2006 IPCC Guidelines for National Greenhouse Gas Inventories (Ministry for the Environment, 2018). Within the 2006 IPCC report, methane emissions from drained organic soils were assumed to be negligible (Evans et al., 2016; IPCC, 2014a). However, the IPCC later released the 2013 Supplement to the 2006 IPCC Guidelines for National Greenhouse Gas Inventories: Wetlands, which set out improved methodologies for organic soils and included emission factors for drained organic soils under different land use classes (IPCC, 2014a). Despite this, New Zealand has opted to exclude this from their emission reporting framework as the use of this supplement is voluntary (Ministry for the Environment, 2019b). The IPCC (2014a) have reported a methane emission factor of 527 kg CH<sub>4</sub> ha<sup>-1</sup> yr<sup>-1</sup> for drainage ditches in temperate shallow-drained grasslands. However, even though the methane emissions within the drainage ditches are large, due to their relatively small spatial extent, the overall methane emissions are relatively small. The whole peatland system including drainage ditches has been estimated to emit 39 kg CH<sub>4</sub> ha<sup>-1</sup> yr<sup>-1</sup> by the IPCC (2014a) and 30 kg CH<sub>4</sub> ha<sup>-1</sup> yr<sup>-1</sup> by Couwenberg (2011). It should be noted that these values have high levels of uncertainty associated with them, mainly due to uncertain proportions of drainage ditches within peatlands, the high variability in methane fluxes between studies and the uneven geographical distribution of studies (Evans et al., 2016; IPCC, 2014a). For shallow drained grasslands, all of the source data that the IPCC used in calculating the emission factors was collected from the Netherlands. The uncertainty range specified within the IPCC report for the drainage ditch emission factor is 285 – 769 kg CH<sub>4</sub> ha<sup>-1</sup> yr<sup>-1</sup> and the 95% confidence interval for entire drained peatland systems is – 2.9 – 81 kg CH<sub>4</sub> ha<sup>-1</sup> yr<sup>-1</sup> (IPCC, 2014a).

Originally, prior to human settlement, New Zealand had an estimated 241,187 ha of peatlands (Landcare Research, 2015). However, since human settlement approximately 90% of wetlands have been drained, primarily for use in agriculture, forestry or peat mining (Ausseil et al., 2015). Currently there is 154,108 ha of peatlands that have been drained for pastoral uses (Landcare Research, 2015). This means that at present there is 154,108 ha of drained peatlands under primarily agricultural use, that do not have their methane emissions accounted for in the current greenhouse gas reporting framework in New Zealand.

Thus, there is a lack of data for drained peatland methane emissions in New Zealand.

#### **1.4 Aims and objectives**

The overall aim of this thesis is to determine the magnitude of methane emissions from a drained peatland under dairy grazing and where and when do the emissions occur throughout the year.

To achieve this aim, the thesis objectives are to:

- Determine where the methane emission hotspots are and when are they active.
- Determine how much methane is emitted by scaling up small-scale chamber measurements.
- Determine total methane emissions as measured by eddy covariance and reconcile this with the small-scale chamber measurements.

The hypotheses are:

- That methane emissions will be elevated in close proximity to drains where the water table is elevated.
- That soil-based methane emissions from a drained peatland under dairy grazing will be elevated compared to a mineral soil
-

## **1.5 Thesis outline**

Chapter 2 is a literature review focused on the production and consumption of methane in soils, specifically drained peatlands. The literature review also covers the research methodology that can be used to measure methane emissions in soil and water bodies.

Chapter 3 contains a description of the study site at Gamma farm

Chapter 4 contain the main experimental part of this thesis and covers where, how much and when methane is emitted from a drained peatland under dairy grazing. Note that this chapter is formatted as a research paper and hence includes methods, results and discussion.

Chapter 5 provides a summary and the conclusions found from this study.





# Chapter Two

## Literature review

---

This literature review chapter begins with an overview of the processes that produce, consume and transport methane within soils before focusing in on methane emissions from drained peat soils. Subsequently, the factors that affect methane emissions from drained peat soils are discussed in section 2.5, followed by the likely impacts of climate change to methane emissions from drained peat soils. Lastly the common methods that are used to measure methane fluxes<sup>1</sup> are discussed.

### 2.1 Methane production and consumption in soil

Soils play a vital role in the methane cycle as methane is both produced (methanogenesis) and consumed (methane oxidation) within soil. The production and consumption of methane in soil is controlled by microbially mediated processes that are dependent on the redox potential of the soil (i.e. the water table level) (Yang et al., 2017). The classical theory of methane dynamics in soils is that methanogenesis only occurs under highly reducing conditions and that methane oxidation is controlled by the availability of oxygen (Yang et al., 2017). Therefore in wetlands, methanogenesis and methane oxidation are controlled by the water table where methanogenesis occurs below the water table and methane oxidation occurs above the water table (Yang et al., 2017). This occurs because the diffusion of oxygen is limited below the water table leading to an anaerobic, reducing environment (Yang et al., 2017). This theory is widely

---

<sup>1</sup> The soil methane flux is simply a measure of the flow of methane gas into or out of the soil (Monson & Baldocchi, 2014). Fluxes are generally measured as a flow (of mass, momentum or heat) per unit area per unit time (e.g.  $\text{kg CH}_4 \text{ ha}^{-1} \text{ yr}^{-1}$ ) (Monson & Baldocchi, 2014). A positive methane flux represents methane emission whereas a negative flux represents methane consumption.

accepted as it encompasses the dominant control on methane production and consumption; which is that the water table controls the oxic-anoxic boundary that separates methanogenesis from methane oxidation (Yang et al., 2017). However, there is increasing evidence that this model does not capture all of the methane that is produced and consumed by soil processes as methanogenesis can occur in anaerobic microsites / hotspots within unsaturated, dry soils and methane oxidation can still occur with other substrates such as nitrate ( $\text{NO}_3$ ), sulphate and organic matter in the absence of oxygen (Figure 2.1) (Yang et al., 2017). Kuzyakov and Blagodatskaya (2015) defined microbial hotspots as “small soil volumes with much faster process rates and much more intensive interactions (between pools) compared to the average soil conditions”. This has led to the emergence of a new “heterogenous” model within which methanogenesis and methane oxidation can both occur throughout the soil profile (Yang et al., 2017). The methane flux is therefore the balance of methane production and methane oxidation (Bridgham et al., 2013).

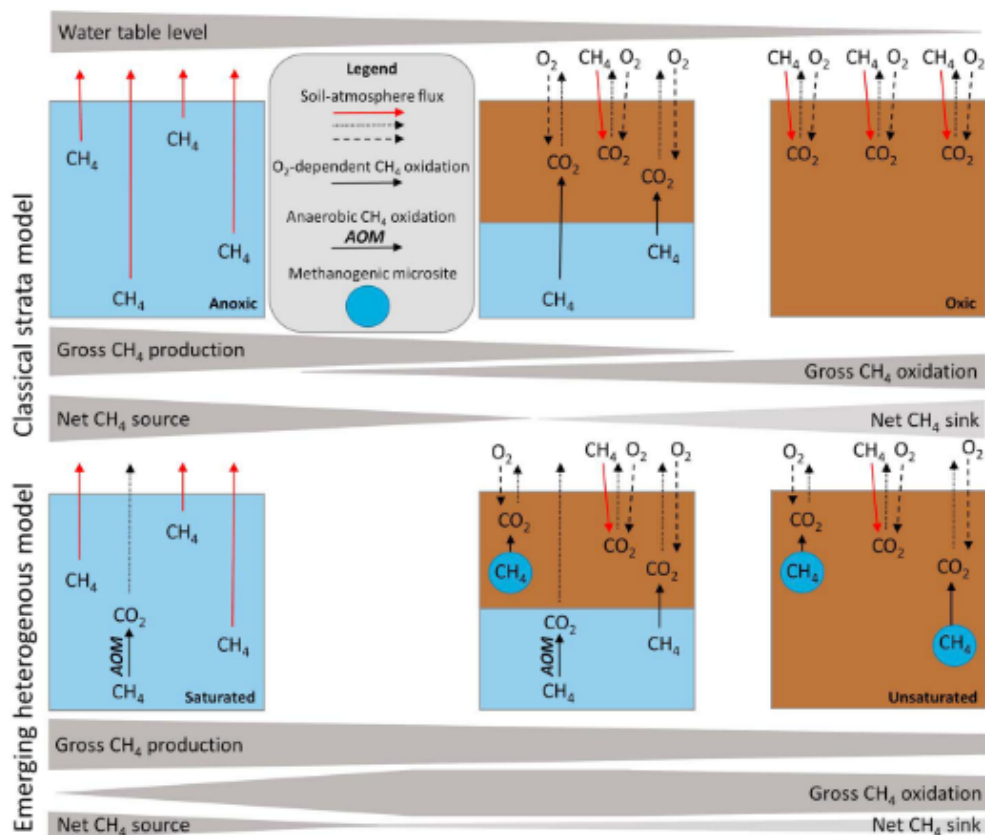


**Figure 2.1** The classical strata model of methane dynamics versus the emerging heterogenous model [Source: (Yang et al., 2017)].

### 2.1.1 Methanogenesis

Methanogenesis or methane production is defined as “the microbial production of methane by the anaerobic breakdown of carbon-containing compounds” (Cammack et al., 2008). This process is carried out by a group of microbes known as methanogens, which are classified within the Archaea domain (Allaby, 2013). Methanogenesis is an anaerobic process and for methanogenesis to occur a redox potential ( $E_h$ ) below -200 mV is required (Le Mer & Roger, 2001). Thus, methanogenesis is typically only presumed to occur in anerobic, reducing environments (e.g. below the water table or in anaerobic microsites) (Yang et al., 2017) Methanogens are unique in that during the metabolism of organic substrates, methane is produced as their major metabolic product (Boone, 1993). The number of substrates that methanogens are capable of using are extremely limited and includes  $H_2 + CO_2$ , formate, acetate, methanol, methylamines, methylsulfides and some alcohols (Boone, 1993). Due to the limited number of substrates available to be used by methanogens, they are reliant on other microbes to convert organic matter into useable substrates (Boone, 1993). The anaerobic decomposition of organic matter is split into three different processes; fermentation; syntrophic acetigenesis and methanogenesis (Boone, 1993).

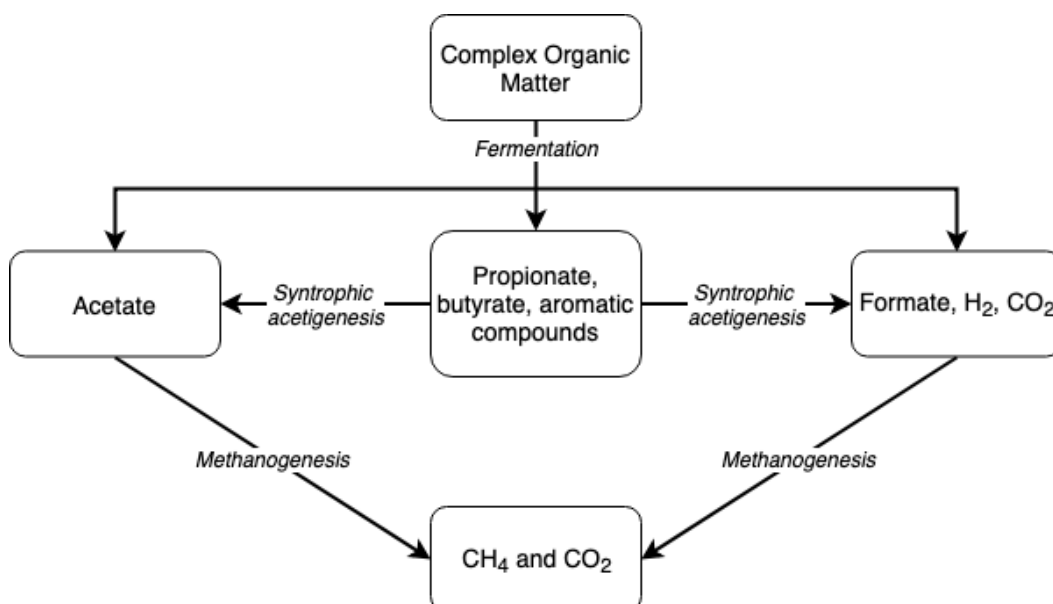


**Figure 2.2** Anaerobic decomposition of organic matter [Adapted from: (Boone, 1993)].

Each process (fermentation, syntrophic acetigenesis and methanogenesis) is catalysed by separate groups of microbes and these reactions typically occur

simultaneously (Boone, 1993). Hence, the concentrations of intermediary products is often small (Boone, 1993). The first step is fermentation, where complex organic matter is converted into useable organic substrates such as acetate, formate, H<sub>2</sub> and CO<sub>2</sub> and unusable volatile fatty acids such as propionate, butyrate and aromatic compounds (Boone, 1993; Ferry, 2010). Next, acetogenic bacteria oxidise the volatile fatty acids to form acetate, CO<sub>2</sub> and H<sub>2</sub> (Boone, 1993). Lastly, methanogenesis occurs, whereby organic substrates produced by fermentative and acetogenic bacteria are converted to methane and CO<sub>2</sub> (Ferry, 2010). There are many different types of methanogens that utilise different pathways and substrates to obtain energy (Ferry, 2010). There are three main pathways that are utilised by methanogens; the CO<sub>2</sub> reduction pathway; the aceticlastic pathway; and the methyltrophic pathway (Ferry, 2010). In the CO<sub>2</sub> reduction pathway, CO<sub>2</sub> is reduced to methane with either formate or H<sub>2</sub> (Ferry, 2010). In the aceticlastic pathway the methyl group of acetate is converted to methane while the carboxyl group is converted to CO<sub>2</sub> (Ferry, 2010). In the methyltrophic pathway the methyl groups of methanol, methylamines and methylsulfides are converted to methane and CO<sub>2</sub> (Ferry, 2010). However, the H<sub>2</sub> + CO<sub>2</sub> and acetate pathways account for the majority of methane that is produced in the soil (Ferry, 2010).

There are a large variety of factors that influence the rate of methane production in soils. These factors include anaerobic conditions and redox potential, electron acceptors, substrate availability, temperature, diffusion, water availability and water table depth, soil pH and salinity, fertiliser and manure additions and amendments, trace metals, competitive inhibition, vegetation, plant species and cultivars and elevated CO<sub>2</sub> concentrations (Dalal et al., 2008). However, the concentration and type of organic matter as well as the concentration of oxygen are the predominant factors in methanogenesis (Dalal et al., 2008).

### **2.1.2 Methane oxidation (methanotrophy)**

Methane oxidation or methanotrophy is defined as a microbial metabolic process where methane is oxidised with O<sub>2</sub> to CO<sub>2</sub> for energy generation (Bürgmann,

2011). Methane oxidation is carried out by methanotrophic bacteria (methanotrophs) who use methane as a sole carbon and energy source (Hanson & Hanson, 1996). Methanotrophic bacteria can be split into two main groups based on the metabolic pathway that they use (Hanson & Hanson, 1996; Serrano-Silva et al., 2014). Type I methanotrophs (gammaproteobacteria) use the ribulose monophosphate (RuMP) pathway whereas Type II methanotrophs (alphaproteobacteria) use the serine pathway (Hanson & Hanson, 1996; Serrano-Silva et al., 2014). Initially there was a third classification; Type X which had the characteristics of both types and was later reclassified within Type I methanotrophs (Hanson & Hanson, 1996; Serrano-Silva et al., 2014). Type I methanotrophs are typically dominant in environments that have limited methane and high levels of nitrogen and copper (Hanson & Hanson, 1996). This is because Type I methanotrophs are unable to fix molecular nitrogen and require copper for growth (Graham et al., 1993). In addition, the RuMP pathway utilised by Type I methanotrophs is the more efficient pathway for carbon assimilation. Conversely Type II methanotrophs are dominant in environments that have high levels of methane and limited nitrogen and copper levels (Hanson & Hanson, 1996). Methanotrophic bacteria are important drivers in the soil methane flux as methanotrophic bacteria at the soil surface are capable of consuming large amounts of the methane that is produced in the soil by methanogenic bacteria (Hanson & Hanson, 1996; Serrano-Silva et al., 2014). It is therefore the balance between methanogenesis and methane oxidation in soil that determines the methane flux. Methane oxidation typically occurs in the aerobic surface layer of soils or within the rhizosphere (Tate, 2015).

There are a large variety of factors that influence the rate of methane oxidation in soils. These factors include temperature, soil water / water filled pore space (WFPS), aeration, gas diffusion and soil texture, soil pH, salinity, substrate and methane concentrations, soil nitrogen, other soil nutrients, fertilisers and amendments, increased concentration of atmospheric CO<sub>2</sub> and herbicides and pesticides (Dalal et al., 2008). However, the effect that these factors have on methane oxidation will depend on the dominant type of methanogen present as Type I methanotrophs are dominant in nutrient rich environments whereas Type

II methanotrophs are dominant in nutrient poor environments (Serrano-Silva et al., 2014).

### **2.1.3 Methane transport**

The transport of methane is an important factor in the net production and consumption of methane in soil (Bridgham et al., 2013). There are three main mechanisms of methane transport from the soil to the atmosphere; diffusion, ebullition and plant-mediated transport (Serrano-Silva et al., 2014). Diffusion of methane occurs along the concentration gradient that is set up by the high concentrations of methane in the deeper soil where methane is produced and the low concentrations of methane in the upper soil where methane is oxidised and emitted to the atmosphere (Serrano-Silva et al., 2014). Although diffusion is the slowest transport mechanism for methane, it is the most important transport mechanism for methane consumption as it increases the time that the methane is available for oxidation before it is emitted to the atmosphere (Serrano-Silva et al., 2014). If the dissolved concentration of methane is sufficiently high, methane gas bubbles may form in the soil that quickly transport the methane to the soil surface, thereby reducing methane oxidation in the aerobic surface layers (Serrano-Silva et al., 2014). The third transport mechanism is plant-mediated transport, which occurs through plant structures known as aerenchyma (Serrano-Silva et al., 2014). Aerenchyma are structures that were developed by vascular plants to adapt to flooded environments and are defined as a “plant tissue containing large, continuous extracellular air spaces” (Cammack et al., 2008; Serrano-Silva et al., 2014). These air spaces are primarily used by the plant to transport oxygen to submerged roots, but can also transport methane from the waterlogged zone to the surface (Cammack et al., 2008; Serrano-Silva et al., 2014). This process bypasses the aerobic zone where methane oxidation occurs (Serrano-Silva et al., 2014). Plant-mediated transport is a relatively fast and efficient means of methane transport and its contribution to the total methane flux varies between wetland systems (Bridgham et al., 2013; Serrano-Silva et al., 2014). However, it typically accounts for 30-100% of the total methane flux (Bridgham et al., 2013). Wetland plants have been shown to vary in their capability to transport methane

and therefore the composition of plants in a wetland could impact on the methane flux (Bhullar et al., 2013). Graminoid plants have been shown to facilitate higher rates of methane transport than shrubs, woody vegetation and forbs (Bhullar et al., 2013).

## **2.2 Soil Methane emissions**

Soil is both a globally important source and sink of atmospheric methane as methane can be either produced or consumed in soils by microbial activity (Yang et al., 2017). For the most part soils either act as methane sources or as methane sinks, with upland soils as the major methane sinks and wetlands as the major methane sources (Ciais, 2013; Yang et al., 2017). Additionally, wetlands are the largest source of methane globally and account for 177-284 Tg CH<sub>4</sub> yr<sup>-1</sup> (Ciais, 2013). This results in wetlands being the dominant driver of interannual variations in the total global methane flux (Ciais, 2013). The IPCC defines wetlands as any area that is covered or saturated by water for all or part of the year and this includes such ecosystems as peatlands, wet soils and waterways (IPCC, 2013; Ministry for the Environment, 2017b). Although, most soils are either a methane source or a methane sink, peat-forming wetlands such as bogs and fens can act as both a methane source or sink depending on the hydrological conditions and the water table depth (Yang et al., 2017). High water tables reduce the availability of oxygen within the soil and results in reducing conditions that are favourable for methanogenesis (Megonigal et al., 2004; Yang et al., 2017). Thus, low water tables increase the oxygen available in the soil, which enhances methanotrophy (methane consumption) and can lead to a reduction in methane production / a switch to net methane consumption (Yang et al., 2017). The lowering of the water table can be as a result of agricultural management processes (e.g. drainage), drought or decreased rainfall and increased evaporation (Yang et al., 2017).

## **2.3 Methane production and consumption in water**

Methane is formed by microbial processes within anaerobic sediment and is released to the atmosphere via three primary pathways; ebullition, diffusion and plant-mediated transport (Duc et al., 2013). Within aquatic environments



methane emissions are comprised of the fluxes between the water's surface and the atmosphere (diffusive flux) and bubbles from the sediment-water interface rising to the water's surface (ebullition) (International Hydropower Association, 2010). However, the methane that is emitted to the atmosphere is controlled by biological (microbial production and oxidation) and physical transport processes (Duc et al., 2013). Methane transported via diffusion can be entirely or partly oxidised as it rises through the water column (Duc et al., 2013). This occurs through two main methods: oxidation by methanotrophs in the presence of dissolved oxygen; and oxidation through the nitrate/nitrite reduction pathway (denitrification-dependent anaerobic methane oxidation) (Liu et al., 2017). The nitrate/nitrite reduction pathway is considered to be more likely to occur than the sulphate reduction pathway although both  $\text{NO}_3/\text{NO}_2^-$  and  $\text{SO}_4^{2-}$  are present in anaerobic water bodies (Liu et al., 2017). This denitrification methane oxidation reaction process consumes methane while producing  $\text{N}_2$  and  $\text{CO}_2$  (Liu et al., 2017). This has the added benefit of reducing the excess nitrogen present in water bodies (Liu et al., 2017). Conversely, methane that is transported by ebullition processes quickly pass through the oxic zone, with little chance for oxidation to occur (Duc et al., 2013).

Methane concentrations in water are influenced by several factors including the mixing regime, the abundance of algal plants and their photosynthetic rates, the quantity of organic matter entering the system and its rate of decomposition, the water residence time and the dissolved oxygen content (International Hydropower Association, 2010). The diffusive gas flux primarily depends on the concentration gradient between the water and the air, convection and physical variables such as wind speed and rainfall (Demarty & Bastien, 2011). Conversely, ebullition primarily depends on the water temperature and hydrostatic pressure (Demarty & Bastien, 2011).

## **2.4 Methane production and consumption in drained peat soils**

Peatlands are defined as wetland ecosystems that are characterised by water-saturated soil and the accumulation of organic matter as peat due to incomplete

decomposition (Hahn et al., 2018). Within natural peatlands, the rate of carbon uptake due to photosynthesis is higher than the rate of loss due to autotrophic and heterotrophic respiration which therefore results in peat accumulation (Kroon et al., 2010). As peatlands are anaerobic in nature due to the high water table, the rate of decomposition of organic matter is significantly lower than in aerobic soils as anaerobic decomposition occurs at lower rates than aerobic decomposition (Couwenberg & Fritz, 2012). Natural peatlands are therefore a sink for atmospheric CO<sub>2</sub> and a source for atmospheric methane (Kroon et al., 2010). Although peatlands only cover approximately 3% of the Earth's surface they are important drivers in both the global methane and carbon dioxide cycles as they are responsible for an estimated 20-30% of global methane emissions each year as well as storing approximately 455 Pg of carbon, or one-third of the global soil carbon pool (Hahn et al., 2018; Kroon et al., 2010; Nungesser, 2003). However, in modern times large areas of natural peatlands have been drained primarily for agriculture, forestry or peat extraction due to the potentially high fertility of the peat soil (Hatala et al., 2012). Natural peatlands tend to have a high water table, which results in anoxic conditions and the peatland acting as a source of methane and a sink of carbon dioxide (Hahn et al., 2018). When drained, the water table within the peatland is lowered which results in the peatland acting as a source of carbon dioxide and having significantly reduced methane emissions or even acting as a small methane sink (Hahn et al., 2018; Tiemeyer et al., 2016). Drained peatlands are complex ecosystems with methane emitting hot and cold spots, due to the variable water table depth as a result of flooded drainage ditches (Baldocchi et al., 2012). Hence, even though methane emissions are significantly reduced, methane fluxes from drainage ditches can remain high (Schrier-Uijl, 2010; Teh et al., 2011). Teh et al. (2011) found that drainage ditches in drained peatlands accounted for less than 5% of the land area yet were responsible for more than 84% of methane emissions. In addition, methane can be emitted from anaerobic microsites located above the water table in the aerobic zone (Yang et al., 2017).

New Zealand's National Greenhouse Gas Inventory defines organic soils as soils that contain greater than 17% organic matter, with further classifications as slightly peaty (17-30% OM), peaty (30-50% OM) and peat soil (>50% OM) (Ministry

for the Environment, 2018). Previous to human settlement, New Zealand had an estimated 241,187 ha of peatlands (Landcare Research, 2015). Subsequently, approximately 90% of peatlands have been drained, primarily for use in agriculture, forestry or peat mining (Environment Waikato, 2006). Currently there is approximately 154,108 ha of drained peatlands used for agriculture (Landcare Research, 2015).

#### **2.4.1 Methane emissions from drained peat soils**

Methane emissions from drained peatland soils are difficult to quantify as there are large spatial and temporal variations, primarily due to variations in the water table depth caused by flooded drainage ditches (Baldocchi et al., 2012; Schrier-Uijl et al., 2010). As such, defining accurate emission factors for methane emissions from drained peatland soils is a difficult task, made more complicated by the limited number of studies that have investigated methane emissions from drained peatlands (Evans et al., 2016). In addition to the limited number of studies, the geographical and typological distribution of sites is highly uneven with more than half of the peatland sites studied located in the Netherlands (Evans et al., 2016). The IPCC (2014a) estimated the methane emissions for drained peatland systems to be  $39 \text{ kg CH}_4 \text{ ha}^{-1} \text{ yr}^{-1}$ , which included emissions from the bulk soil as well as the drainage ditches. And although the total emissions were relatively low, the methane emissions from just the drainage ditches themselves were estimated to be  $527 \text{ kg CH}_4 \text{ ha}^{-1} \text{ yr}^{-1}$  (IPCC, 2014a). It is the relatively low spatial extent of the drainage ditches compared to the whole system that results in the significantly lower methane emissions from the whole peatland system. Taking the IPCC emission factor for drained peatlands ( $39 \text{ kg CH}_4 \text{ ha}^{-1} \text{ yr}^{-1}$ ) and the area of drained peatlands under agricultural use in New Zealand (154,108 ha), it can be calculated that drained peatlands under agricultural use emit 6010.2 ton  $\text{CH}_4$  (150.26 kt  $\text{CO}_2$ -eq) per year (IPCC, 2014a; Landcare Research, 2015). A meta-analysis by Evans et al. (2016) summarised previous reviews of drained peatlands to determine the methane fluxes of drainage ditches in peatlands under different land uses, shown in Figure 2.3.

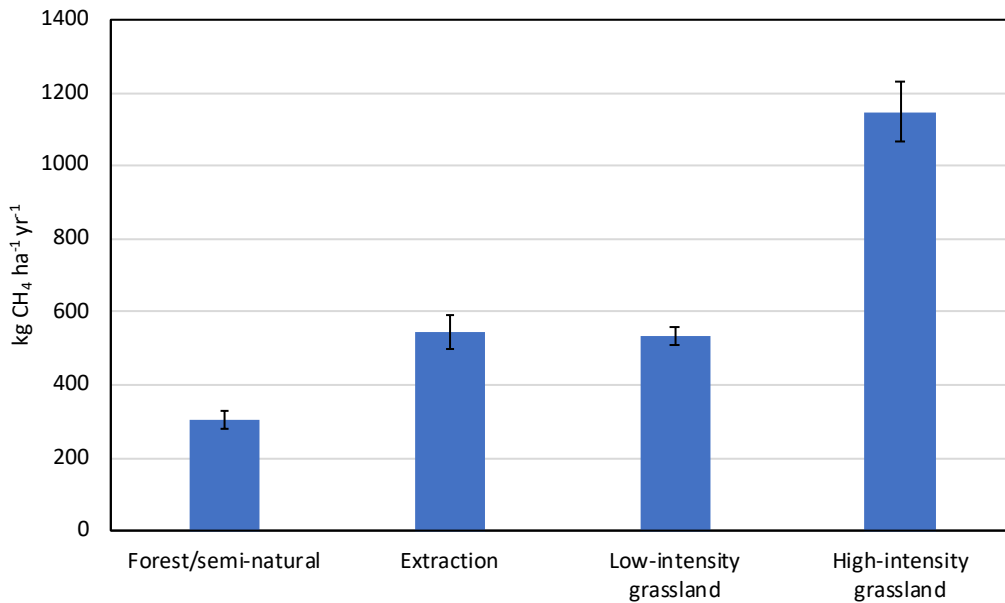


**Figure 2.3** Mean methane emissions from peatland drainage ditches under different land uses. Error bars show 95% confidence interval for the per study means only [Adapted from: (Evans *et al.*, 2016)].

Drainage ditches within agricultural grasslands were shown have methane emissions in the range of 500-1000 kg CH<sub>4</sub> ha<sup>-1</sup> yr<sup>-1</sup> (Evans *et al.*, 2016). A study completed by Schrier-Uijl *et al.* (2010) investigated the methane emissions for an intensively and an extensively managed peatland. They split each peatland into three sections: drains/ponds (i.e. open water); drain edges (i.e. saturated land) and the drier field between the drains (Schrier-Uijl *et al.*, 2010). Their results showed that for managed peatland systems the methane emissions from drainage ditches contributed approximately 60-70% of the total methane emissions. A summary of the results found by Schrier-Uijl *et al.* (2010) with comparisons to other studies in drained peatlands are shown in Table 2.1.

**Table 2.1** Comparison between the CH<sub>4</sub> emission rates reported in studies on drained peatland ecosystems. Mean CH<sub>4</sub> emission rates are in mgCH<sub>4</sub>m<sup>-2</sup>h<sup>-1</sup> and the three middle columns represent the landscape elements [Source: Schrier-Uijl et al. (2010)].

<b>Ecosystem</b>	<b>Field</b>	<b>Drain Edge / Saturated land</b>	<b>Drain / pond</b>	<b>Reference</b>
Boreal fen	-0.04 – 0.04		15.72 up to 25 in summer	Minkkinen and Laine (2006)
Eutrophic fen abandoned agriculture	1.6	15.3	5.6	Hendriks et al. (2007)
Boreal fen	0.0 – 1.0		5.8 up to 38.2 in summer	Bubier et al. (1993)
Less eutrophic fen	1.0 – 10.0			Bellisario et al. (1999)
Boreal fen	0.1 – 0.9	1.2 – 8.2		Pelletier et al. (2007)
Boreal fen		2.0 – 9.2		Liblik et al. (1997)
Less eutrophic fen	0.9 – 2.3	11.8		Van den Pol-van Dasselaar et al. (1998b)
Less eutrophic fen			2.9	Waddington and Day (2007)
Eutrophic aquifer	0.0 – 8.0			Adrian et al. (1994)
Boreal fen			up to 8.0	Hutten et al. (2003)
Less eutrophic fen			4.6 – 7.5	Hamilton et al. (1994)
Less eutrophic fen		5.3 – 12.4		Chanton et al. (1993)
Eutrophic fen (intensively managed)	0.7 – 0.8	4.8 – 6.0	4.5 – 7.0	Schrier-Uijl et al. (2010)
Eutrophic fen (extensively managed)	0.8 – 0.9	2.7 – 4.4	4.5 – 5.3	Schrier-Uijl et al. (2010)

As shown by Table 2.1, multiple studies have consistently found that drainage ditches are a methane emission hotspot within drained peatland environments.

However, Table 2.1 also highlights the large variations in the measured methane flux within and between studies.

## **2.5 Controls of methane emissions from drained peat soils**

The predominant factors that control methane fluxes are soil temperature and the water table position. However, studies have shown that the controls of methane fluxes are often complicated and include substrate availability, pH, nutrients/fertiliser addition, vegetation and electron acceptors in addition to the temperature and water table level (Adhya et al., 1998; Dunfield et al., 1993; Segers, 1998; Teh et al., 2011; Turetsky et al., 2014). Thus, the controls for methane fluxes in peatland soils are incredibly complex, interrelated and we still do not completely understand what is driving the variability in the methane flux (Turetsky et al., 2014).

### **2.5.1 Substrate availability**

Substrate availability is one of the most important factors in the production of methane as methanogens require carbon substrates to function (Dalal et al., 2008; Segers, 1998). The carbon substrates that are utilised by methanogens are sourced from the anaerobic decomposition of soil organic matter, roots, root exudates, microbial biomass, and above ground organic matter such as plant biomass and leaf litter (Dalal et al., 2008). The rate of methane production has been shown to increase with the addition of direct methanogenesis substrates such as H<sub>2</sub> and acetate as well as indirect substrates such as glucose and leaf leachate that require other microbes for conversion into a useable substrates for methanogenesis (Segers, 1998).

### **2.5.2 Water**

The availability of water is the main control of microbial activity, carbon mineralisation, substrate availability and oxygen availability, thereby controlling the extent of the anaerobic conditions and the redox potential of the soil (Dalal et al., 2008). Therefore, the water availability is a major factor in the rate of

methanogenesis as methanogens require anaerobic conditions as well as carbon substrates to function (Dalal et al., 2008). The rate of methanogenesis has been shown to be dependent on the height of the water table and increase with the height of the water table (Dalal et al., 2008). This is because methanogenesis occurs below the water table where there is limited oxygen and as methane is produced it travels above the water table into the aerobic soil above where it is available for oxidation (Topp & Pattey, 1997). Therefore, the larger the aerobic zone, (i.e. the lower the water table) the more methane that can be oxidised and less methane that can be produced.

However, the relationship between methane dynamics and the water table depth has been shown to be complex, with various direct and indirect controls (Goodrich et al., 2015). For example, drainage ditches tend to result in large spatial variations in the methane flux due to their effect on the water table (Schrier-Uijl et al., 2010; Teh et al., 2011). This is because drainage ditches increase the water availability in the areas surrounding the drain, thereby increasing the redox potential of the soil and increasing the methane flux.

### **2.5.3 Temperature**

Temperature is a major control on the rate of both methane production and consumption, with rates increasing at higher temperatures (Dalal et al., 2008). It has been shown that the  $Q_{10}^2$  value of methanogenesis varies between 1.7 – 16 (van Huissteden et al., 2016). Conversely, the  $Q_{10}$  value of methane consumption varies between 1.4 – 2.1 (van Huissteden et al., 2016). The optimum temperature of methane production and consumption is approximately 25-30°C in peat soils although methanogenesis shows a higher temperature sensitivity than methane oxidation (Dunfield et al., 1993). It has been shown that the methanogenic population is able to adapt to long term temperature conditions and carbon

---

<sup>2</sup> The  $Q_{10}$  or temperature coefficient of a reaction describes the factor by which the reaction changes with a 10°C increase in temperature (Cammack et al., 2008). A  $Q_{10}$  of 2 indicates that for every 10°C increase in temperature the reaction rate doubles.

supply, resulting in different optimum temperatures depending on which type of methanogen is dominant (Dalal et al., 2008). Chin et al. (1999) found that at high temperatures *Methanosarcinaceae* is dominant and is able to use both H<sub>2</sub> + CO<sub>2</sub> and acetate for methanogenesis. Conversely *Methanosaetaceae* is dominant at low temperatures and only uses acetate as a substrate for methanogenesis (Chin et al., 1999). Thus, *Methanosaetaceae* produces less methane compared to *Methanosarcinaceae*. Castro et al. (1995) found that temperature was only effective at controlling methane oxidation at temperatures between -5°C and 10°C and had no influence at temperatures between 10°C and 20°C. Additionally Horz et al. (2005) found that the structure of the methanotrophic community changed, with the relative abundance of Type II methanotrophs decreasing as rainfall and temperature increased. In addition, wetland methane fluxes have been shown to exhibit a seasonal pattern, with higher rates of emissions during the warmer months (Smemo & Yavitt, 2006). Temperature also serves as a proxy for primary productivity and therefore the supply of labile carbon and nutrients that stimulate the methane flux (Turetsky et al., 2014).

#### **2.5.4 Vegetation**

Vegetation in peatlands is a major control on the methane flux as it influences both the production and consumption of methane by (i) supplying carbon substrates that are able to be used by methanogens; (ii) transporting oxygen into anoxic soil layers, thereby allowing methane to be oxidised in the rhizosphere; (iii) transporting methane through aerenchymous tissue, thereby bypassing oxic soil layers; and (iv) some plants such as *Sphagnum* mosses are able to form mutualistic associations with methanotrophic bacteria (Turetsky et al., 2014). Therefore, the type and amount of vegetation present can greatly influence methane emissions from soil.

#### **2.5.5 Soil pH**

Methane consumption can occur under a wide variety of soil pH, with acidophilic methanotrophs functioning at pH down to 3.5 and alkaliphilic methanotrophs functioning at pH up to 9.5 (Dalal et al., 2008). However, it has been observed that



increased soil acidity significantly reduces the rate of methane oxidation (Dalal et al., 2008). Similarly, methane production can occur under a wide variety of soil pH, from pH below 4 to pH above 9 (Chaban et al., 2006). However, the optimum pH range for methane production is 5–7.5, and within this range the methane production is positively correlated with soil pH (Inubushi et al., 2005).

### **2.5.6 Electron acceptors**

Microbial respiration generates energy by the transfer of electrons from an electron donor (substrate) to an electron acceptor (i.e. as organic matter is oxidised to produce chemical energy) (Gao et al., 2019). Electron acceptors include  $O_2$ ,  $NO_3^-$ ,  $Fe^{3+}$ ,  $Mn^{4+}$  and  $SO_4^{2-}$  (Dalal et al., 2008). However, different electron acceptors are not all thermodynamically equal and yield different amounts of energy and therefore microbial respiration follows a sequence that is governed by the energy produced (Knorr et al., 2009). This sequence is oxygen reduction, nitrate reduction, iron reduction, manganese reduction and sulphate reduction (Boyd, 1995). As organic matter decomposition using electron acceptors is thermodynamically more favourable than methanogenesis, the presence of electron acceptors results in a suppression of methanogenesis (Dalal et al., 2008). Under water-logged conditions such as those found in peatlands, oxygen is quickly consumed, and other electron acceptors are reduced allowing methanogenesis to occur (Gao et al., 2019). The decomposition of organic matter using electron acceptors produces  $CO_2$  as an end product, whereas methanogenesis produces methane as an end product (Gao et al., 2019). Thus, the availability of electron acceptors in the soil determines the ratio of  $CO_2$  to  $CH_4$  that is produced. However many studies have found that the concentrations of inorganic dissolved and particulate electron acceptors and their electron accepting capacities were not sufficient to explain the high ratio of  $CO_2$  produced compared to methane (Gao et al., 2019). It was subsequently proposed that peat organic matter may act as an additional organic terminal electron acceptor (TEA) for anaerobic respiration in addition to the inorganic electron acceptors (Gao et al., 2019; Heitmann et al., 2007; Klüpfel et al., 2014). It has been shown that in systems with low concentrations of inorganic TEA's and high organic matter contents such as

peatland ecosystems, organic matter (OM) may be the most important TEA in relation to its capacity to accept electrons (Gao et al., 2019; Keller et al., 2009; Lau et al., 2014). The electron accepting capacity of organic matter (EAC<sub>OM</sub>) is made up of two fractions; the particulate organic matter fraction (EAC<sub>POM</sub>) and the dissolved organic matter fraction (EAC<sub>DOM</sub>) and 26-56% of the non-methanogenic CO<sub>2</sub> formation could be attributed to organic matter, with the majority of EAC<sub>OM</sub> being provided by the particulate fraction (EAC<sub>POM</sub>) (Gao et al., 2019). Therefore, for methanogenesis to occur, anaerobic conditions are required for a prolonged period of time, until all TEA's including organic matter have been sufficiently depleted. (Gao et al., 2019). It should also be noted that within peatlands EAC<sub>OM</sub> and other electron acceptors are able to be periodically regenerated (i.e. re-oxidised) during water table fluctuations (Gao et al., 2019; Klüpfel et al., 2014). Thus, this "redox cycling" of electron acceptors has the potential to suppress methane formation in temporarily anaerobic systems such as drained agricultural peatlands (Klüpfel et al., 2014).

### **2.5.7 Fertiliser / nutrient addition**

Both nitrogen and phosphorus fertilisers have been shown to have a direct effect on the methane production rate in peat soils. For example, Klüber and Conrad (1998) found that the addition of nitrate and its denitrification products (nitrite, NO, N<sub>2</sub>O) resulted in decreased methane production. They found that nitrate, nitrite and N<sub>2</sub>O significantly decreased the partial pressure of H<sub>2</sub>, with nitrate and N<sub>2</sub>O decreasing H<sub>2</sub> concentrations below the threshold of methanogens, thereby reducing and even stopping exergonic<sup>3</sup> methane production (Klüber & Conrad, 1998). Furthermore, the addition of nitrate and N<sub>2</sub>O resulted in increased concentrations of the electron acceptors Fe<sup>3+</sup> and SO<sub>4</sub><sup>2-</sup> (Klüber & Conrad, 1998). Klüber and Conrad (1998) also found that the competition with denitrifiers for H<sub>2</sub> was a significant factor in the inhibition of methanogenesis. In addition, methane consumption can be significantly inhibited by the application of nitrogen fertilisers (Crill et al., 1994). This can be partly explained by NH<sub>4</sub><sup>+</sup> being a competitive

---

<sup>3</sup> Describes a reaction where energy is released (e.g. cellular respiration) (Cammack et al., 2008).

inhibitor of CH<sub>4</sub> monooxygenase, and Liu et al. (2017) showed that the application of NH<sub>4</sub><sup>+</sup> reduced methane oxidation and therefore increased the methane flux. However, some studies have shown that there is no effect of NH<sub>4</sub><sup>+</sup> on methane oxidation or that NH<sub>4</sub><sup>+</sup> actually increases methane oxidation (Jacinthe & Lal, 2006; Kiese et al., 2003; Tate et al., 2006). These inconsistent findings are likely a result of different methanotrophic communities as nitrogen fertiliser application generally inhibits methane oxidation by Type II methanotrophs, but increases methane oxidation by Type I methanotrophs (Dalal et al., 2008). Thus, the co-existence of different methanotrophic communities may reduce the inhibitory effect of NH<sub>4</sub><sup>+</sup> (Dalal et al., 2008). The effect of phosphorus on methane production in peat soils was shown to vary by Adhya et al. (1998) depending on the source of the phosphorus. They found that methane production was stimulated by the addition of K<sub>2</sub>HPO<sub>4</sub> and Jordan rock phosphate and inhibited by the addition of Mussorie rock phosphate and single superphosphate (Adhya et al., 1998). However the addition of K<sub>2</sub>HPO<sub>4</sub> only stimulated methane production in phosphorus deficient soils (Adhya et al., 1998). Their results showed that it was the sulphur content of the phosphorus sources that determined the effect on methane production, with higher levels of sulphur inhibiting methane production (Adhya et al., 1998). This is because sulphate is an electron acceptor that inhibits methanogenesis. Addition of nutrients can also be sourced from the urine and dung of grazing animals (Hahn et al., 2018). The addition of dung to a drained peatland has been shown to increase the methane flux and change the microbial community due to the addition of rumen-associated methanogens (Hahn et al., 2018).

## **2.6 Climate change and methane emissions from drained peatlands**

The effect that global climate change will have on peatland greenhouse gas emissions is a significant problem that is not yet fully understood. The production, consumption and transport of greenhouse gases in peatland systems is a complex series of interactions between microbial communities (e.g. methanogens and methanotrophs), plants and environmental variables (e.g. water table level and temperature). The uncertainty of the peatland response is due to the incomplete

understanding of the combined response of CH<sub>4</sub> and CO<sub>2</sub> fluxes to environmental variables and land use change (Petrescu et al., 2015). Typically, natural peatlands act as a sink of CO<sub>2</sub> and a source of CH<sub>4</sub> (e.g. Urbanová et al., 2013). This is due to an imbalance between photosynthetic uptake and respiration losses within peatlands caused by a high water table leading to anaerobic respiration which proceeds at a slower rate than aerobic respiration and produces CH<sub>4</sub> as the final catabolic product (Boone, 1993; Urbanová et al., 2013). Drainage of peatlands turns them into sources of CO<sub>2</sub> and significantly reduces CH<sub>4</sub> emissions and in some cases turns peatlands into small CH<sub>4</sub> sinks (Urbanová et al., 2013). The predominant factors that are typically assumed to control the fluxes of methane from drained peatlands are the water table level, the temperature and the vegetation composition. It has been extensively shown in the literature that an increase in soil temperature leads to increased methane emissions from peat soils (Frolking et al., 2011). However, there is no clear relationship between the magnitude of temperature increase and the magnitude of increase in the methane flux, and this is reflected in reviews of peatland methane fluxes from a wide variety of climatic conditions (Frolking et al., 2011). The water table level is known to be a strong control on methane emissions from peatlands, with drier conditions leading to a lowered water table and decreased methane emissions and wetter conditions leading to a higher water table and increased methane emissions (Frolking et al., 2011). Furthermore, the water table is also a direct control on the vegetation composition which also impacts the methane flux (Frolking et al., 2011).

Climate change is anticipated to have the largest impact on the near-surface peat zone through changing water table levels and peat temperatures (Glaser et al., 2016). Global climate change models have consistently projected that the temperature will increase by 2-6°C in temperate areas, although predictions vary for changes in the precipitation (Christensen et al., 2007; Flato et al., 2013; Frolking et al., 2011). The predicted impacts of climate change within New Zealand are shown in Figure 2.4.

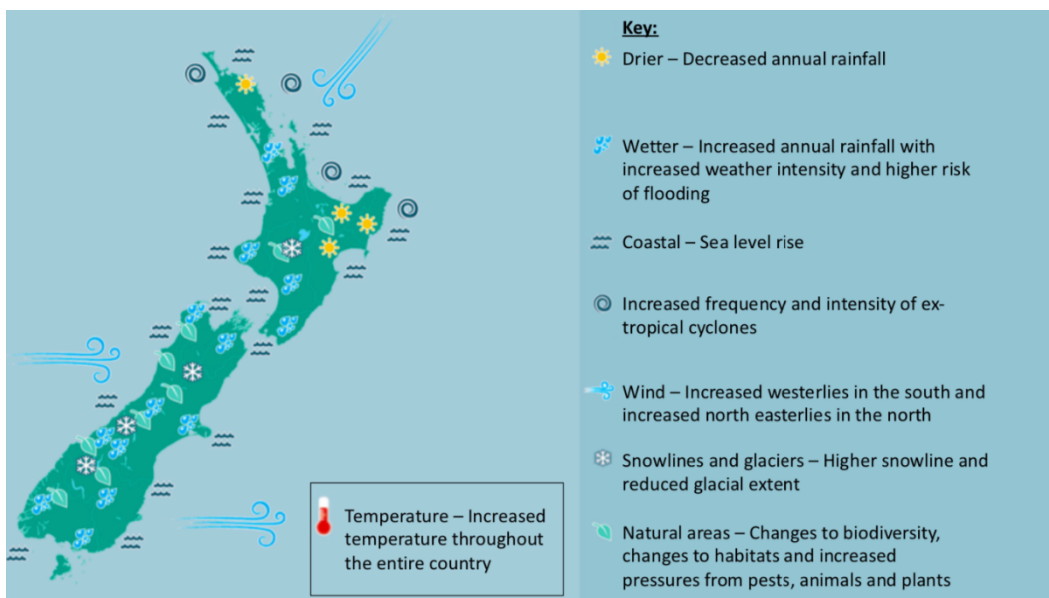


**Figure 2.4** Map of regional climate change impacts in New Zealand [Adapted from: Ministry for the Environment (2017a)].

Overall, New Zealand is likely to experience longer, hotter and drier summers with warmer winters that have more frequent and intense rainfall events (Ministry for the Environment, 2019a). The impact that climate change will have on peatlands is highly uncertain due to the interactive effects of individual impacts and the high rates of climate change predicted for the 21<sup>st</sup> century (Frolking et al., 2011). However, it should be noted that it is likely that drained peatlands will be impacted to a greater amount compared to natural peatlands due to their limited buffering capacity to changes in the water table (Frolking et al., 2011).

## 2.7 Methane measurement methods

The techniques used to measure methane fluxes depend on the goal of the study and the resources available (Topp & Pattey, 1997). In particular, the measurement method depends on the required spatial and temporal coverage, expected magnitude of the methane flux and the required resolution (Topp & Pattey, 1997). Methane measurements can be made at a variety of different spatial and temporal scales, from large-scale global inversion studies of methane emissions to small-scale measurements of individual sources (National Academies of Sciences, 2018). When aiming to measure the methane flux in peat soils, there are a variety of

measurement techniques that can be utilised, although the most commonly used to measure soil methane flux are chambers and eddy covariance (Teh et al., 2011).

### **2.7.1 Incubation**

Incubation is a laboratory-based measurement technique where soil cores taken from the experimental site can be compared under controlled conditions (Topp & Pattey, 1997). Thus, the soil gas flux that is measured from the incubated soil cores are able to give a relative measurement of gas flux between different treatments. This is important when the influence of a single parameter on soil gas flux is being investigated (Oertel et al., 2016). Incubation methods are commonly used due to their low cost, and the high level of control that can be achieved over the experimental conditions (e.g. temperature, light levels, moisture content etc.) (Topp & Pattey, 1997). Additionally, soil incubation methods allow for cumulative measurements (Topp & Pattey, 1997). Incubation methods can either be done with intact soil cores or with sieved homogeneous soil samples (Oertel et al., 2016). Intact soil cores cause minimal disturbances on the soil structure and microbial life, however due to the heterogeneous nature of soil cores, a large sample size is needed (Oertel et al., 2016). Using homogenised soil samples allows the effects of any variable to be seen more easily (Oertel et al., 2016). The main disadvantages of using soil incubation methods is that there is no spatial integration of the samples and there are significant disturbance on the soil samples (Topp & Pattey, 1997).

### **2.7.2 Chambers**

Chambers are one of the most commonly used methods for measuring trace gas fluxes as they are simple to use, portable and are relatively cheap (Denmead, 2008). The general principle of chambers is to restrict the volume of air within which gas exchange can occur by covering a known area of soil with a chamber (Denmead, 2008; Pihlatie et al., 2013). This allows gas exchange between the soil below the chamber and the chamber headspace, thereby changing the gas concentration in the chamber headspace (Pihlatie et al., 2013). The change of gas concentration over time can be precisely measured and a flux can be determined

(Pihlatie et al., 2013). The size of the chambers used can vary dramatically, with the chamber size only limited by practical considerations (McGinn, 2006). Smaller chambers have the advantage of being cheaper, allowing for replicates to be conducted (McGinn, 2006). However, due to their small size they are prone to uncertainty if the source is spatially variable and they therefore require many chamber measurements to determine the average gas flux (i.e. to determine the spatial variability of the methane flux) (McGinn, 2006). Larger chambers can be used to reduce the effect of spatial variability, although as the chamber increases in size the chamber becomes more resource demanding which decreases the amount of replicates that can be conducted (McGinn, 2006).

There are two main types of chambers; flow-through/open chambers and closed chambers. Flow-through chambers require a constant flow of air through the headspace of the chamber allowing a gas flux to be calculated by measuring the difference in concentration between the air entering the chamber and the air leaving the chamber (Denmead, 2008). The flux density,  $F_g$  ( $\text{kg m}^{-2} \text{s}^{-1}$ ) is calculated by:

$$F_g = v(\rho_{g,o} - \rho_{g,i})/A$$

where  $v$  ( $\text{m}^3\text{s}^{-1}$ ) is the volume flow rate,  $\rho_{g,o}$  ( $\text{kg m}^{-3}$ ) is the gas concentration leaving the chamber,  $\rho_{g,i}$  ( $\text{kg m}^{-3}$ ) is the gas concentration entering the chamber and  $A$  ( $\text{m}^2$ ) is the surface area of the chamber (Denmead, 2008). The advantage of using a flow-through chamber rather than a closed chamber is that the increase in the gas concentration within the chamber can be controlled by the volume flow rate, thereby reducing the likelihood of high gas concentrations limiting the gas flux (Denmead, 2008). However, they are disadvantageous when the gas flux is small (Denmead, 2008). Closed chambers have no outside air entering the chamber and measure the gas flux as an increase in concentration over time (Denmead, 2008). The flux is therefore calculated by:

$$F_g = (V/A)d\rho_g/dt$$

where  $F_g$ ,  $\rho_g$  and  $A$  are defined as previously,  $V$  ( $\text{m}^3$ ) is the chamber headspace volume and  $t$  (s) is the time (Denmead, 2008). Closed chambers are typically used over flow-through chambers due to their simplicity and the larger changes in gas concentrations, which are easier to detect (Denmead, 2008). There are two types

of closed chamber; static and dynamic. Static closed chambers have no air circulation between the chamber and a gas sensor and the gas flux is measured by taking regular samples from the chamber headspace over time (Denmead, 2008). Dynamic chambers have a closed loop between the chamber and the sensor and are therefore able to continuously monitor the concentration of gas in the chamber headspace (Denmead, 2008). This allows for the gas concentrations in the chamber headspace to be monitored to prevent the gas flux being inhibited by high gas concentrations (Denmead, 2008).

When calculating a flux from a closed chamber, the change in concentration of the gas of interest over time ( $d\rho_g/dt$ ) is determined. As this increase in concentration within the chamber changes the diffusion gradients between the soil and the chamber headspace, a non-linear increase is expected with a higher rate of change immediately after chamber closure and decreasing over time (de Klein & Harvey, 2015; Hüppi et al., 2018). To account for this non-linearity a number of different models have been developed, all with their own advantages and disadvantages. The conventional methods that are used are linear regression, Hutchinson & Mosier, quadratic regression, non-steady state diffusive flux estimator (NDFE), HMR method and chamber bias correction method (CBC) (de Klein & Harvey, 2015). However, choosing what model to use is challenging as each model has its own bias and variance and there is currently no “perfect” model for all flux applications (de Klein & Harvey, 2015). Linear regression is the most common method to use as it is simple to apply and is the least sensitive to measurement error (de Klein & Harvey, 2015; Forbrich et al., 2010). However, it has been shown to systematically underestimate the true flux (de Klein & Harvey, 2015).

Chamber design is a hotly debated topic, with no clear consensus on a standard method for chamber design and deployment (Pihlatie et al., 2013; Rochette, 2011). Using a chamber to measure soil gas flux has inherent biases that need to be minimised (Rochette, 2011). The use of chambers can disturb the soil and have effects on the soil moisture, soil temperature, pressure, humidity and therefore on the soil gas flux (Parkin & Venterea, 2010; Rochette, 2011). Parkin and Venterea (2010) recommend that chambers be constructed out of two parts; a permanent



anchor / collar and a flux chamber cap. The chamber should be constructed out of non-reactive and reflective / white materials such as PVC, stainless steel or aluminium (Parkin & Venterea, 2010). Parkin and Venterea (2010) state that the chamber should cover at least 182 cm<sup>2</sup>, and recommend using a circular chamber with a diameter of 20 cm (314 cm<sup>2</sup>) (Parkin & Venterea, 2010). The chamber should contain a vent tube (at least 10 cm long and 4.8 mm in diameter) to minimise pressure changes in the chamber, and a sampling port to remove samples (Parkin & Venterea, 2010).

When using a chamber to take gas flux measurements, the collars should be installed at least 8 cm deep and extend no more than 5 cm above the ground surface (Parkin & Venterea, 2010). Due to soil disturbances the collar should be installed at least 24 hours before the first flux measurement (Parkin & Venterea, 2010). To measure the soil gas flux, the chamber should be closed for a maximum of 60 minutes, with at least 3 samples taken at regular time intervals (e.g. 0, 30, 60 min or 0, 20, 40 min) (Parkin & Venterea, 2010). However, Rochette (2011) states that at least 4 samples should be taken and that the first sample (time = 0) should be taken from the chamber rather than assuming it is equal to the ambient air concentrations. Additionally, Rochette (2011) recommends that chambers be closed no longer than 30 minutes as errors associated with the chamber environment and leakage increase with time. The volume of the sample removed is dependent on the gas analysis that will be used, although the volume is typically in the range of 5-30ml (Parkin & Venterea, 2010).

When measuring gas fluxes from water surfaces, a floating chamber should be used and measurements made while the chamber is floating freely with the water (International Hydropower Association, 2010). This is because fixing the chamber in place can result in turbulence being artificially enhanced by the friction between the chamber walls and the water leading to significant overestimates of the gas flux (International Hydropower Association, 2010). In addition, the turbulence can be increased by the chamber wall sitting flush with the water's surface (Matthews et al., 2003). Thus, best practice is to have the chamber's wall extending below the

water's surface as chambers that sit flush with the water's surface have been found to increase the measured gas flux by up to 3-5 times (Matthews et al., 2003).

The advantages and disadvantages of the chamber method for measuring gas fluxes are summarised in Table 2.2.

**Table 2.2** Advantages and disadvantages for measuring soil gas fluxes [Adapted from Denmead (2008); Topp and Pattey (1997)].

<b>Advantages</b>	<b>Disadvantages</b>
<ul style="list-style-type: none"> <li>• Simple, low cost, portable and easy to use</li> <li>• They do not require large experimental sites</li> <li>• Can be highly sensitive</li> <li>• Allows for multiple replicates</li> <li>• Can measure very small flux</li> <li>• No or low electrical supply required</li> </ul>	<ul style="list-style-type: none"> <li>• High gas concentrations in the chamber headspace may influence gas fluxes</li> <li>• Pressure differences inside and outside the chamber can influence the gas fluxes</li> <li>• Initial soil disturbance</li> <li>• Needs multiple replicates due to small surface area if source is spatially variable</li> <li>• Labour intensive</li> <li>• Enclosures can affect the microclimate</li> <li>• Some gas fluxes have different emission cycles, therefore measurements should be taken at various times of the day / night</li> </ul>

### 2.7.3 Eddy Covariance

Eddy covariance is a micrometeorological technique that is used to measure the gas flux to or from a surface (McGinn, 2006). Micrometeorological methods utilise the measurement of moving air masses (eddies) over ecosystems to determine the gas flux (Dalal et al., 2008). The principle behind the eddy covariance method is that the vertical flux of a gas can be represented as the covariance of the vertical wind velocity and the gas concentration hence the vertical flux density ( $F_g$ ) of a gas can be calculated by:

$$F_g = \overline{\rho w' s'}$$

where  $\bar{\rho}$  is the dry air density  $\bar{w}$  is the vertical wind speed,  $\bar{s}$  is the scalar mixing ratio (i.e. the dry mole fraction of the gas of interest in the air) and the overbar indicates time averaging (Burba, 2013; Paw et al., 2000).

Eddy covariance measurements are typically collected within the surface boundary layer at frequencies of 10 Hz or higher (Denmead, 2008; Foken et al., 2012). It is assumed that the fluxes are constant within the surface boundary layer and therefore the measurements collected are representative of the fluxes from the underlying ground surface (Foken et al., 2012). The average flux density is then calculated over the sampling period, which is typically 30 minutes (Burba, 2013). The vertical wind speed is typically measured with a 3-D sonic anemometer and gas concentrations are typically measured with fast-response gas analysers (Denmead, 2008). The flux footprint of an eddy covariance tower is the area where the measured gas fluxes originate (i.e. fluxes generated in this area are registered by the instruments on the eddy covariance tower) (Burba, 2013). The flux footprint area is dependent on the tower height, the surface roughness and the atmospheric thermal stability (Burba, 2013). In general, an increase in tower height, a decrease in surface roughness or a higher thermal stability will result in a larger flux footprint (Burba, 2013). For a forest system the flux footprint is typically 2-3 km<sup>2</sup> and for a grassland or cropland system the flux footprint is several hectares (Dalal et al., 2008). This is primarily because for a forest system, the eddy covariance tower is set at a higher height compared to a grassland system (Burba, 2013).

There are a variety of different designs for eddy covariance towers, instrument configuration and tower location (Munger et al., 2012). However, the design used is typically a balance between the needed precision / accuracy and the lowest cost (Munger et al., 2012). In general, the ideal eddy covariance system is located in an area that has flat and even terrain, a uniform source/sink strength and a short roughness length (Munger et al., 2012). Additionally, the tower should be placed in a position that maximises the exposure time of the land surface being measured, with the upwind fetch as long as possible (Munger et al., 2012).

The biggest advantage of using eddy covariance over other micrometeorological techniques such as relaxed eddy accumulation or flux gradient methods is that it is a direct measurement of the vertical flux at the measurement point and it therefore does not require the same simplifying assumptions that other micrometeorological techniques do (Denmead, 2008). In addition, the eddy covariance method does not cause any disturbances to the soil or ecosystem (e.g. plants). Other advantages include the high temporal resolution, the reliability and repeatability of the results (Burba, 2013). However, eddy covariance requires a relatively large and homogeneous surface to measure the gas flux from (Munger et al., 2012; Topp & Pattey, 1997). Other disadvantages include the high cost and complexity of the system (Topp & Pattey, 1997).

Traditionally eddy covariance measurements integrate fluxes across the entire flux footprint as it is assumed that the flux footprint is homogenous (Wall et al., 2019). However, this presents a problem within agricultural systems where the flux is integrated across several paddocks wherein each paddock can have different paddock-scale management regimes even though they have the same land use (Wall et al., 2019). This is primarily caused by minor differences in management practices such as variation in the timing, duration or stocking density of grazing (Wall et al., 2019). This therefore violates the assumption that the eddy covariance source area is homogenous and can lead to skewed integrated fluxes as measurements made by the eddy covariance tower are dominated by the paddocks closest to it (Wall et al., 2019). However, footprint analysis can be used to calculate the fraction of the measured flux derived from a defined area and can therefore provide estimates of the fluxes derived from each paddock (Wall et al., 2019). The measurement of paddock scale fluxes has several advantages; (a) the integrated signal from multiple paddocks can be separated and thus different management effects identified; (b) the influence of spatial variability of the fluxes can be limited and (c) the ability to calculate separate fluxes from two adjacent paddocks allows an experimental design where one variable can be measured against a control in adjacent paddocks with one eddy covariance tower (Wall et al., 2019).



# Chapter Three

## Site description

---

The study was carried out on Gamma Farm, a pastoral dairy farm under rotational grazing. Gamma Farm is approximately 330 ha in area and is located on the remnants of the Moanatuatua peatlands approximately 20 km southeast of Hamilton, New Zealand (Figure 3.1). Approximately 1000 cows are grazed in three herds of approximately 330 cows each, with each field grazed 8 – 10 times per year. Approximately 130 kg-N ha<sup>-1</sup> yr<sup>-1</sup> is applied in the form of urea.

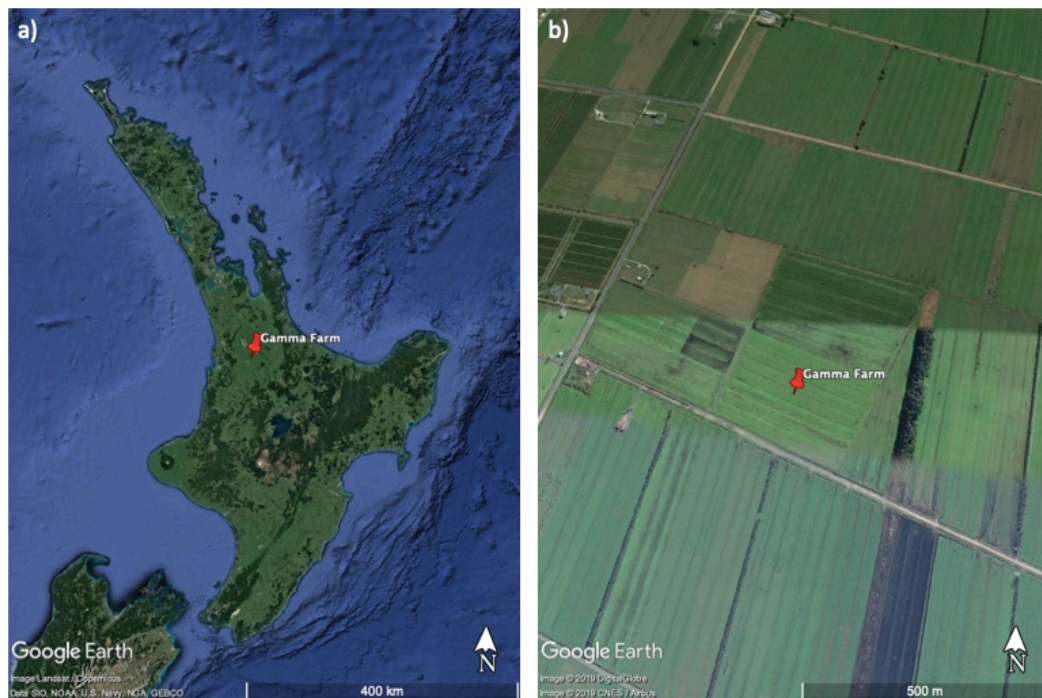


**Figure 3.1** Location of Gamma Farm: (a) in relation to the North Island of New Zealand and; (b) showing the location of the study site, a pair of paddocks within Gamma Farm [Source: Google Earth (2019)].

Within the Hamilton basin peatlands began to form approximately 14,000 years ago on impervious pumiceous silt that had accumulated between the levées of paleochannels of the Waikato River and the surrounding hills and between the levées of roughly parallel paleochannels (McCraw, 2011). This resulted in a poorly drained and swampy environment perfect for peat formation (McCraw, 2011). Within these areas peat began to form as conditions at the time were particularly

favourable for peat formation with increased net rainfall and a warming climate (McCraw, 2011). This led to the formation of the Moanatuatua peatland which is classified as an oligotrophic raised bog and in its original state once covered an estimated 8,500 ha , although the majority of this has now been drained and converted into pasture (Environment Waikato, 2006; Pronger et al., 2014). Drainage began in the late 1800s to early 1900s, although intensive drainage efforts did not begin until the late 1950s (Pronger et al., 2014). Currently, only two small remnants of the natural peatland remain. The Moanatuatua peatland has two main soil types; the Motumaoho series (NZSC: Mellow Humic Organic Soils) which typically occurs on shallow peat deposits (<1m) and the Kaipaki series (NZSC: Mellow Mesic Organic Soils) which occurs on deeper peat deposits (>1m) (Pronger et al., 2014).

The study site at Gamma Farm consists of two paddocks (total area is 7.8 ha) which are drained by a series of shallow “spinner” drains that discharge water into deeper “border” drains (Figure 3.2).

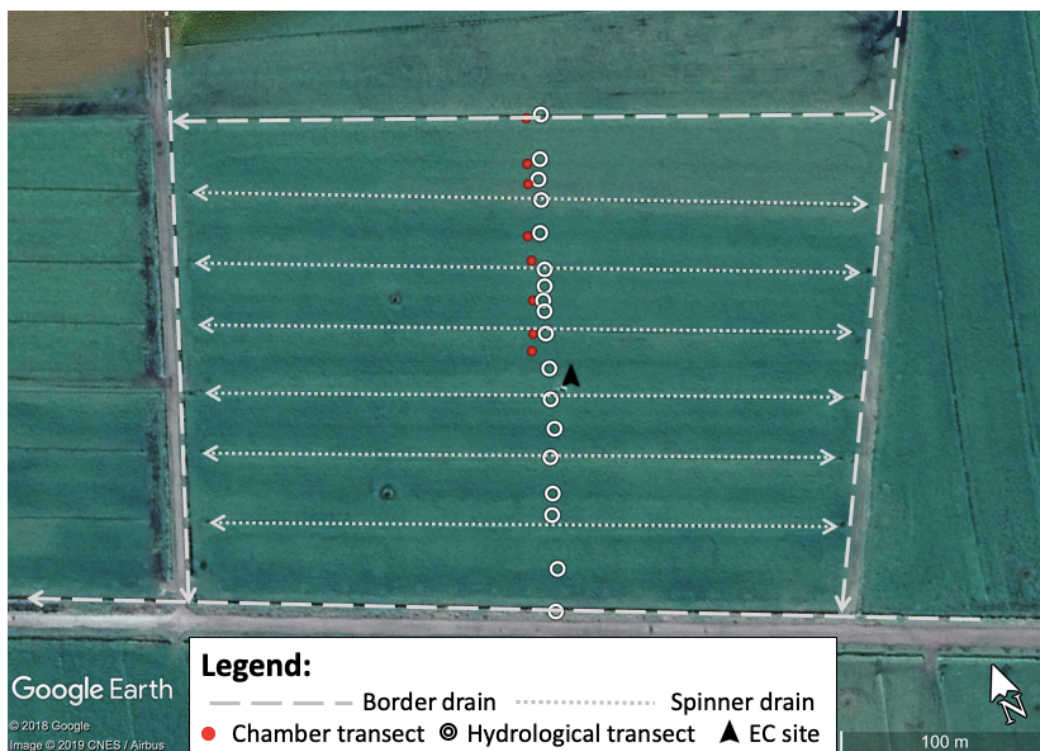


**Figure 3.2** Features of the study site, showing the location of the shallow “spinner” drains and deeper “border” drains. Arrows indicate flow direction. Also shown is the location of the chamber and hydrological dip-well transect and eddy covariance flux tower [Adapted from: Google Earth (2019)].

In 1978 the peat depth of the Moanatuatua peat bog was measured to be a maximum of 11.5 m thick and a mean of 4.1 m thick (Davoren, 1978; Pronger et al., 2014). Recent measurements show that the peat depth at Gamma Farm is currently approximately 7 m thick. The pasture is predominantly composed of perennial ryegrass (*Lolium perenne L.*) and white clover (*Trifolium repens L.*). The climate at Gamma farm was approximated using nearby weather stations. Cambridge weather station was used for rainfall (approximately 10 km away) and Hamilton weather station (approximately 20 km away) was used for temperature. The long term annual temperature (1981 – 2010) is 13.8°C and the long term annual rainfall (1981 – 2010) is 11,167.39 mm (NIWA, n.d.).





# Chapter Four

## Methane emissions from a drained peatland under dairy grazing

---

### 4.1 Introduction

Methane is a greenhouse gas that has a global warming potential 28 times higher than CO<sub>2</sub> and is the second most important anthropogenic greenhouse gas behind CO<sub>2</sub> (IPCC, 2014b).. Atmospheric concentrations of methane have been steadily rising since pre-industrial times to over 1858.6 ppb today (Dlugokencky, 2019; Prather & Holmes, 2017). Natural peatlands act as a sink for atmospheric CO<sub>2</sub> and as a source of methane due to their high water tables and anaerobic conditions (Kroon et al., 2010). However, large areas of natural peatlands have been drained primarily for agriculture, forestry or peat extraction (Hatala et al., 2012). When a peatland is drained, the water table is lowered and this results in the peatland changing to a significant source of CO<sub>2</sub> and having significantly reduced methane emissions or even having a small net uptake of methane (Hahn et al., 2018). Drained peatlands are complex ecosystems with methane emitting “hot and cold spots”, due to their variable water table depth as a result of flooded drainage ditches (Baldocchi et al., 2012). However, New Zealand does not report methane emissions from drained peatlands as it is assumed that methane emissions are negligible (Ministry for the Environment, 2018). There are a limited number of studies that have investigated methane emissions from drained peatlands, and the few that have been published have been focused in the Northern Hemisphere.

The aim of this study was to determine the magnitude of methane emissions from a drained peatland under dairy grazing and where and when do the emissions occur throughout the year. In order to achieve this aim, the objectives of this study were to:

- (1) Use static closed chambers to identify methane emission hotspots linked to the location and hydrology of drainage ditches and to cow dung patches;
- (2) Determine the effect of soil physical and chemical properties on methane fluxes. The measured properties were soil temperature, soil pH, water table depth, soil moisture content, bulk density, ammonium concentration, nitrate concentration and Olsen-P;
- (3) Determine the effect of the physical and chemical properties of drainage ditch water on methane fluxes. The measured properties were pH, dissolved oxygen, electrical conductivity, water temperature, water depth, nitrate concentrations and dissolved phosphorus;
- (4) Use eddy covariance to determine annual and seasonal methane fluxes;
- (5) Estimate the net annual methane flux using eddy covariance and compare it to the default IPCC emission factor for drained peatlands. In addition, the impact of these fluxes on New Zealand's greenhouse gas inventory was explored in relation to New Zealand's annual agricultural emissions and total annual methane emissions.

## 4.2 Methods

### 4.2.1 Chamber measurements of methane fluxes

Static closed chambers were used to determine the spatial and temporal variation in methane fluxes across the field site, in particular across the different peatland landforms. The study site was classified into four distinct landform types that represented the dominant features of the peatland. These landforms were categorised as: drainage ditch; ditch edge; slope and crown (Figure 4.1).

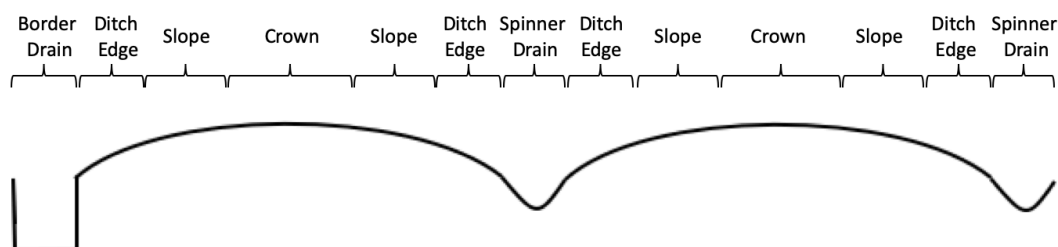


**Figure 4.1** Diagram of the dominant landforms at the study site

Crown landforms are typically the highest areas of the paddock and have a slight convex shape with little slope. Slope landforms are defined as the areas downslope from the crown landform and connect them with the lower topographical features such as drainage ditches and are characterised by their gentle slope. The ditch edge is defined as the land immediately adjacent to the drainage ditch which is subjected to the hydrological effects of the drainage ditch. The drainage ditch is a man-made feature that is typically used to lower the water table within the peatland to below the plant rooting zone in order to improve plant growing conditions. Over the study period the water level within the drainage ditches varied and during the dry periods over summer dropped below the bottom of the drainage ditches. The drainage ditch landform at Gamma farm consisted of two drainage ditch types; shallow “spinner” drains and deeper “border” drains.

Chamber measurements were taken in a transect that was set out approximately perpendicular to the drainage ditches (Figure 3.2). Chambers were placed such that they were representative of the dominant landform features (drainage ditch, ditch edge, slope and crown). The transect covered the entire study site and provided a general overview of methane fluxes from the different peatland landforms. Within the transect, an additional two chambers were used as “free” chambers that were placed in areas identified as possible methane emission “hotspots” (e.g. over cow dung). Sampling was undertaken in seven campaigns between March 2019 and September 2019. Measurement campaigns were situated to capture a wide variety of environmental conditions throughout both summer and winter.

The chambers that were used in this study had been designed and used for N<sub>2</sub>O flux measurements, hence were designed in accordance with the guidelines for N<sub>2</sub>O flux measurements set out in de Klein and Harvey (2012). The chambers consisted of a stainless-steel collar and an opaque cylindrical PVC chamber that was 0.213 m high and 0.24 m in diameter and covered a soil area of 0.0452 m<sup>2</sup>. The collars were inserted approximately 0.15 m into the soil such that the collar rim sat level and flush with the ground. As Gamma Farm is an operational dairy farm, the collars were not able to be installed permanently, and were instead

installed at least 48 hours in advance of flux measurements. Collars were used on land and within the drainage ditches when the ditch water level was sufficiently low (<10 – 15 cm). When the ditch water level was higher than 10 – 15 cm, a floating chamber was used. Floating chambers were constructed by attaching polystyrene floats to the chambers such that the bottom of the chamber extended into the water by approximately 3 cm. The chambers were modified to include a vent tube in order to equalise the pressure between the chamber headspace and the ambient air (Figure 4.2). Based on an extensive literature search, the best practice for chamber design is to include the use of a mixing system (e.g. a small fan or gas manifold) within the chamber. However, we opted not to include any mixing system within our chambers because of the added complexity. However, we believe the un-mixed chambers still provide an adequate point of comparison to other studies as many studies do not include mixing systems within their chambers (e.g. Beetz et al., 2013; Berglund, 2011; Cooper et al., 2014; Eickenscheidt et al., 2015; Green et al., 2018; Lazar et al., 2014; Minkinen & Laine, 2006; Naser et al., 2018; Teh et al., 2011).



**Figure 4.2** Chambers installed on collars for methane flux measurements in (a) soil (b) shallow standing water and (c) a floating chamber.

During measurements, chambers were sealed by fitting them into the water-filled rim of the collar and gas fluxes were calculated from four measurements across a 45-minute chamber closure time (0, 15, 30 and 45 minutes). All measurements were taken during daytime between 9am and 3pm. A 50 ml syringe was used to

take a 50ml gas sample from the chamber headspace before a needle was attached and 35 ml of the sample was discharged to remove any air present in the needle. The remaining 15 ml of sample was then injected into pre-evacuated glass vials. Samples were analysed the same day using a continuous wave quantum cascade laser (CW-QCL) installed as the eddy covariance N<sub>2</sub>O/CH<sub>4</sub>/H<sub>2</sub>O scalar analyser at the Gamma Farm site. When injecting samples into the CW-QCL the air intake was switched from the eddy covariance flux tower to an injection line. The injection line consisted of a methane free carrier gas (N<sub>2</sub>), a 0.45 µm filter (to prevent over-pressurising the system from the carrier gas) and an injection port. During injections the flow rate was adjusted to 4 - 6 L min<sup>-1</sup>, while the CW-QCL optical cell pressure was maintained at 30 Torr. An insulin syringe was used to inject three 1 ml samples into the CW-QCL. A full standard line consisting of 0.5 ml, 0.6 ml, 0.7 ml, 0.8 ml, 0.9 ml, 1 ml, 2 ml, 3 ml, 5 ml and 10 ml samples of known methane concentration were injected into the CW-QCL at the beginning and end of sample injections. In addition, 1 ml and 5 ml standards were injected after each set of chamber samples. The peak area of each injection was calculated by integrating the area under the peak. A regression relationship for peak area versus methane concentration (calculated from the standard line) was used to convert the peak area of each injection to methane concentration (ppm). Methane concentrations were converted to mass units using the ideal gas law.

$$m_{CH_4} = \frac{C_{CH_4} \times M \times P \times V}{R \times T}$$

where  $m_{CH_4}$  is the mass of methane (µg),  $C_{CH_4}$  is the concentration of methane (ppm),  $M$  is the molecular weight of methane (16.04 g mol<sup>-1</sup>),  $P$  is atmospheric pressure (Pa),  $V$  is the chamber enclosure volume (m<sup>3</sup>),  $T$  is the temperature (K) and  $R$  is the universal gas constant (=8.3143). The methane flux was then calculated by:

$$F_{CH_4} = \frac{dm_{CH_4}}{dt} / A$$

where  $F_{CH_4}$  is the methane flux (µg CH<sub>4</sub> m<sup>-2</sup> min<sup>-1</sup>),  $A$  is the chamber cross-sectional area of the chamber (m<sup>2</sup>) and  $\frac{dm_{CH_4}}{dt}$  is the slope of the change in methane concentration over time. The slope was calculated using linear least squares regression and data were accepted if  $R^2 > 0.7$ . However, when the fluxes were

close to zero, lower  $R^2$  values were common, and fluxes were still deemed acceptable if, upon visual inspection of the slope, a linear trend was clearly evident. Data were only rejected if the relationship was clearly non-linear and the y-intercept was not close to zero.

#### **4.2.2 Soil physical properties**

Soil temperature, water table depth, soil moisture content, bulk density and porosity were measured for each chamber location. Soil temperature was measured before and after the chamber measurements to a depth of 5 cm using a Dostmann P700 thermometer. The water table depth at each chamber site was approximated using a transect of dip-wells that ran parallel to, and approximately 7 m from, the chamber transect (Figure 3.2). Soil volumetric moisture content and bulk density were calculated by drying a soil core of known volume (6.45 cm diameter, 7 cm height, 228.72 cm<sup>3</sup>) at 100°C for 48 hours and recording the weight before and after drying (Figure 4.3a). The soil core was taken from within each chamber collar at the conclusion of the flux measurements. The porosity was calculated by saturating eight soil cores of known volume (6 cm diameter, 5 cm height, 141.37 cm<sup>2</sup>) collected across the field site and drying them at 100°C for 72 hours and recording the weight before and after drying. Soil cores were saturated by placing them in a tray filled with water and leaving them for 72 hours.

#### **4.2.3 Soil chemical properties**

The soil pH, nitrate concentration, ammonium concentration, Olsen-P and total carbon and nitrogen were measured for each chamber. At the conclusion of the flux measurements, six small soil cores (approximately 39.27 cm<sup>3</sup>) were taken from within each chamber collar and bulked together (Figure 4.3b). The bulked soil cores were passed through a 2 mm sieve and a 2 M KCl soil extraction was performed on the fresh soil within 24 hours of collection for ammonium and nitrate analysis. The remaining sieved soil was then air dried for 72 hours for pH and Olsen-P analysis. Ammonium concentrations were determined by colorimetric analysis as described in Baethgen and Alley (1989). Nitrate concentrations were measured using ion chromatography. Total carbon and

nitrogen were measured using stable isotope analysis. pH was measured using a H<sub>2</sub>O suspension as described in Blakemore et al. (1987). Olsen-P was measured using a 0.5 M NaHCO<sub>3</sub> soil extraction as described by Olsen et al. (1954), followed by colorimetric analysis based on the method described by Murphy and Riley (1962).



**Figure 4.3** Soil cores: (a) large volumetric soil core used for soil physical property analysis and (b) small soil core used for soil chemical property analysis.

#### **4.2.4 Water analysis**

When the chambers were placed within standing water the water was analysed for temperature, dissolved oxygen, electrical conductivity and pH using an xplorer GLX (PASCO Scientific, Roseville, CA) at the conclusion of the flux measurements. The xplorer GLX was calibrated for dissolved oxygen and pH on each sampling date. A water sample was taken from inside the chamber collar or adjacent to the floating chamber at the conclusion of the chamber sampling. Nitrate concentration and Olsen-P analysis on the water samples was made using the methods outlined above (section 4.2.3).

#### **4.2.5 Spatially integrated methane fluxes**

The area of the different landforms was calculated through the use of a GPS survey outlining the study area boundary and drainage ditch lengths; a peat surface



elevation transect and field measurements of the drainage ditch widths. The GPS survey was analysed using ArcGIS software and the peat surface elevation data was analysed using MATLAB. Net methane fluxes for the study site were calculated for each chamber sampling date. For each sampling date the individual chamber measurements from each landform were averaged. The average landform flux for each chamber sampling date was weighted by the total landform area and summed to determine the net methane flux for the study site.

#### **4.2.6 Eddy covariance**

An eddy covariance flux tower was used to determine the 30-minute, daily, seasonal and annual methane fluxes from the study site. The eddy covariance tower was placed along the fence line between the two study site paddocks. The eddy covariance tower was placed in a strategic location such that the dominant wind direction maximises exposure to the study area. A range of sensors were used to record environmental variables and record them onto dataloggers as 30-minute averages or totals. Environmental variables that were measured include air temperature and relative humidity, soil temperature and volumetric moisture content at 10 cm soil depth, rainfall, down-welling and up-welling longwave and shortwave radiation, net radiation and soil heat flux at 8 cm soil depth. The eddy covariance measurements were made using a 3-D sonic anemometer (CSAT3B, Campbell Scientific, Logan, UT) to measure sonic temperature and 3-dimensional wind speed components and a continuous-wave quantum cascade laser absorption spectrometer (CW-QCL, Aerodyne, Billerica, MS) to measure atmospheric CH<sub>4</sub>, N<sub>2</sub>O, and H<sub>2</sub>O. Measurements were made at a height of 2 m at a frequency of 10 Hz and fluxes were computed over 30-minute intervals. The CW-QCL was run in a temperature-controlled housing that typically kept the instrument within  $\pm 0.1^{\circ}\text{C}$  (30-minute mean) of a set temperature as the CW-QCL requires a stable temperature to operate. Air samples pass through the CW-QCL at a rate of 15 L min<sup>-1</sup>. A detailed description of the eddy covariance system installed at the study site can be found in Liang et al. (2018) and Wecking et al. (2020). Note that the design of the EC system at the study site was only slightly modified from the system described in Liang et al. (2018) and Wecking et al.

(2020). The half-hourly eddy covariance flux data were filtered to remove poor quality methane flux measurements such as those made when cows were present in the study paddocks, the wind was blowing over the CW-QCL enclosure and when the developed turbulence (friction velocity) was below  $0.15 \text{ ms}^{-1}$ . In addition, all methane fluxes above an arbitrary limit of  $10 \text{ mg CH}_4 \text{ m}^{-2} \text{ h}^{-1}$  were removed. This limit was chosen because the vast majority of the measured methane fluxes were below  $3 \text{ mgCH}_4\text{m}^{-2}\text{h}^{-1}$ , hence we determined any flux measurement above  $10 \text{ mgCH}_4\text{m}^{-2}\text{h}^{-1}$  were more likely to be affected by distant cow emissions, or erroneous, than not. Due to the similarity of methane fluxes throughout the year, the annual net methane emission was calculated as the mean value of the daily mean of valid 30-minute methane fluxes.

## 4.3 Results

### 4.3.1 Climate / hydrological setting

Monthly air temperatures were generally close to the long-term normal temperature (Figure 4.4). However, over the summer period (December to March), monthly average temperatures were slightly higher than normal by  $0.8 - 1.7^\circ\text{C}$ .

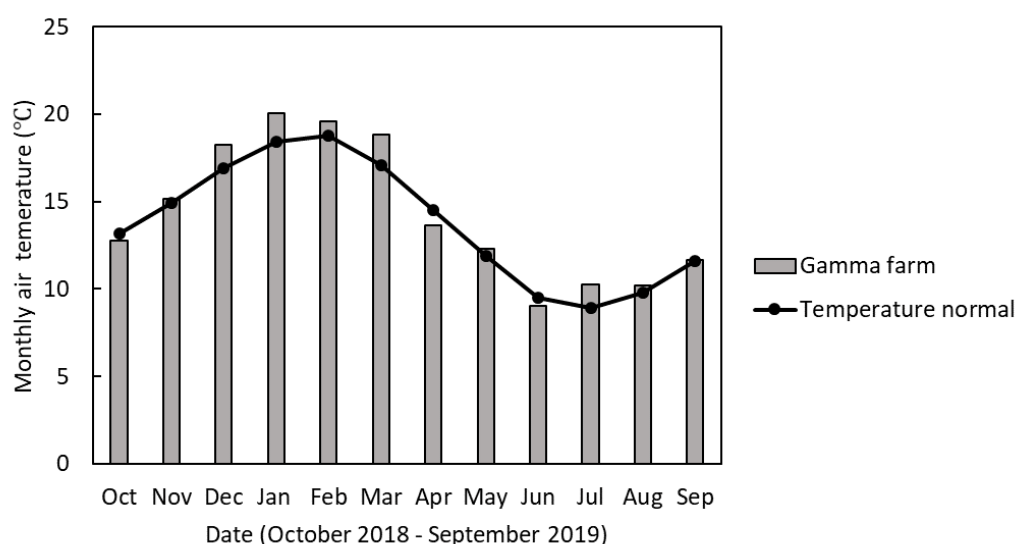


**Figure 4.4** Monthly average air temperature from October 2018 to September 2019. Also shown are the monthly temperature normal, measured in Hamilton over the period 1981 – 2010 [Source: NIWA (n.d.)].

The amount of rainfall deviated considerably from the long-term normal pattern (Figure 4.5). In December 2018, the monthly rainfall was 282.3 mm, which is significantly higher than the long term normal of 105.8 mm (266% of the normal December rainfall). As a result of the high rainfall in December, the water table rose to a maximum level of approximately -70 mm relative to the soil surface (Figure 4.6). However, the amount of rainfall that occurred from January to June was lower than normal (Figure 4.5). Over this period, the rainfall was 55% of the normal rainfall amount. The rainfall then increased from July when the rainfall returned to normal or greater than normal levels.

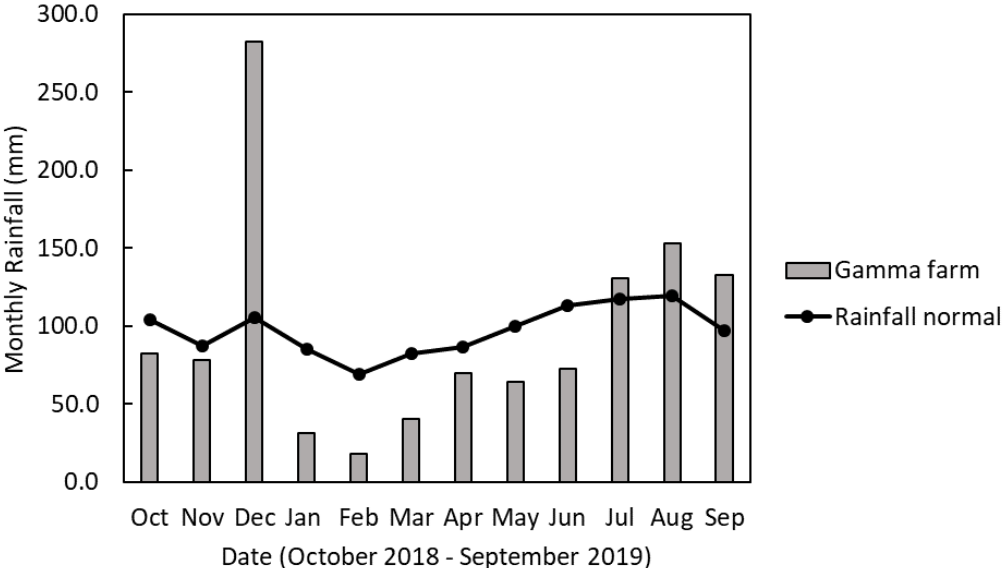


**Figure 4.5** Monthly total rainfall from October 2018 to September 2019. Also shown is the monthly rainfall normal, measured in Cambridge over the period 1981 – 2010 [Source: NIWA (n.d.)].

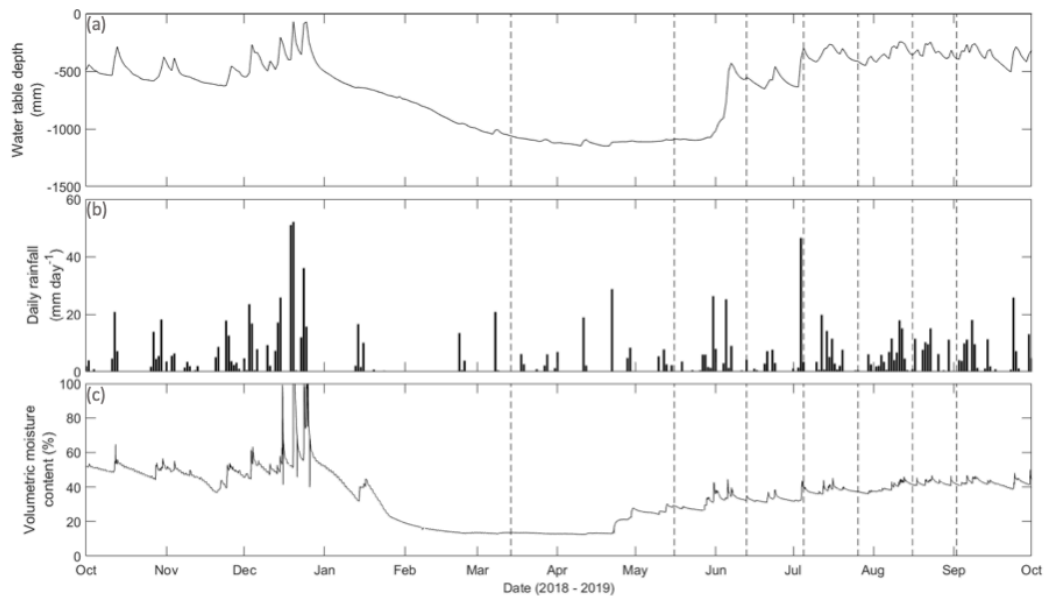


**Figure 4.6** Water table depth (a), daily rainfall (b) and soil volumetric moisture content (c) at 10 cm depth. Vertical lines represent the chamber sampling dates.

This long period of dry weather over summer and autumn led to a significant drawdown of the water table depth, with the depth to the water table continuing to increase over early autumn, peaking mid- to late-April (Figure 4.6). Over late autumn there was a very slight decrease in the depth to the water table. However, the water table showed no meaningful change until early June when it “stepped” up after a period of rain in late May / early June. Over the subsequent winter months (June – August) there was a general decrease in the depth to the water table. The soil volumetric moisture content followed the same general pattern as the water table depth, decreasing over summer and autumn, before increasing in winter. However, the volumetric moisture content dropped to a minimum in February and remained constant over the autumn period, in contrast to the water table, which was continually dropping. In addition, the volumetric moisture content began to recover from late-April with more frequent rainfall, in contrast to the water table, which did not start to recover until June.

### 4.3.2 Soil characteristics

Soil bulk density was found to vary between the different landforms. The crown and slope landforms had a soil bulk density ( $\pm$  standard error of the mean) of  $0.31 \pm 0.01$  and  $0.31 \pm 0.004$  g cm<sup>-3</sup> respectively, while the ditch edge and floor of the

drainage ditch had bulk densities of  $0.27 \pm 0.01$  and  $0.16 \pm 0.02$  g cm<sup>-3</sup> respectively (Table 4.1).

**Table 4.1** Soil bulk density of the different landforms. Sampling depth was 8cm.

	Bulk density (g cm <sup>-3</sup> )	n
Crown	$0.31 \pm 0.01$	18
Slope	$0.31 \pm 0.004$	18
Ditch Edge	$0.27 \pm 0.01$	12
Drainage Ditch	$0.16 \pm 0.02$	5

In addition, the soil organic matter fraction was found to be  $87.6 \pm 0.6\%$  while the total carbon and total nitrogen were  $48.0 \pm 1.1$  and  $2.3 \pm 0.1\%$  respectively, with C:N ratio 21:1. Total porosity was measured to be  $78.3 \pm 0.7\%$ .

### 4.3.3 Temporal variation in the methane flux

There were six main chamber campaigns between March and September 2019, plus one campaign dedicated to measuring the spatial variation in methane fluxes from the drainage ditches on 16 August 2019. Figure 4.7 shows the average methane emission for each peatland landform for each sampling campaign.

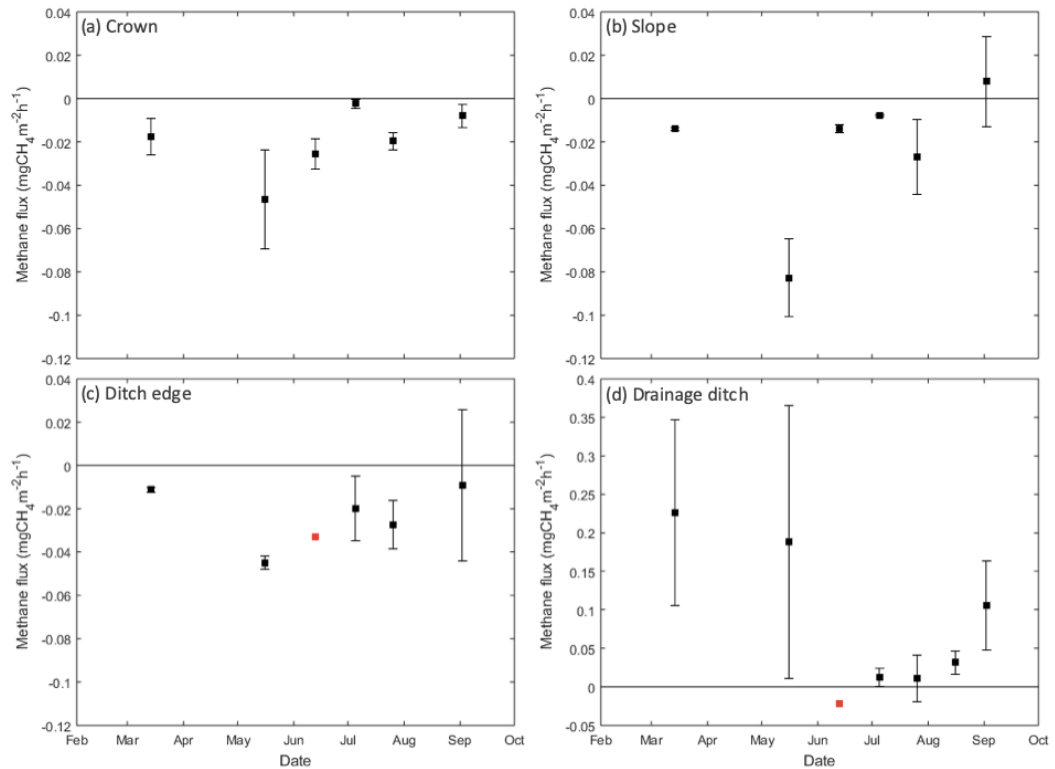


**Figure 4.7** Temporal variation in net methane fluxes from (a) crown (b) slope (c) ditch edge and (d) drainage ditch landforms. Error bars show the standard error of the mean, which was calculated where  $n \geq 2$ . Red points indicate values where  $n=1$ . Note that (d) has a different y-axis scale.

Over the course of the sampling period the slope, crown and ditch edge microforms generally had net negative fluxes, except for 2 September when the individual methane fluxes from the slope landform ranged from  $-0.023 - 0.047$  mg CH<sub>4</sub> m<sup>-2</sup> h<sup>-1</sup> and the net flux was  $0.008 \pm 0.021$  mg CH<sub>4</sub> m<sup>-2</sup> h<sup>-1</sup>. All of the different microforms follow the same general pattern, wherein the fluxes were at a minimum in May / June and subsequently increased over time. The first two sampling dates (14 March and 16 May 2019) had significantly different climatic setting compared to all of the later chamber measurements. This is highlighted by Figures 4.4 and 4.6 which show that during these two chamber sampling campaigns soil temperatures were higher, the water table was lower and VMC was lower. The later methane flux sampling dates occurred with lower temperatures and wetter conditions (Figure 4.6). Additionally, for the first two sampling dates there was no water within the drainage ditches (i.e. the water table was below the bottom of the drains). For all subsequent measurements there was water present

in the drains. Hence, the highest methane fluxes occurred when standing water was not present in the drains.

#### 4.3.4 Spatial variation in the methane flux

Methane fluxes across the different peatland landforms were found to be relatively low with the crown, slope and ditch edge landforms primarily having negative fluxes in contrast to the drainage ditches which primarily had positive fluxes (Figure 4.8).

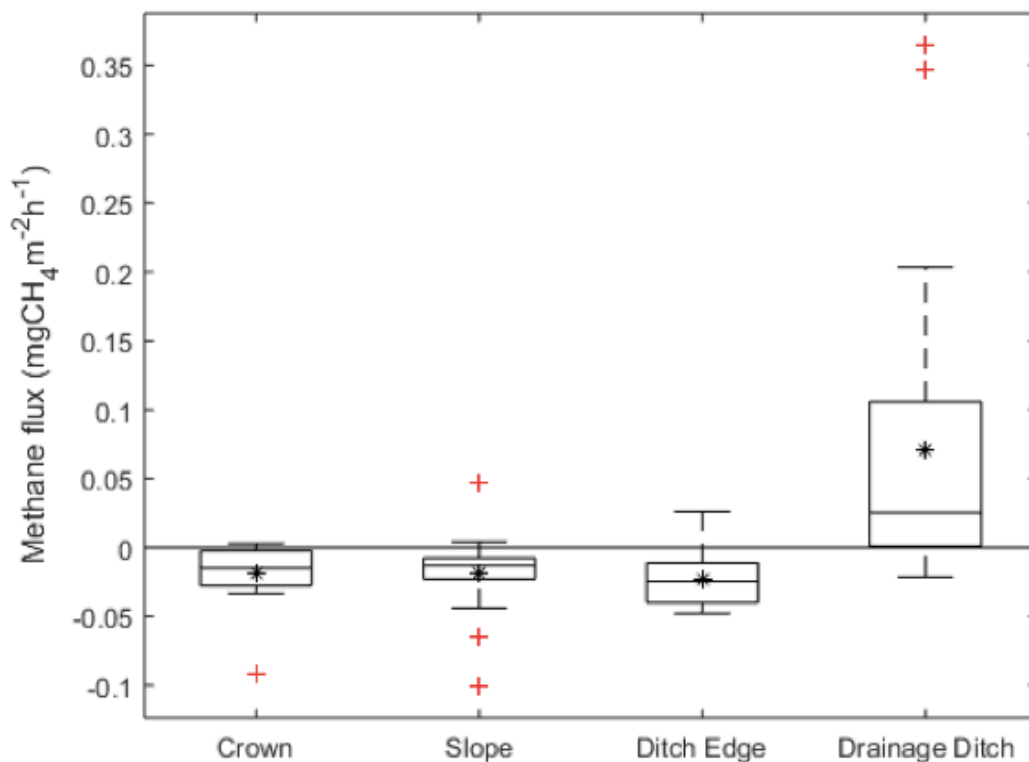


**Figure 4.8** Variation in the measured methane fluxes from the different landforms (crown, slope, ditch edge and drainage ditch). The \* shows the mean methane flux and the + shows the outliers.

Methane fluxes from the crown, slope and ditch edge microforms ranged from  $-0.091 - 0.003 \text{ mg CH}_4 \text{ m}^{-2} \text{ h}^{-1}$ ,  $-0.1 - 0.047 \text{ mg CH}_4 \text{ m}^{-2} \text{ h}^{-1}$  and  $-0.048 - 0.026 \text{ mg CH}_4 \text{ m}^{-2} \text{ h}^{-1}$ , respectively (Table 4.2).

**Table 4.2** Methane fluxes ( $\pm$  standard error of the mean) by landform. Values are reported in  $\text{mg CH}_4 \text{ m}^{-2} \text{ h}^{-1}$ .

	Crown	Slope	Ditch Edge	Drainage Ditch
Mean	-0.019 $\pm 0.005$	-0.019 $\pm 0.008$	-0.023 $\pm 0.006$	0.071 $\pm 0.021$
Median	-0.015	-0.013	-0.025	0.025
Min	-0.091	-0.101	-0.048	-0.022
Max	0.003	0.047	0.026	0.365
Stdev	0.021	0.032	0.021	0.106
Skewness	-2.08	-0.77	0.85	1.57

On average the crown, slope and ditch edges were net methane sinks with average fluxes ( $\pm$  standard error of the mean) of  $-0.019 \pm 0.005 \text{ mg CH}_4 \text{ m}^{-2} \text{ h}^{-1}$ ,  $-0.01 \pm 0.008 \text{ mg CH}_4 \text{ m}^{-2} \text{ h}^{-1}$  and  $-0.023 \pm 0.006 \text{ mg CH}_4 \text{ m}^{-2} \text{ h}^{-1}$  respectively (Table 4.2). The ditch edge was found to have the highest average rate of net methane oxidation, although the highest individual rate of net methane oxidation (minimum flux) was less than that which was found for both the crown and slope landforms. The higher average rate of net methane oxidation is due to the ditch edge having consistently higher rates of net methane oxidation throughout the study period. Average methane fluxes for the crown, slope and ditch edge landforms were not significantly different from each other ( $p > 0.05$ ). However, the average methane flux for the drainage ditch was significantly different from the other landforms ( $p < 0.05$ ). The drainage ditches had primarily positive methane fluxes that ranged from  $-0.022 - 0.365 \text{ mg CH}_4 \text{ m}^{-2} \text{ h}^{-1}$ . The drainage ditches had an average flux of  $0.071 \pm 0.021 \text{ mg CH}_4 \text{ m}^{-2} \text{ h}^{-1}$ . The variation in methane fluxes from the crown, slope and ditch edge microforms was relatively low with standard deviations of just 0.021, 0.032 and 0.021  $\text{mg CH}_4 \text{ m}^{-2} \text{ h}^{-1}$  (Table 4.2). In contrast, the drainage ditch had a much higher degree of variation in methane fluxes between measurements. This is reflected in a standard deviation of  $0.106 \text{ mg CH}_4 \text{ m}^{-2} \text{ h}^{-1}$ . A skewness test revealed that all of the landforms had skewed distributions of methane fluxes with the crown and drainage ditches being highly skewed and the slope and ditch edges being moderately skewed (Table 4.2).



To investigate the spatial variation within the drainage ditches more closely twelve chamber measurements were made on 16 August 2019, with six chambers in the spinner drains and six chambers in the deeper border / main drains (Figure 4.9).

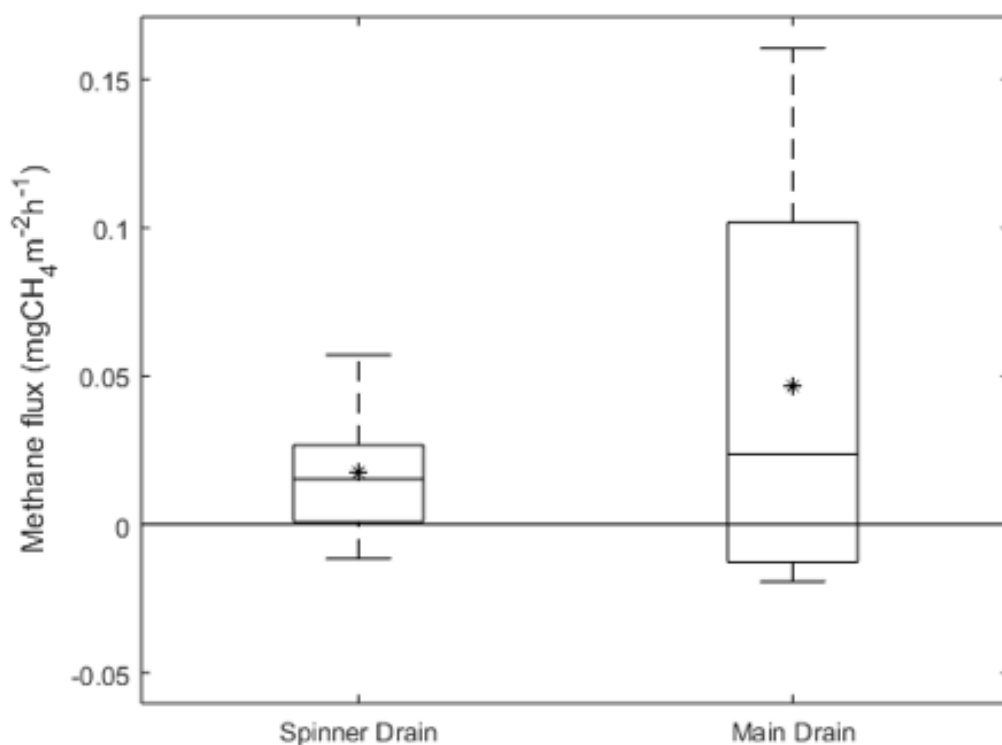


**Figure 4.9** Spatial variation in methane fluxes from the drainage ditches. The drainage ditch landform is comprised of two different drainage ditch types, the shallow “spinner drain” and the deeper main / border drain.

At the time of sampling the spinner drains had more water in them compared to the main drains. The average water depth within the spinner drains was 8.42 cm compared to 6.9 cm in the main drain. In addition, the average water temperature in the spinner drains was higher at 13.3°C compared to 10.7°C in the main drain. The main drainage ditch had much greater spatial variation in the methane flux ranging from  $-0.019 - 0.16 \text{ mg CH}_4 \text{ m}^{-2} \text{ h}^{-1}$  compared to the much lower range of  $-0.011 - 0.057 \text{ mg CH}_4 \text{ m}^{-2} \text{ h}^{-1}$  in the shallower spinner drains, although the median values were fairly similar at 0.015 and 0.024  $\text{mg CH}_4 \text{ m}^{-2} \text{ h}^{-1}$  for the spinner and main drains respectively. However, there was no statistical difference ( $p = 0.36$ ) between the spinner and main drain methane fluxes. A skewness test revealed that fluxes from both the spinner and main drains are moderately skewed with a skewness of 0.57 and 0.71 respectively.

In addition to the peatland microforms, methane flux measurements were also made from cow dung that was present from grazing events. There were six grazing events over the study period with cows in one of the two study site paddocks on 22 – 23 March, 16 – 24 May and 21 – 26 August 2019. Methane fluxes from cow dung were primarily positive with a maximum recorded methane flux of 12.3 mg CH<sub>4</sub> m<sup>-2</sup> h<sup>-1</sup>. This flux was considerably higher than the methane fluxes measured from the peatland landforms. However, methane fluxes from cow dung were highly variable and tended towards zero as the days since grazing increased (Figure 4.10).

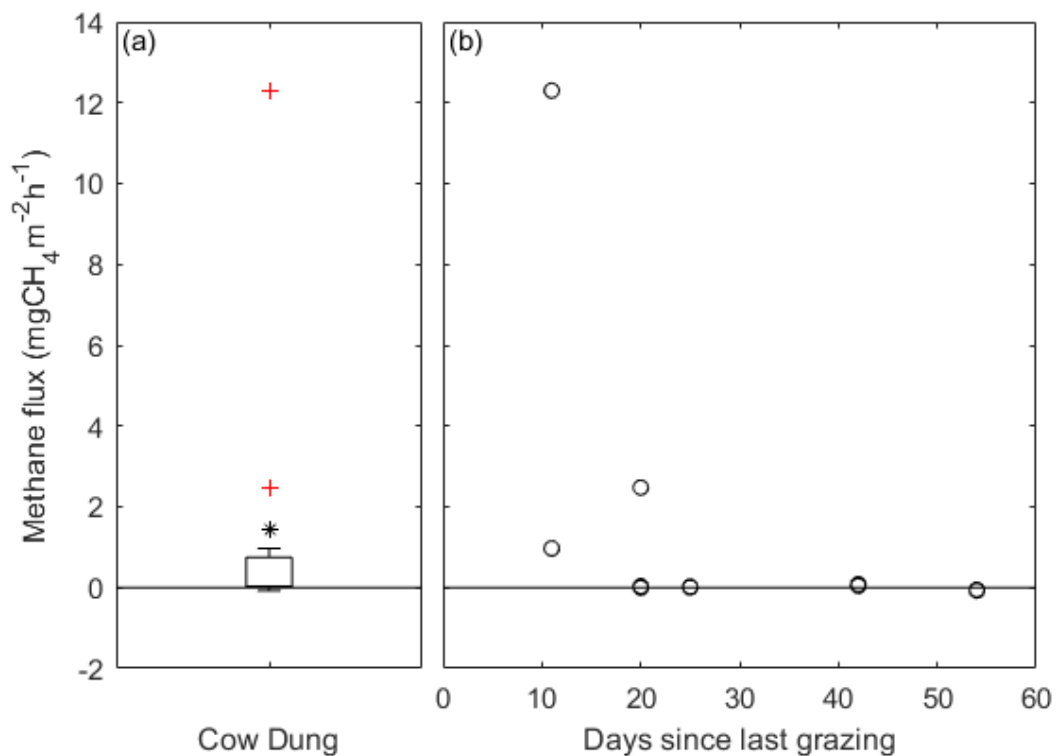


**Figure 4.10** Methane fluxes measured from cow dung, (a) boxplot showing the distribution of methane fluxes and (b) methane fluxes from cow dung vs days since the last grazing. The \* in (a) shows the mean methane flux.

Cow dung had an average flux ( $\pm$  standard error of the mean) of  $1.44 \pm 1.1$  mg CH<sub>4</sub> m<sup>-2</sup> h<sup>-1</sup> (Table 4.3). Methane fluxes from cow dung varied widely, ranging from -0.034 – 12.3 mg CH<sub>4</sub> m<sup>-2</sup> h<sup>-1</sup>. The associated standard deviation was 3.683 mg CH<sub>4</sub> m<sup>-2</sup> h<sup>-1</sup>, which highlights the extremely high variability in methane fluxes. Although the number of measurements made over cow dung was limited there was a general trend of methane fluxes to decrease as the days since grazing increased, with very high initial methane fluxes, quickly decreasing and trending towards zero

flux. Although, one measurement made 20 days after grazing had a negative flux, net methane oxidation was not seen until measurements made 54 days after grazing.

**Table 4.3** Methane fluxes from cow dung ( $\text{mg CH}_4 \text{m}^{-2} \text{h}^{-1}$ )

Mean	$1.44 \pm 1.1$
Median	0.034
Min	-0.074
Max	12.3
Standard deviation ( $\sigma$ )	3.683

#### 4.3.5 Soil physical properties

##### Temperature

Methane fluxes showed no apparent relationship to soil temperature, despite soil Temperatures spanning a wide range, from 9.5 – 24.3°C (Figure 4.11).

##### Water table depth

Methane fluxes showed a linear relationship to the water table depth, increasing as the depth to the water table decreased (i.e. the water table moved closer to the peat surface). This relationship holds true for all three landforms and the  $R^2$  were 0.47, 0.59 and 0.48 for the crown, slope and ditch edge landforms respectively. As all three landforms showed the same relationship between methane fluxes and the water table depth the linear regression shown in Figure 4.11b includes measurements from all three landforms. The  $R^2$  for the overall linear regression was 0.43.

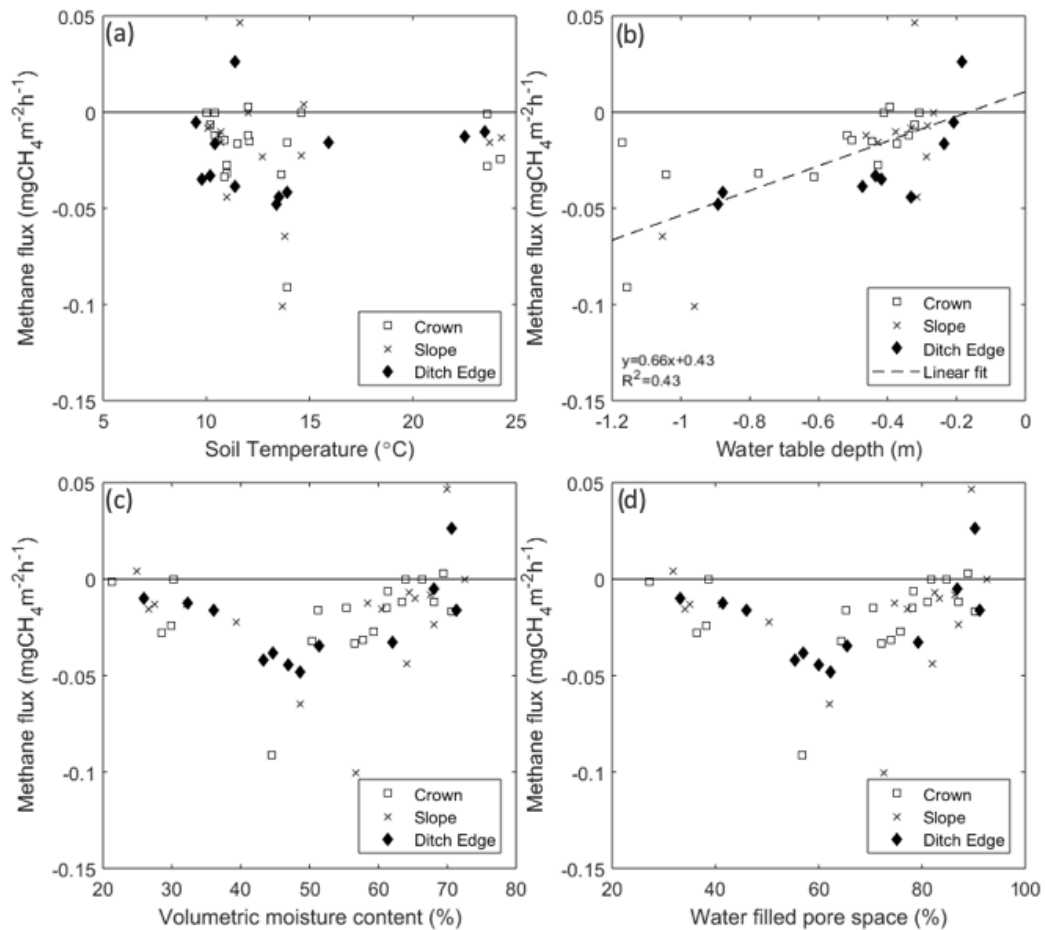


**Figure 4.11** Relationship between methane fluxes and (a) soil temperature (b) water table depth (c) volumetric moisture content and (d) water filled pore space. The dashed line (b) shows the linear regression between methane fluxes and water table depths for all three landforms.

### Volumetric moisture content

Figure 4.11c shows that at high VMC (above 40%), methane fluxes tended to increase as the VMC increased. Methane fluxes were at a minimum in the 40 – 50% VMC range, with methane fluxes tending towards zero at VMCs below 40%.

### Water filled pore space

The WFPS shows the same relationship as the VMC. This is because it was calculated as a function of the VMC and the total soil porosity. However, the WFPS has a slightly higher value than the VMC. Thus, minimum methane fluxes occur in the 50 – 60% WFPS range.

### Effect of water table depth on VMC

The water table depth was shown to influence both the volumetric moisture content and hence the water filled pore space (Figure 4.12).

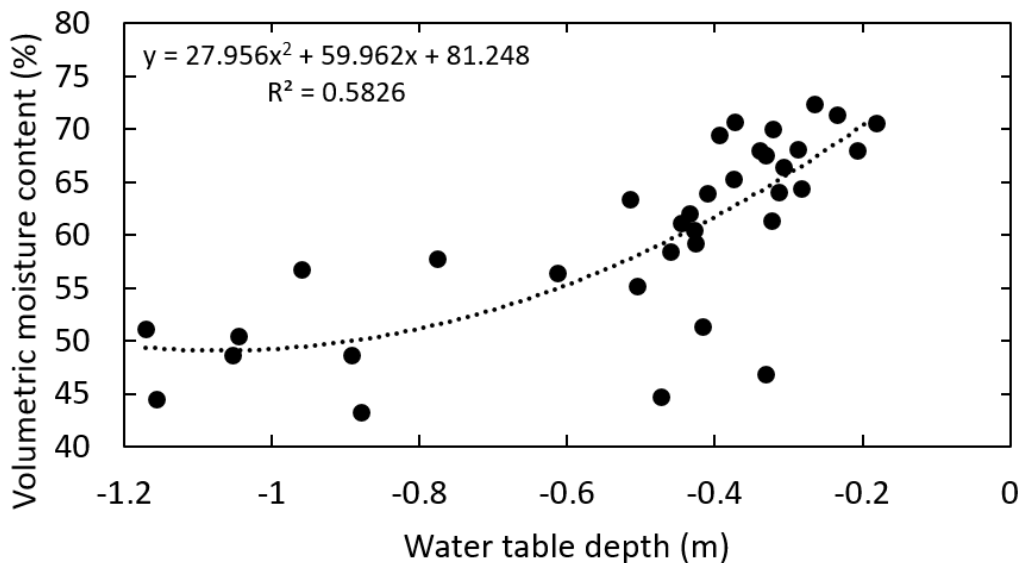


**Figure 4.12** Effect of water table depth on the volumetric moisture content. Note that the VMC has a different range than shown previously (Figure 4.11c) due to no water table depth measurements occurring during the 14 March 2019 sampling date when the lowest VMC values were measured.

At shallow water table depths (above  $-0.5$  m) the relationship appears to be linear but as the water table progresses deeper and deeper the change in the VMC decreases.

### 4.3.6 Soil chemical properties

#### pH

Methane fluxes did not have any apparent relationship with the pH, with the pH ranging from 4.95 – 6.92 (Figure 4.13a). The pH of each landform was fairly consistent throughout the study period with the crown and slope landforms having pH between 5.5 – 7, while the ditch edge landform had pH between 4 – 5.

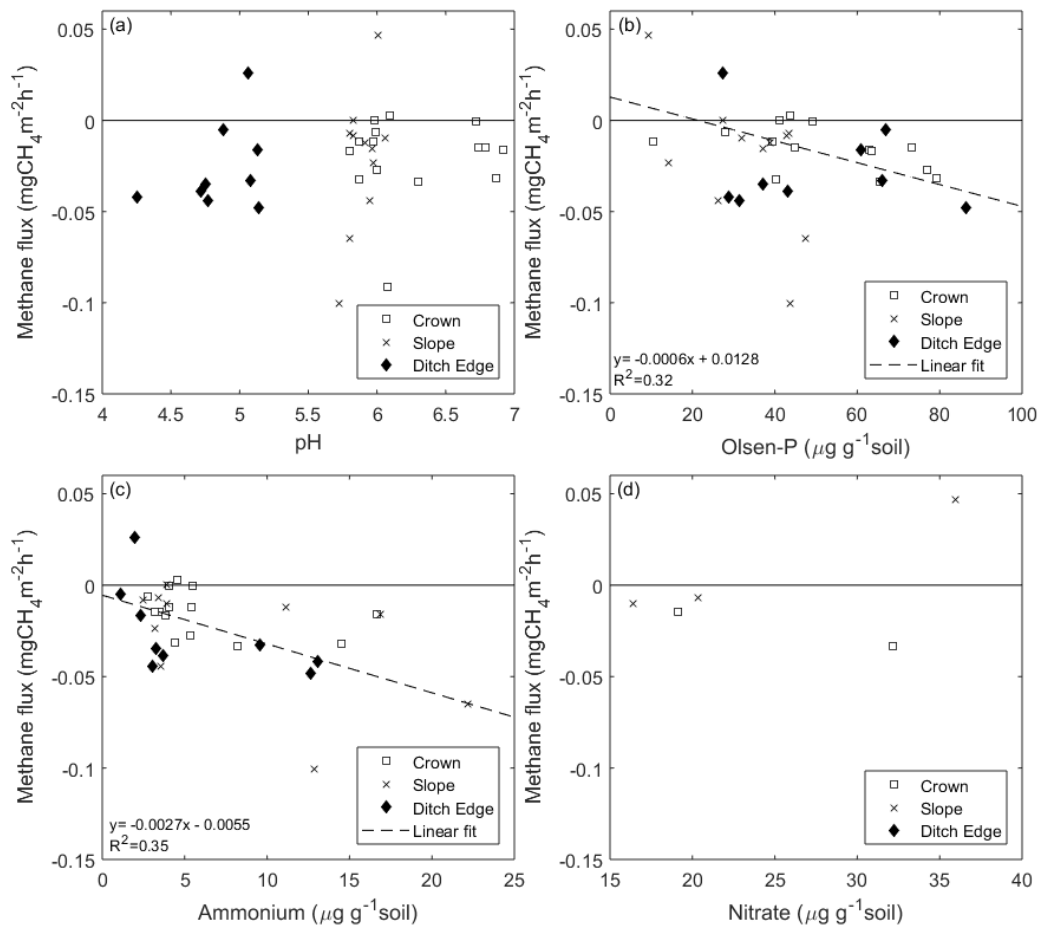


**Figure 4.13** Effect of (a) pH (b) Olsen-P (c) ammonium concentration and (d) nitrate concentration on methane fluxes.

### Olsen-P

Methane fluxes showed little to no relationship with Olsen-P. In the slope and ditch edge landforms there was no relationship between methane fluxes and Olsen-P. However, there appeared to be a slight inverse relationship ( $R^2 = 0.32$ ) in the crown landform wherein methane fluxes tended to decrease as the availability of phosphorous in the soil increased.

### Ammonium

Methane fluxes and soil ammonium concentrations were found to have an inverse relationship with methane fluxes decreasing as the ammonium concentration increased. The strength of the relationship between methane fluxes and ammonium concentrations was moderate with an  $R^2$  of 0.51, 0.27 and 0.33 for the crown, slope and ditch edge landforms respectively. As all three landforms

showed the same relationship between methane fluxes and the ammonium concentration, the linear regression shown in Figure 4.13c includes measurements from all three landforms. The  $R^2$  for the linear regression was 0.35.

### **Nitrate**

For the most part, there was no nitrate detected in any of the soil cores taken from the crown, slope and ditch edge landforms. However, small amounts of nitrate between 16.4 – 36  $\mu\text{g g}^{-1}$  soil were detected in five of the crown and slope soil cores. Hence, no relationship between methane fluxes and nitrate concentration could be identified.

### **4.3.7 Drainage ditch chemical and physical properties**

There was no apparent relationship between methane fluxes and any water properties (pH, conductivity, dissolved oxygen, water temperature, water depth, nitrate concentration and dissolved phosphorus) or soil properties (VMC and WFPS) that were measured (Figure 4.14).

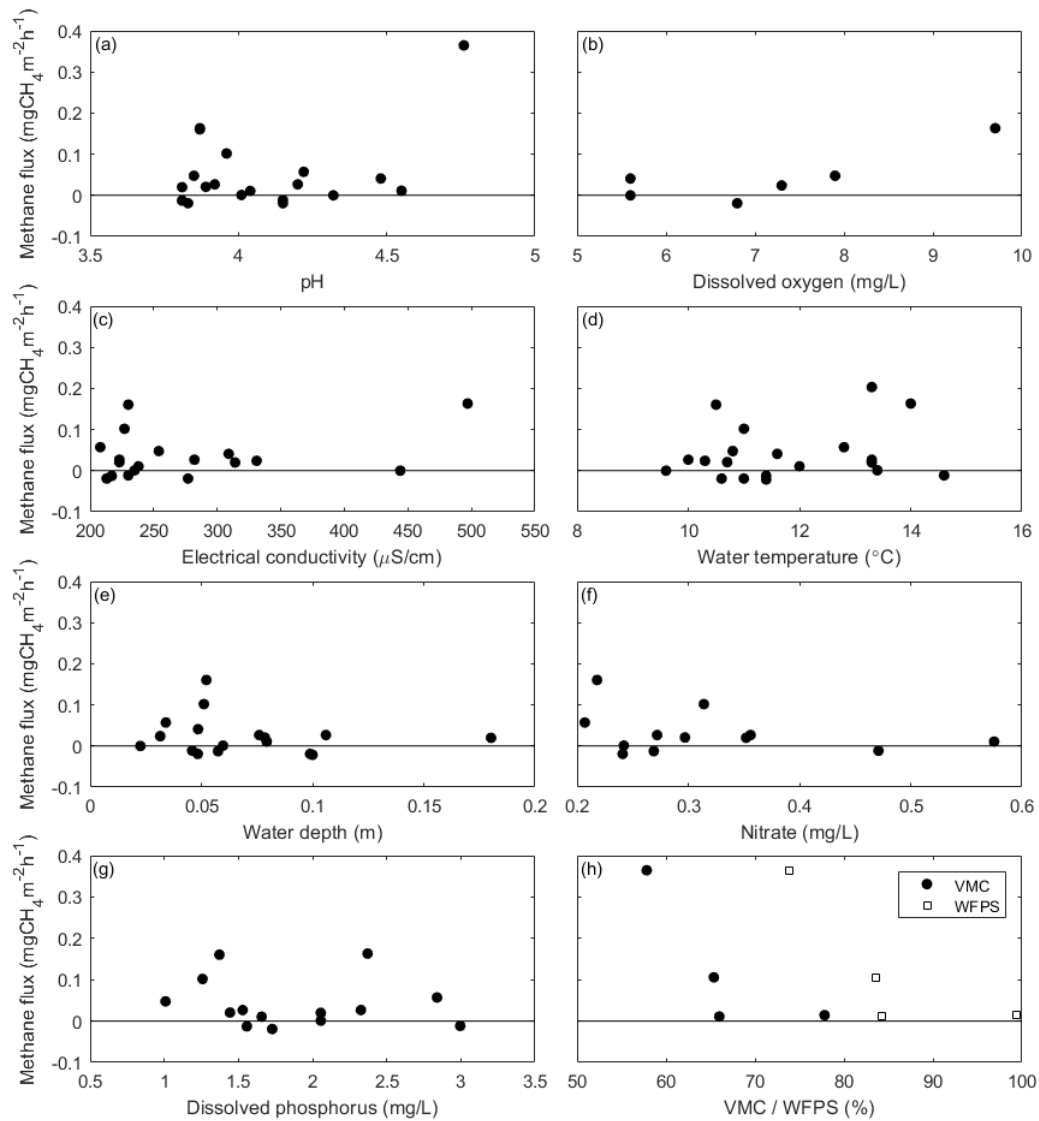


**Figure 4.14** Effect of (a) pH (b) dissolved oxygen (c) electrical conductivity (d) water temperature (e) water depth (f) nitrate concentration (g) dissolved phosphorus and (h) volumetric moisture content and water filled pore space on methane fluxes in the drainage ditch landform. The soil moisture content and water filled pore space measurements were made when there was no standing water in the drainage ditch landforms. The rest of the measurements were from water samples.

### 4.3.8 Eddy covariance

The annual net methane emissions from the study site was calculated using eddy covariance measurements made over the period 1 October 2018 to 30 September 2019 (Figure 4.15). The primary driver of large emissions of methane are cows, and the large peaks of methane fluxes seen in Figure 4.15a are associated with fluxes recorded when cows were present in the eddy covariance footprint area.



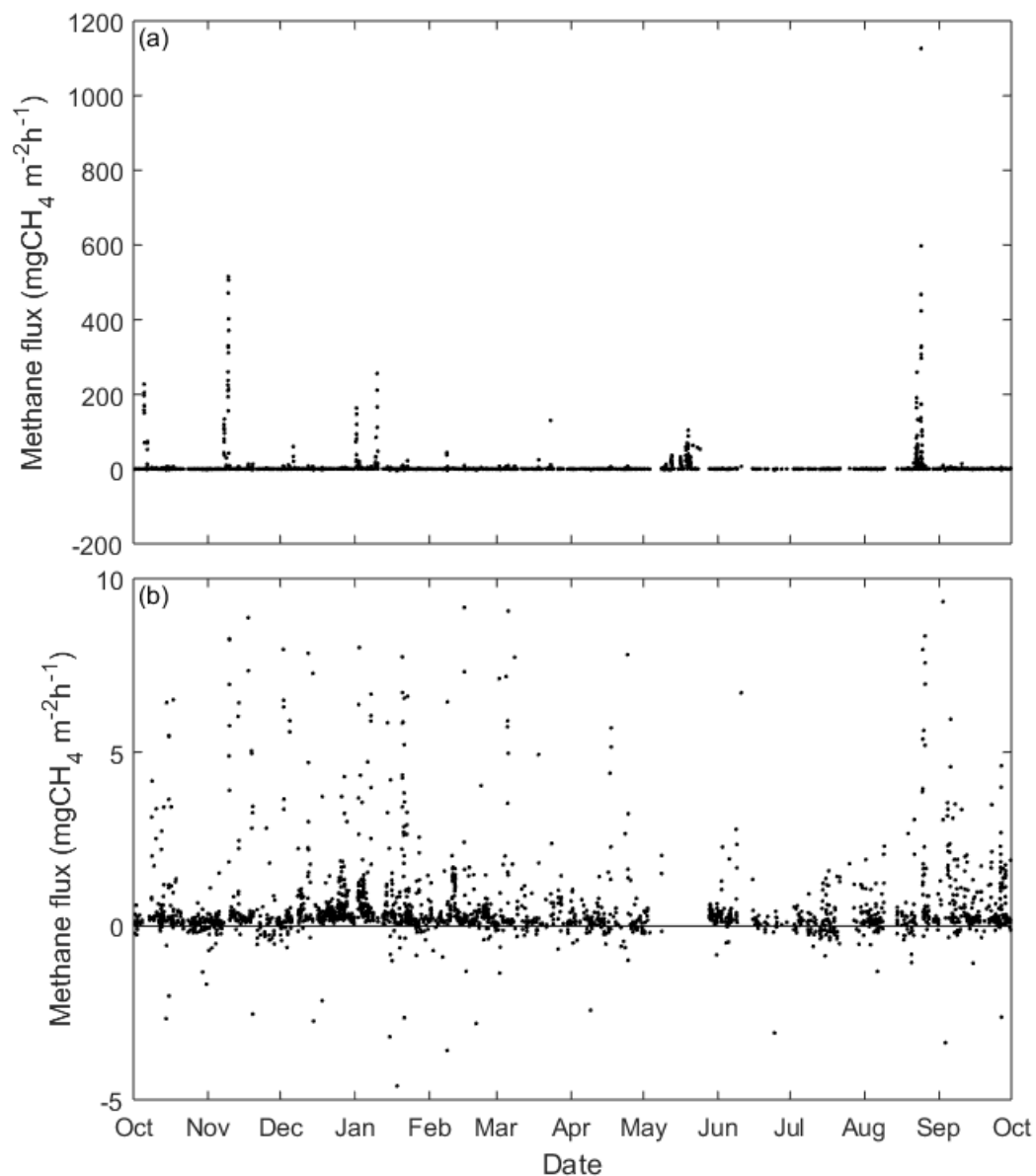


**Figure 4.15** Half-hourly methane fluxes as measured by eddy covariance (a) methane fluxes before filtering of grazing events (b) methane fluxes after filtering out grazing events (October 2018 – September 2019).

Although most of the peaks correlate with the grazing records for the two paddocks in the study area, some of the small peaks did not correlate with the grazing records. However, due to the high readings compared to the background, we postulate that these peaks occurred when cows were present in the paddocks surrounding the study area and the EC footprint extended past the two paddocks of the study area. As the objective of this study was on soil methane fluxes, all peaks that were correlated with the recorded grazing events were removed and also any peaks above an arbitrary set threshold of 10 mg CH<sub>4</sub> m<sup>-2</sup> h<sup>-1</sup>. The mean daily methane flux was calculated from the resulting filtered data (Figure 4.16).

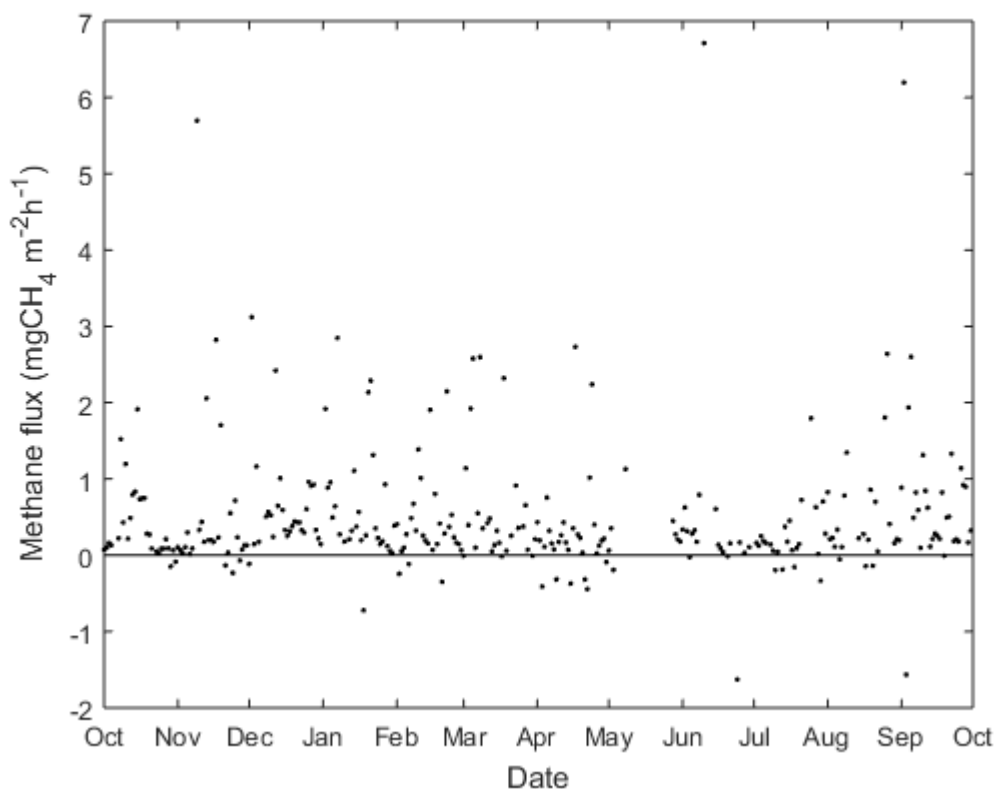


**Figure 4.16** Mean daily methane fluxes measured by eddy covariance. Fluxes were filtered to remove grazing events any peaks above an arbitrary set threshold of  $10 \text{ mg CH}_4 \text{ m}^{-2} \text{ h}^{-1}$  (October 2018 – September 2019).

Mean daily fluxes were primarily positive, with the bulk of the data falling within the  $0 - 1.5 \text{ mg CH}_4 \text{ m}^{-2} \text{ h}^{-1}$  range. However, there were some larger daily fluxes of up to  $7 \text{ mg CH}_4 \text{ m}^{-2} \text{ h}^{-1}$  recorded. There were a small number of days with negative daily fluxes, although they were all relatively minor with only two days  $< -1 \text{ mg CH}_4 \text{ m}^{-2} \text{ h}^{-1}$ . Examining Figure 4.16, there was no obvious seasonal pattern to the methane flux. When seasonal averages are calculated, there is a noticeable seasonal pattern. Spring and summer had relatively similar fluxes of  $0.601 \pm 0.05$  and  $0.681 \pm 0.04 \text{ mg CH}_4 \text{ m}^{-2} \text{ h}^{-1}$  respectively, with summer having the overall highest mean methane flux. Winter fluxes were the lowest at  $0.443 \pm 0.06 \text{ mg CH}_4 \text{ m}^{-2} \text{ h}^{-1}$  and autumn fluxes were slightly higher at  $0.507 \pm 0.07 \text{ mg CH}_4 \text{ m}^{-2} \text{ h}^{-1}$  (Table 4.4). Statistical analysis revealed that there was only a significant difference between the summer and winter methane fluxes ( $p = 0.0092$ ).

**Table 4.4** Seasonal mean methane fluxes ( $\pm$  standard error of the mean) as measured by eddy covariance from October 2018 to September 2019.

Season	Methane flux ( $\text{mg CH}_4 \text{ m}^{-2} \text{ h}^{-1}$ )
Spring	$0.601 \pm 0.05$
Summer	$0.681 \pm 0.04$
Autumn	$0.507 \pm 0.07$
Winter	$0.443 \pm 0.06$

Methane fluxes showed a diurnal variation with the highest methane fluxes occurring at night from around 2400 to 0400 (Figure 4.17).

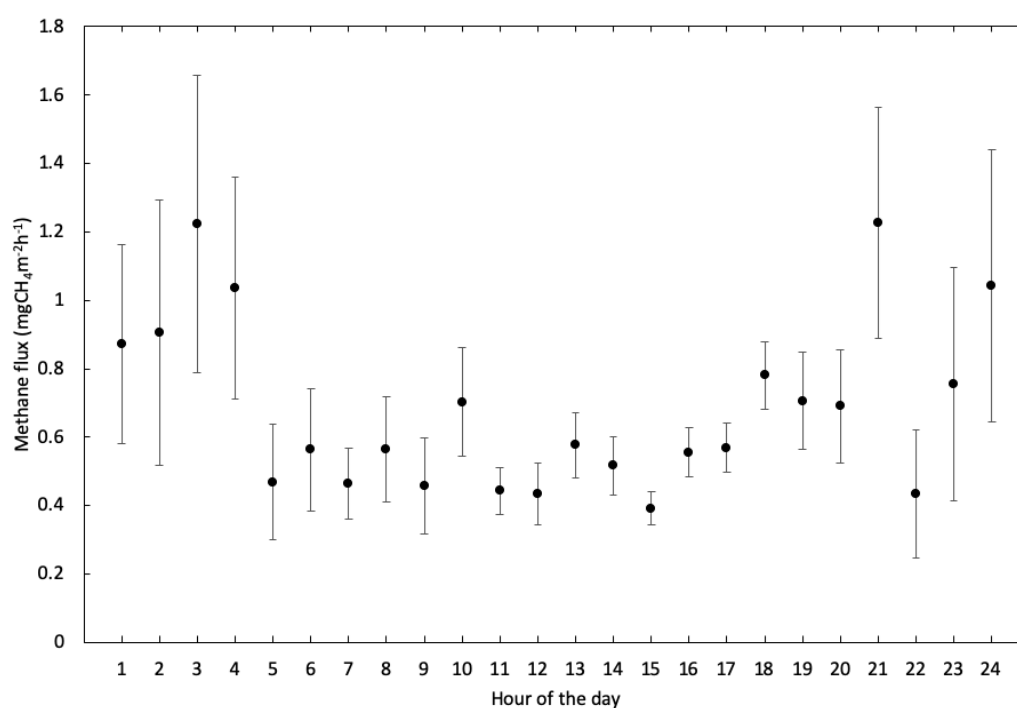


**Figure 4.17** Average methane fluxes recorded for each hour of the day. Error bars show the standard error of the mean (October 2018 – September 2019).

Daytime methane fluxes were in the range of  $0.4 - 0.6 \text{ mg CH}_4 \text{ m}^{-2} \text{ h}^{-1}$ , while the night-time fluxes averaged up to  $1.2 \text{ mg CH}_4 \text{ m}^{-2} \text{ h}^{-1}$ .

The net annual methane flux was calculated to be  $44.72 \text{ kg CH}_4 \text{ ha}^{-1} \text{ yr}^{-1}$ .

#### 4.3.8.1 Eddy covariance footprint analysis

An analysis of the eddy covariance footprint shows that for the most part the  $x_{\text{peak}}$  distance (i.e. the distance from the flux tower to the peak of the flux footprint

probability distribution) was relatively close to the flux tower at less than 25 m (Figure 4.18). In addition,  $X_{70}$  (i.e. the distance from the flux tower within which 70% of the measured flux was sourced) was relatively small and was generally less than 150 m and therefore generally within the boundaries of the study site.

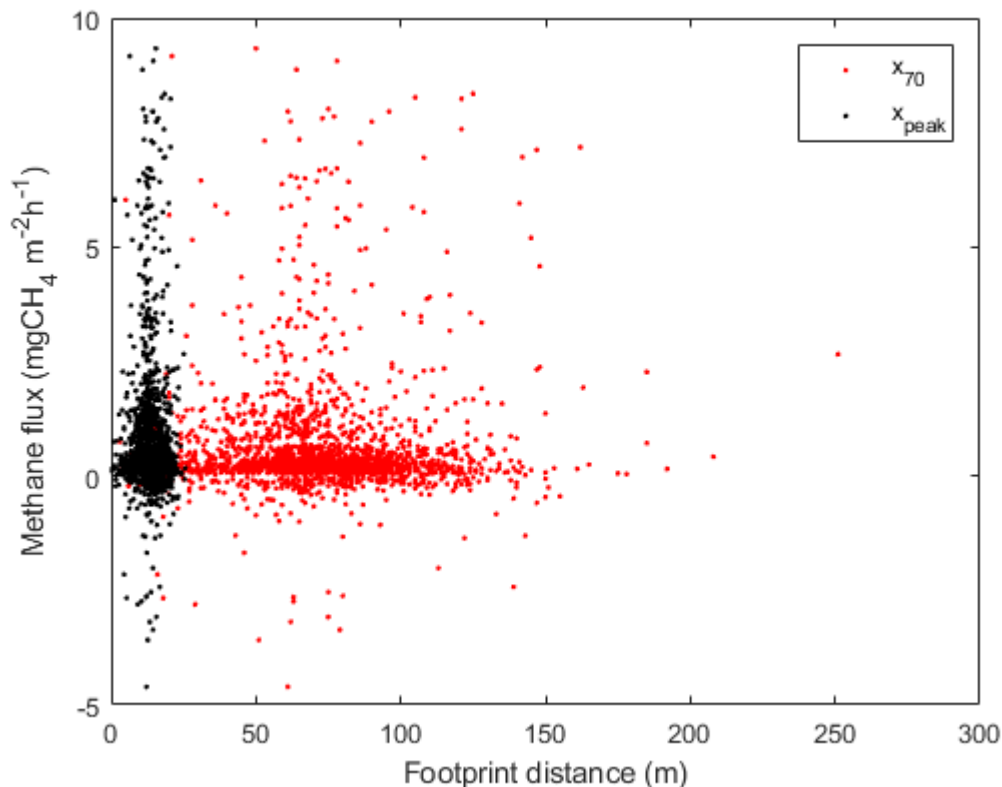


**Figure 4.18** Eddy covariance methane fluxes versus footprint distance. The footprint distance is shown as both footprint peak distance ( $X_{\text{peak}}$ ) and footprint distance from which 70% of the measured flux is sourced ( $X_{70}$ ).

Examining wind directions associated with the measured methane fluxes (Figure 4.19), there was a higher density of fluxes measured between 225 and 270° (i.e. a greater proportion of high fluxes were measured when the wind was blowing from the southwest). In addition, when the wind was blowing from the southwest, the footprint peak distance ( $X_{\text{peak}}$ ) was typically less than 18 m (Figure 4.20).

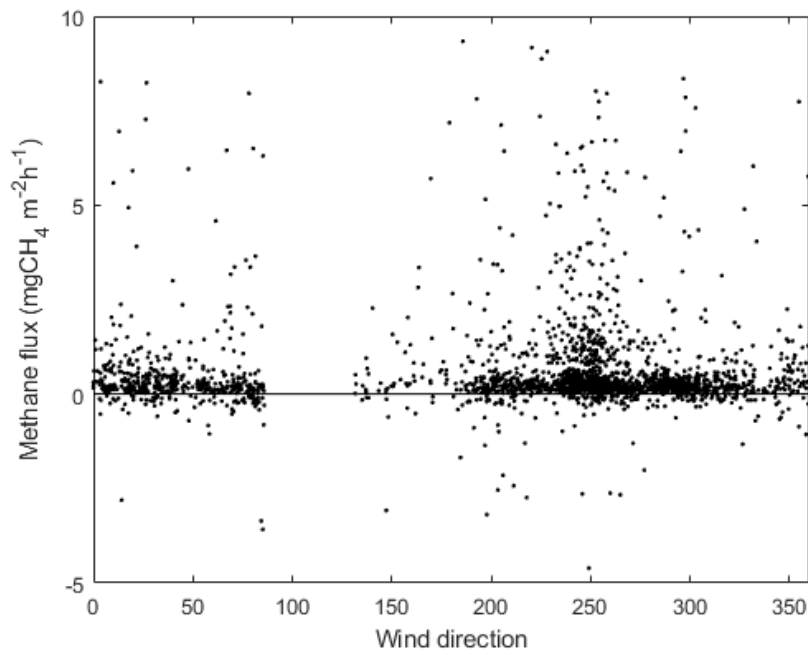


**Figure 4.19** 30-minute eddy covariance methane fluxes versus wind direction. Note that the gap observed around 86 - 130° is due to the filtering of fluxes measured when the wind is blowing over the QCL enclosure at the study site.

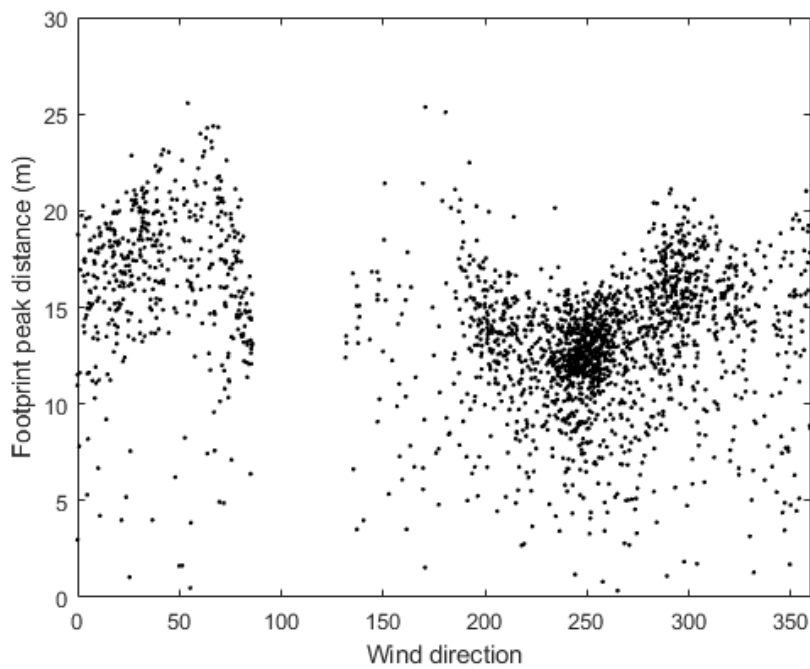


**Figure 4.20** Eddy covariance footprint peak distance ( $X_{\text{peak}}$ ) versus wind direction. Note that the gap observed around 86 - 130° is due to the filtering of fluxes measured when the wind is blowing over the QCL enclosure at the study site.

#### 4.3.8.2 Environmental variables

Unlike the chamber measurements there did not seem to be as clear a trend between the EC methane flux and the water table depth (Figure 4.21). In addition, there was no clear trend between the EC methane flux and the soil temperature, volumetric moisture content or the air temperature.

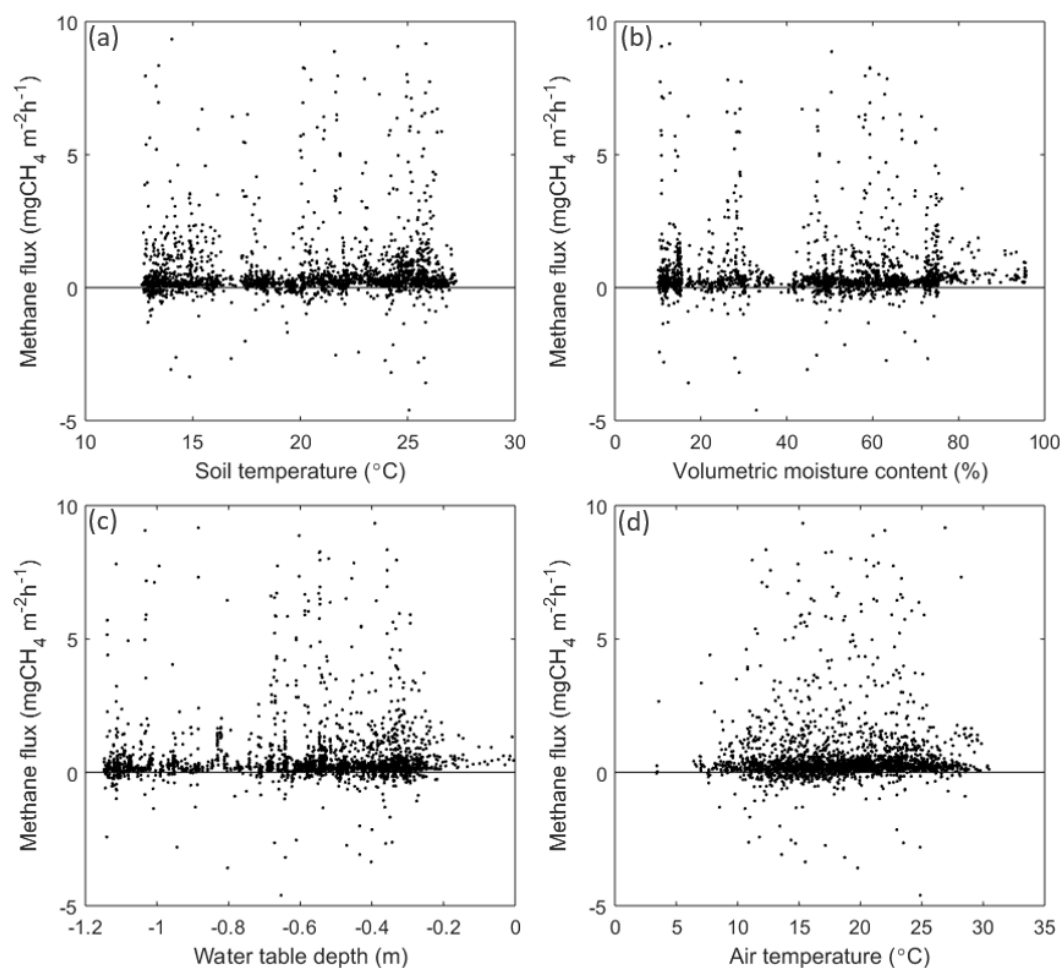


**Figure 4.21** Methane fluxes vs (a) soil temperature (b) volumetric water content (c) water table depth and (d) air temperature. Methane fluxes were measured with eddy covariance and are mean half-hourly fluxes. Air temperature was measured at the EC flux tower and soil temperature, volumetric moisture content and water table depth were measured in close proximity to the flux tower. The soil temperature was measured at 20 cm depth.

Although there is no apparent relationship between the EC methane flux and the air temperature in the half-hourly flux measurements, there was a relationship in both the monthly averaged air temperature and soil temperature and the EC fluxes, whereby methane fluxes were larger at higher temperatures (Figure 4.22). However, the strength of the relationship was much higher between methane

fluxes and mean monthly air temperatures ( $R^2 = 0.32$ ), rather than the mean monthly soil temperature ( $R^2 = 0.17$ ).

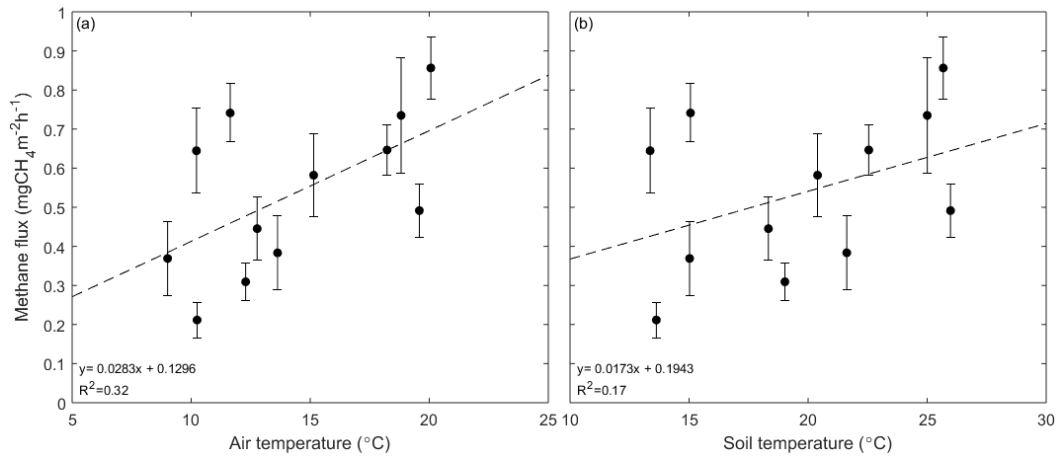


**Figure 4.22** (a) Mean monthly air temperature and (b) mean monthly soil temperature at 20 cm depth vs methane fluxes measured by eddy covariance. Error bars show the standard error of the mean.

#### 4.3.9 Eddy covariance versus chamber measurements

The crown and slope landforms at the study site make up the majority of the land area accounting for approximately 43 and 50% of the land area respectively (Figure 4.23). The ditch edges accounts for 4% of the land area, while the drainage ditches account for 3% of the land area. Thus, when looking at net emissions, 97% of the study site was a methane sink while 3% was a methane source (Figure 4.8 & 4.23).

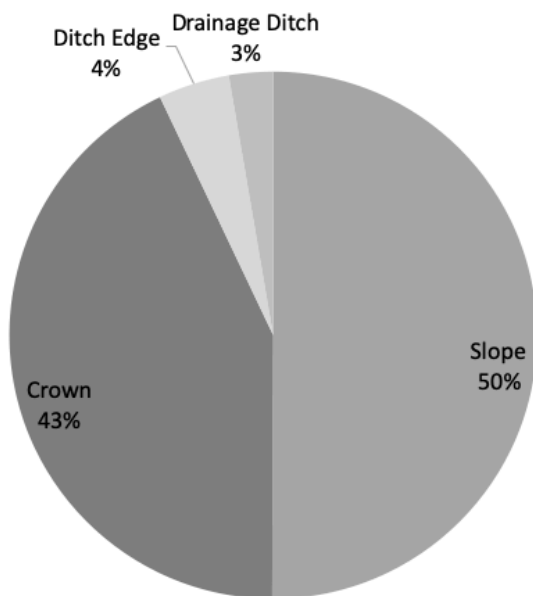


**Figure 4.23** Area coverage of the different landforms.

The net paddock-scale methane flux for each chamber sampling date was estimated by weighting the average landform flux (Figure 4. 7) by the corresponding landform area. When net methane fluxes were calculated using the chamber measurements, the overall net methane fluxes were small and close to zero. Over the first five sampling dates net methane fluxes were small but negative and ranged from -0.005 – 0.058 mg CH<sub>4</sub> m<sup>-2</sup> h<sup>-1</sup> (Figure 4.24). However, on the last sampling date (2 September 2019), the net methane flux was very small at 0.003 mg CH<sub>4</sub> m<sup>-2</sup> h<sup>-1</sup>.

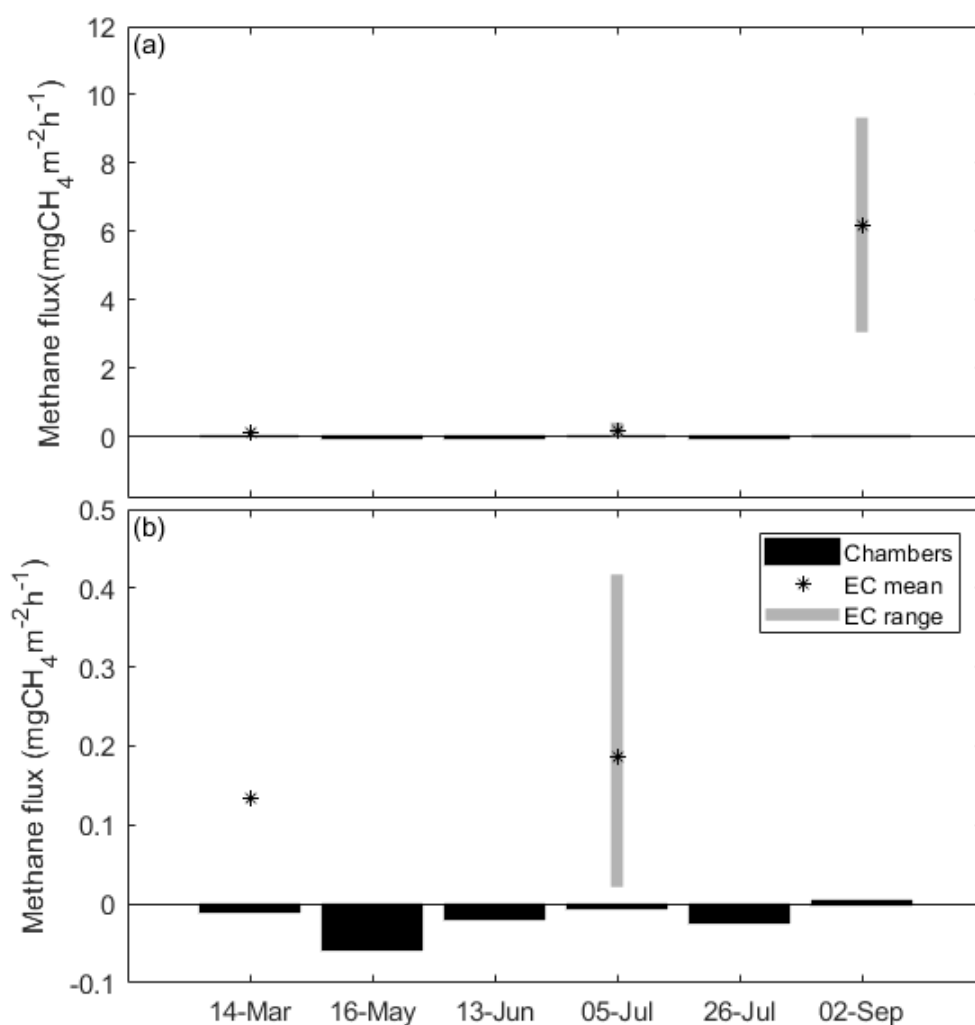


**Figure 4.24** Net methane emissions. The black bars show the upscaled chamber measurements for each sampling date. The grey bars show the range of EC flux measurements, where they were available on the chamber sampling date and the \* shows the mean EC flux. Shown in (a) is the full extent of the data; (b) is a zoomed in view of (a).

When the net fluxes estimated from the chamber measurements were compared to the measured fluxes from the eddy covariance flux tower, there was a large discrepancy between the two measurement techniques. The eddy covariance



mean daily methane fluxes shown in Figure 4.16 were all positive fluxes and the methane fluxes measured on the sampling dates (Figure 4.24) were again positive. In addition, on 2 September the net methane flux from the EC measurements was  $6.2 \text{ mg CH}_4 \text{ m}^{-2} \text{ h}^{-1}$ , which is considerably larger than the majority of the methane fluxes measured at the study site (Figure 4.16). These net positive methane fluxes measured by eddy covariance are in contradiction to the generally net negative methane fluxes estimated by the chamber measurements.

## 4.4 Discussion

### 4.4.1 Methane emission hotspots

#### 4.4.1.1 Spatial variation in the methane flux

Methane fluxes from our study site (a drained peatland under dairy grazing) were found to be highly variable, both spatially and temporally. A wide range of methane fluxes were recorded from chamber measurements across the peatland with maximum emissions of  $0.365 \text{ mg CH}_4 \text{ m}^{-2} \text{ h}^{-1}$ , and a maximum uptake of  $-0.101 \text{ mg CH}_4 \text{ m}^{-2} \text{ h}^{-1}$ . It has been well established in the literature that methane emissions from drained peatlands are difficult to quantify due to the spatial and temporal variation that is primarily a result of variations in the water table depth caused by drainage ditches (e.g. Baldocchi et al., 2012; Schrier-Uijl et al., 2010). To show the major sources of spatial variation in methane fluxes across the peatland, it was classified into four landforms; crown, slope, ditch edge and drainage ditches. The crown, slope and drain edge landforms had consistently negative methane fluxes, indicating that they are a net sink of methane. Interestingly, and contrary to hypothesis one (section 1.4), the ditch edge landform was found to be the strongest sink of methane with an average flux of  $-0.023 \pm 0.006 \text{ mg CH}_4 \text{ m}^{-2} \text{ h}^{-1}$ . The crown and slope landforms were a slightly weaker sink of methane at  $-0.019 \pm 0.005 \text{ mg CH}_4 \text{ m}^{-2} \text{ h}^{-1}$  and  $-0.019 \pm 0.008 \text{ mg CH}_4 \text{ m}^{-2} \text{ h}^{-1}$  respectively. Although the ditch edges had the highest average rate of net methane oxidation, both the crown and slope landforms had higher individual rates. The higher average rate was due to the ditch edge having much more consistent methane fluxes when compared to the crown and slope landforms (Figure 4.8). The drainage ditches were a small methane source, emitting  $0.071 \pm 0.021$

mg CH<sub>4</sub> m<sup>-2</sup> h<sup>-1</sup>. These results are somewhat consistent with what other researchers have found for methane emissions in drained peat soils in regard to the fact that drainage ditches act as a source of methane, while the “field” soil (i.e. crown, slope and ditch edge landforms) have negligible or slightly negative methane fluxes (e.g. Alm et al., 2007; Couwenberg, 2011; Schrier-Uijl et al., 2010; Teh et al., 2011). However, other studies have shown that ditch edges are also a source of methane. For example Schrier-Uijl et al. (2010) found that the ditch edges emitted 4.8 – 6.0 mg CH<sub>4</sub> m<sup>-2</sup> h<sup>-1</sup> in an intensively managed eutrophic fen, and 2.7 – 4.4 mg CH<sub>4</sub> m<sup>-2</sup> h<sup>-1</sup> in an extensively managed eutrophic fen. This is likely because their drains were permanently filled with water and the ditch edge was saturated compared to the other landforms (Schrier-Uijl et al., 2010). This is in contrast to our study site where there was little difference in the volumetric moisture content, water table depth and the WFPS between the crown, slope and ditch edge landforms (Figure 4.11). As water availability is a major control on methane fluxes (Frolking et al., 2011), it is likely that this is the reason that these three landforms overall have similar methane fluxes. The link between methane fluxes and water availability is further discussed in section 4.4.2.1

Although the observed pattern of negative methane fluxes in the field area and positive methane fluxes in the drainage ditches at our study site is consistent with the literature, the measured strength of the fluxes in the drainage ditches is significantly lower than what has been reported in the literature (Table 4.5).

**Table 4.5** Comparison between net methane emissions from drainage ditches reported in studies on drained peatland ecosystems. Mean CH<sub>4</sub> emission rates are in mg CH<sub>4</sub> m<sup>-2</sup> h<sup>-1</sup> [Adapted from: Schrier-Uijl et al. (2010)].

<b>Drain / pond CH<sub>4</sub> flux</b>	<b>Reference</b>
15.72 up to 25 in summer	Minkkinen and Laine (2006)
5.6	Hendriks et al. (2007)
5.8 up to 38.2 in summer	Bubier et al. (1993)
2.9	Waddington and Day (2007)
up to 8.0	Huttunen et al. (2003)
4.6 – 7.5	Hamilton et al. (1994)
4.5 – 7.0	Schrier-Uijl et al. (2010)
4.5 – 5.3	Schrier-Uijl et al. (2010)
0.071 ± 0.021	This study

The drainage ditches were found to have a net methane emission rate of 0.071 mg CH<sub>4</sub> m<sup>-2</sup> h<sup>-1</sup>, which is considerably lower than methane fluxes reported from other studies in Table 4.5. Even the maximum measured methane emission rate of 0.364 mgCH<sub>4</sub>m<sup>-2</sup>h<sup>-1</sup> was still considerably lower than other published values. The reason that methane fluxes from the drainage ditches at the study site were lower than other studies is not entirely clear. One possible explanation is the high spatial and temporal variability in the methane flux. It is possible that the chamber measurements simply did not capture any high flux events, as during each sampling campaign only two chambers were used in the drainage ditches. However, this is unlikely to be the cause of the low measured fluxes as one sampling campaign on 16 August 2019 was dedicated to identifying the spatial variation in methane fluxes from the drainage ditches. During this campaign all 12 chambers were placed in the drainage ditches and all measured similar fluxes compared to the other campaigns.

#### **4.4.1.2 Temporal variation in the methane flux**

Methane fluxes were highly variable over the sampling period and in the crown slope and ditch edge landforms, methane fluxes followed a similar pattern (Figure 4.7). In these landforms methane fluxes decreased to a minimum (maximum net methane oxidation) over the first two sampling campaigns (14 March 2019 and 16

May 2019). This pattern is likely to be largely driven by changes to the water content of the soil as the water table is a major control on methane fluxes with methane oxidation increasing as the depth to the water table increases (Topp & Pattey, 1997). Examining the water table depth (Figure 4.6a), there was a large difference between the first two sampling dates (14 March 2019 and 16 May 2019) and the rest. However, this large difference is not as readily apparent when examining the VMC (Figure 4.6c) as over the study period the VMC was steadily increasing. From both the water table depth and the VMC data, it can be concluded that the soil was initially dry and got progressively wetter through the study period. Hence, the measured methane flux increased over the study period as methane fluxes increase with increasing water saturation (Dalal et al., 2008). However, the first measurement on 14 March had a higher methane flux. This was likely caused by the extremely dry conditions as VMC measurements made within the chamber collars showed that the average VMC for the crown, slope and ditch edge landforms on 14 March was only 28.02%. An increase in methane fluxes at low soil moistures is often attributed to a reduction in the rate of methane oxidation due to biological water stress (Kammann et al., 2001). This is because some water is required for the diffusion of oxygen and methane within soils and methanotrophs have a physiological requirement for water (Kammann et al., 2001; Mancinelli, 1995).

In the drainage ditches, the highest fluxes were measured during the first two sampling campaigns (14 March 2019 and 16 May 2019) decreasing to a minimum in late May / early June and increasing over the winter period (Figure 4.7). This pattern of methane fluxes in the drainage ditches does not reflect the changes in the water table. During the first two sampling campaigns the water table was lower than during the later sampling campaigns (Figure 4.6). Hence, the expectation is that methane fluxes would be lower than those observed in the later sampling campaigns. In addition, during the first two sampling campaigns the water table was below the bottom of the drainage ditches (i.e. there was no water in the drainage ditches). Although the water table was low, the soil within the drainage ditches was still partially saturated with an average VMC of 76 and 62% for the 14 March 2019 and 16 May 2019 sampling campaigns respectively. The

water table is a primary control on methane fluxes with methanogenesis primarily occurring below the water table and methane oxidation occurring above the water table (Yang et al., 2017). Hence the height of the water table determines the relative rates of methane production and consumption and therefore the overall net flux. Maximum net methane fluxes in peat soils typically occur when the soil is completely saturated, and the water table is close to the soil surface. This is because in these conditions there is minimal aerobic soil or water and therefore minimal rates of methane oxidation (Bubier, 1995; Couwenberg & Fritz, 2012). This is possibly why the methane emissions in the drainage ditches was at a maximum in the first two sampling dates as the soil was relatively wet and there was no water present in the drainage ditches where the methane is able to be oxidised as it diffuses to the surface. On 13 June 2019 there was only one chamber measurement made from the drainage ditches and therefore the validity of the chamber measurement for this sampling date is unable to be determined. Over the remaining sampling campaigns, it was found that methane fluxes within the drainage ditches tended to increase. Similarly to the crown, slope and ditch edge landforms it was concluded that this increase is likely to have been primarily driven by changes in the temperature and water availability. Over these four sampling campaigns the water temperature tended to increase. The average water temperature for 5 July, 26 July, 16 August and 2 September was 10.0, 11.3, 12.0 and 12.4°C respectively.

In addition, over this period the monthly rainfall increased, which resulted in the depth to the water table decreasing (Figures 4.5 & 4.6). Hence, over this period, the water depth in the drainage ditches increased and for 5 July, 26 July, 16 August and 2 September the average water depth was 0.03, 0.05, 0.08 and 0.09 m above the bottom of the drainage ditch. Methanogenesis has been shown to increase with increasing temperatures and decreasing water table depths (Dalal et al., 2008). Hence, it can be inferred that temperature and rainfall are likely the cause of the increasing methane fluxes over this period.

#### **4.4.1.3 Methane fluxes from cow dung patches**

High methane emissions from cow dung patches occur because fresh dung carries all of the requirements for methanogenesis; a suitable population of microbes / methanogens and it is warm and moist with a readily available carbon supply (Saggar et al., 2004). Methane fluxes are typically only high in freshly voided dung with methane fluxes returning to background levels fairly quickly (Jarvis et al., 1995; Maljanen et al., 2012; Mori & Hojito, 2015; Saggar et al., 2004). Hence, cow dung patches are only a significant source of methane for approximately 10-35 days before the measured methane fluxes are indistinguishable from those from the soil (Mori & Hojito, 2015). As the number of cow dung chamber measurements was limited, there were not enough data points to positively determine the trend that the methane fluxes from cow dung have over time (Figure 4.10). However, the pattern observed does align with high initial fluxes decreasing over time, as described in the literature (e.g. Jarvis et al., 1995; Maljanen et al., 2012; Mori & Hojito, 2015).

The maximum measured methane flux from cow dung was  $12.3 \text{ mg CH}_4 \text{ m}^{-2} \text{ h}^{-1}$ , which was measured 11 days after grazing. This is within the range of values reported in other studies, such as Maljanen et al. (2012) who reported maximum flux rates of  $>8.3 \text{ mg CH}_4 \text{ m}^{-2} \text{ h}^{-1}$ , Jarvis et al. (1995) who reported maximum methane fluxes of approximately  $27 \text{ mg CH}_4 \text{ m}^{-2} \text{ h}^{-1}$  and Saggar et al. (2003) who reported maximum methane fluxes of up to  $20 \text{ mg CH}_4 \text{ m}^{-2} \text{ h}^{-1}$ . Although, all of these studies were conducted on mineral soils, Jarvis et al. (1995) reported that the majority of the methane emissions came from the dung itself, with only a small positive interaction with the soil. Hence, these values serve as an appropriate comparison to cow dung patches on peat soils.

#### **4.4.2 Controls on methane emissions**

##### **4.4.2.1 Soil physical properties**

The majority of literature that surrounds the controls of methane fluxes in peat soils report that the soil temperature and the water table position are the dominant controls on methane fluxes (e.g. Bridgham et al., 2006; Frohling et al.,

2011). Water controls methane fluxes primarily through its effects on the diffusion of oxygen, methane and carbon substrates (Dalal et al., 2008). Methanogenesis is an anaerobic process, while methane oxidation is an aerobic process (Yang et al., 2017). Thus methanogenesis primarily occurs in saturated soil, primarily below the water table but can also occur in anaerobic microsites within generally unsaturated soil (Yang et al., 2017). Hence, it is usually assumed that methane fluxes are positively correlated with water saturation since, in dry soil (low WTD, VMC and WFPS), methane oxidation dominates and in wet soil (high WTD, VMC and WFPS), methanogenesis dominates (Couwenberg & Fritz, 2012). Hence, in dry soil net methane fluxes are typically negative and in wet soil net methane fluxes are typically positive (Couwenberg & Fritz, 2012). In temperate peatlands significant emissions of methane only occur when the water table is above  $-0.2$  m, as 20 cm of oxic peat is typically sufficient to oxidise the methane produced in the peat column (Couwenberg & Fritz, 2012). In addition, when the water level is above the peat surface, methane emissions can often decrease as methane can be consumed in the oxygenated water (Bubier, 1995; Couwenberg & Fritz, 2012). The methane fluxes that were measured are somewhat consistent with this pattern, with positive methane fluxes starting to be observed at a water table depth of  $-0.4$  m (Figure 4.11b). However, all but one measurement in the crown, slope or ditch edge landforms had a water table depth below  $-0.2$  m (Figure 4.11b). Methane fluxes from the drainage ditches, when there was standing water were on occasion negative, indicating that methane was likely being consumed within the oxygenated water. Interestingly, it was found that in particularly dry soil with a volumetric moisture content below 40%, methane fluxes tended towards zero. This indicates that in extremely dry soil, where water is limiting, methane oxidation is suppressed. This is attributed to biological water stress as methanotrophs have a physiological requirement for water (Kammann et al., 2001; Mancinelli, 1995).

It is typically expected that temperature should influence methane fluxes, with the rates of both methanogenesis and methane oxidation increasing at higher temperatures (Dalal et al., 2008). However, the results of this study showed that methane fluxes displayed no correlation with shallow soil temperatures when

examining individual chamber flux measurements (Figure 4.11a). Although it should be noted that due to the very low measured methane fluxes when compared to the literature, any temperature dependence was likely to be difficult to detect. Within the literature, many studies have shown a relationship between methane fluxes and temperature, however many have not (Moore & Roulet, 1993). There are several possible factors that can influence the relationship between methane fluxes and temperature. Firstly, there is a high degree of spatial and temporal variation in methane fluxes that can make it difficult to discern clear correlations. Secondly, methane fluxes are the net result of two separate processes; methanogenesis and methane oxidation. These two processes occur at different depths within peat soils, with methanogenesis usually occurring deeper than methane oxidation (Baird et al., 2019). Temperatures at these different depths can be different from each other and have different patterns over time. Hence, when comparing methane fluxes to a temperature recorded from a fixed depth, it is not surprising that there is no relationship between the two variables. As stated in Baird et al. (2019) “It is therefore, perhaps more noteworthy when relationships exist between the methane flux and the temperature recorded at a single fixed depth than when they do not”. In addition, both processes have a different response to a change in temperature with methanogenesis being more sensitive to the temperature. This is reflected in  $Q_{10}$  values of 1.7 – 16 and 1.4 – 2.1 for methanogenesis and methane oxidation respectively (van Huissteden et al., 2016). This is likely to be the reason why no relationship was apparent between measured methane fluxes and soil temperatures (Figure 4.11a) as the soil temperature was measured at a depth of 5 cm. Lastly, there is the influence of other variables that may mask any correlation between methane fluxes and soil temperature. For example, the influence of temperature on methane fluxes can be obscured by the influence of water saturation (Fang & Moncrieff, 2001; Oertel et al., 2016). This was shown by Luan and Wu (2015), who found that in the wet season only soil temperature and methane fluxes were correlated, while in the dry season only the water table depth and methane fluxes were correlated.

Although methane fluxes measured by chambers in the present study showed little correlation with soil temperature during individual flux measurements, on



longer timescales such as monthly averages there was a linear relationship between means of methane fluxes measured by eddy covariance and both the air temperature and soil temperature (Figure 4.22). The monthly average temperature likely shows a higher correlation to methane fluxes than the individual shallow soil temperature measurements because the longer-term average is indicative of relative warming or cooling of the temperatures at all depths within the peat profile.

#### **4.4.2.2 Soil chemical properties**

There did not appear to be any correlation between methane fluxes and soil pH. However, this is likely because over the study period there was no significant change in the pH in each of the landforms. For the most part pH measurements from the ditch edge landforms were between 4 – 5, measurements from the slope landforms were between 5 – 6 and measurements from the crown landforms were between 6 – 7.

The role that mineral nitrogen (i.e. ammonium and nitrate) has on methane oxidation has been found to vary. In the past it was often assumed that methane oxidation is inhibited by the addition of mineral nitrogen and hence the addition of mineral nitrogen to soils was seen to increase methane fluxes (Bodelier & Laanbroek, 2004). However, many studies have since shown that the addition of nitrogen can have no effect or in some cases can increase the rate of methane oxidation (e.g. Bodelier et al., 2000; Jacinthe & Lal, 2006; Kiese et al., 2003; Tate et al., 2006). The inconsistencies between findings is likely a result of the composition of the microbial community as Type I methanotrophs are typically stimulated by nitrogen addition while Type II methanotrophs are typically inhibited (Mohanty et al., 2006). The results showed that methane oxidation increased as the concentration of ammonium increased. However, the majority of soil samples taken did not have any detectable nitrate. If nitrate was present, concentrations were between 16 – 35  $\mu\text{g g}^{-1}$ soil. Hence, the relationship between methane fluxes and nitrate concentrations was unable to be determined. In addition, this study was not a controlled experiment, which makes identifying a relationship more difficult as there are a range of interrelated factors that can

influence methane fluxes. The decrease in methane fluxes associated with an increased ammonium concentration could indicate that the primary methanotrophs present at the study site are Type II. As Type II methanotrophs are typically dominant in environments where nitrogen levels are limited, this is what was expected as the majority of the soil samples had no detectable nitrate (Hanson & Hanson, 1996). The lack of nitrate in the soils is likely due to denitrification occurring in the soil. Figure 4.11 shows that the WFPS was mostly above 55%, with a few measurements associated with the March chamber sampling campaign below 50%. Denitrification is an anaerobic process that uses nitrate as a terminal electron acceptor to oxidise organic matter and typically is dominant in soils with a WFPS above 60% (Heinen, 2006; Meixner & Yang, 2006). Thus, it is likely that the nitrate within the soil is denitrified to nitrogen gas. In addition, nitrate reduction is thermodynamically more favourable than methanogenesis and hence outcompetes methanogens for available substrates (Dalal et al., 2008)

Methane fluxes showed no correlation with the soil Olsen-P within the slope and ditch edge landforms and a slight inverse relationship between methane fluxes and Olsen-P in the crown landform. The  $R^2$  was 0.32, which shows that there is a moderate correlation between methane fluxes and the Olsen-P. The effect that phosphorus has on methane oxidation is still not fully understood with different studies finding positive correlations, some finding negative correlations and some finding no correlation (Veraart et al., 2015). Due to this and the fact that this study was not a controlled experiment, no conclusion about the relationship between methane fluxes and Olsen-P can be drawn.

#### **4.4.2.3 Drainage ditch physical and chemical properties**

The microbial processes within drainage ditches that regulate methane fluxes are variables such as sediment / water temperature, dissolved oxygen concentration, organic matter availability and composition, sediment and water chemistry, availability of electron acceptors, pH, conductivity and water depth (as cited in Schrier-Uijl et al., 2011). The physical and chemical properties of water in the drainage ditches were analysed and it was found that there was no correlation

between methane fluxes and any measured variable. This included pH, dissolved oxygen, conductivity, water temperature, water depth, dissolved phosphorus and nitrate concentrations. Also, the water filled pore space / soil moisture content from the drainage ditches when there was no water present in the drains was not correlated to methane fluxes.

The National Policy Statement for Freshwater Management 2014 sets out the water quality requirements for freshwater in New Zealand. The national bottom line for nitrate and dissolved oxygen in rivers is 6.9 mg/L and 5 mg/L respectively (New Zealand Government, 2017). The 5 mg/L bottom line for dissolved oxygen refers to the threshold below which aquatic life is harmed. The point at which anoxic conditions are assumed to occur are at dissolved oxygen concentrations below 0.5 mg/L (Zogorski et al., 2006). The nitrate concentration in the drainage ditches ranged from 0.21 – 0.58 mg/L and the dissolved oxygen concentration ranged from 5.6 – 9.7 mg/L. Hence, the concentration of nitrate observed within the drainage ditches are an acceptable level, which is unlikely to cause eutrophication or anoxic conditions. This is further shown by the dissolved oxygen concentration being above 5 mg/L, which shows that the drainage ditches are in an aerobic state (Figure 4.14b). This likely reduced the amount of methane emitted from the drainage ditch as the methane is able to be oxidised as it diffuses through the water. Additionally, nitrate is an electron acceptor and as such will act to suppress methanogenesis as nitrate reduction is thermodynamically more favourable than methanogenesis (Dalal et al., 2008).

In the drainage ditches there was no relationship between methane fluxes and temperature, pH or dissolved phosphorus. The pH of the water within the drainage ditches was fairly consistent over the study period, ranging between 3.5 – 4.5 (Figure 4.14a). This is lower than what other studies have reported for drainage ditches. For example, Schrier-Uijl et al. (2011) measured the pH in their drainage ditches to be between 6.8 – 9. In addition, the optimum pH range of methane production is 5 – 7.5 (Inubushi et al., 2005), which means that the low pH in the drainage ditches could be inhibiting the rate of methane production and therefore

could be one mechanism to explain why methane fluxes from the drainage ditches were so low when compared to other studies (Table 4.5)

Within drainage ditches methane emissions are comprised of diffusive fluxes from the water's surface, plant transport and from ebullition events (methane gas bubbles) rising through the water column from the sediment-water boundary (Barber et al., 1988). As the methane rises through the water column, it is able to be consumed through two main processes. The first is oxidation by methanotrophs in the presence of dissolved oxygen and the second is through the nitrate / nitrite reduction pathway (denitrification-dependent anaerobic methane oxidation) (Liu et al., 2017). The localised and stochastic nature of ebullition events makes them extremely difficult to measure or quantify (Couwenberg & Fritz, 2012; Goodrich et al., 2011). In addition, ebullition can occur as a steady stream of small bubbles which can appear as a linear increase in chamber headspace methane concentrations (Coulthard et al., 2009). Hence, the relative contribution of ebullition and diffusive fluxes to measured methane fluxes was unable to be determined. However, there were no large "steps" in the chamber headspace concentration time series, which would indicate that no ebullition events were captured in any of the chamber measurements. If the methane flux is primarily the result of diffusion rather than ebullition, this could be another possible mechanism to explain why methane fluxes from the drainage ditches were so low when compared to other studies (Table 4.5) as the methane is available for oxidation as it diffuses through the water.

### **4.4.3 Annual and seasonal methane fluxes**

#### **4.4.3.1 Eddy covariance**

Eddy covariance measurements of methane fluxes were made using a CW-QCL over one year, including the period of chamber measurements discussed in the previous sections, and also form the basis of larger-scale spatial and temporal estimates. Mean daily methane fluxes at the study site were primarily positive, with mean fluxes generally within the 0 – 1.5 mg CH<sub>4</sub> m<sup>-2</sup> h<sup>-1</sup> range (Figure 4.16). All but three mean daily fluxes were below 3.5 mg CH<sub>4</sub> m<sup>-2</sup> h<sup>-1</sup>. There were a small

number of negative mean daily fluxes, although only two of the negative methane fluxes were  $<-1 \text{ mg CH}_4 \text{ m}^{-2} \text{ h}^{-1}$ . It is typically expected that there is a seasonal variation in methane fluxes as they respond to changes in the temperature and water availability (via rainfall). Although this seasonal variation is not obvious in the mean daily methane fluxes (Figure 4.16), there is a seasonal variation to mean seasonal methane fluxes (Table 4.4). The mean methane fluxes were highest in summer and lowest in winter at  $0.681$  and  $0.443 \text{ mg CH}_4 \text{ m}^{-2} \text{ h}^{-1}$  respectively. The summer and winter methane fluxes were statistically different ( $p = 0.0092$ ), although no other pairing of the seasonal mean methane fluxes was statistically different. It is likely a combination of temperature and rainfall that drives the seasonal pattern in methane fluxes that were observed. Saarnio et al. (1997) noted that that methane fluxes are best correlated to peat temperature. This is because the temperature can influence the rates of both methanogenesis and methane oxidation (Saarnio et al., 1997). There was found to be a linear relationship between mean monthly methane fluxes and both air temperature and soil temperature at our site (Figure 4.22). This would indicate that temperature is one factor driving the seasonality of methane fluxes. Water availability is also likely to influence methane fluxes, along with temperature. It is likely to be the water availability that drives the variance in methane fluxes between spring and autumn as the spring methane flux ( $0.601 \text{ mg CH}_4 \text{ m}^{-2} \text{ h}^{-1}$ ) was higher than the autumn methane flux ( $0.515 \text{ mg CH}_4 \text{ m}^{-2} \text{ h}^{-1}$ ), despite having a lower mean air temperature of  $13.2^\circ\text{C}$  versus  $14.9^\circ\text{C}$  respectively. Hence, it is likely the lower emissions in autumn were a result of the low amount of rain during the autumn period and the resulting low water table and volumetric moisture content (Figures 4.5 & 4.6). Goodrich et al. (2015) investigated the influence of temperature and water table dynamics in a New Zealand, raised bog. Although their study was on a natural peatland it still provides a useful comparison as the peat characteristics and overall climatic setting are relatively similar to our study site due to the close geographical location of the two study sites. They found that the water table regulated the temperature sensitivity of methane fluxes, and that at shallow water table depths this temperature sensitivity was the highest. Below a critical water table depth that they estimated as  $-0.1 \text{ m}$ , the water table exerted a stronger control on methane fluxes, while methane fluxes were less responsive to

temperature (Goodrich et al., 2015). They also observed a seasonal pattern of methane fluxes, with higher summer fluxes and lower winter fluxes and concluded that in wet conditions methane fluxes are driven by temperature, while in dry conditions methane fluxes are driven by the water table depth. Hence, the methane flux dynamics were ultimately controlled by water.

In addition to a seasonal pattern in methane fluxes, a diel pattern was also found in this study, whereby fluxes were higher at night and lower during the day (Figure 4.17). Typical daytime fluxes were between  $0.4 - 0.6 \text{ mg CH}_4 \text{ m}^{-2} \text{ h}^{-1}$ , while night-time fluxes ranged from  $0.6 - 1.2 \text{ mg CH}_4 \text{ m}^{-2} \text{ h}^{-1}$ . There have been a number of studies that have investigated diel variations in methane fluxes from peatlands, however no consensus has been reached, with some studies reporting higher daytime fluxes, some reporting higher night-time fluxes and some reporting no diel variation (e.g. Dooling et al., 2018; Kowalska et al., 2013; Mikkela et al., 1995; Thomas et al., 2010). There are two main processes that influence methane fluxes to cause a diel variation. Firstly, the daily temperature cycle can influence methane fluxes by controlling the rates of both methanogenesis and methane oxidation (Dunfield et al., 1993; Le Mer & Roger, 2001; Serrano-Silva et al., 2014). Secondly, photosynthetic activity during the day can influence methane fluxes. This is due to the resulting production of root exudates that are able to be utilised by methanogens, thereby increasing methane fluxes (Dooling et al., 2018). High methane fluxes often occur at night due to the lag period between photosynthetic activity, root exudate production, utilisation by methanogens and transport to the soil surface. In addition, within drainage ditches methane oxidation can be reduced during the night as less oxygen will be produced which will lower the redox potential and increase methanogenesis (Schrier-Uijl et al., 2011). It is likely that all three of these factors influence the diel variation in methane fluxes to some degree. In addition, the relative importance of each of these factors is likely to vary with other factors, particularly water saturation. As mentioned previously, temperature has a higher influence under wet conditions (Goodrich et al., 2015). Additionally, it is unlikely that root exudates would stimulate methanogenesis during dry conditions as methanogenesis primarily occurs below the water table, which under dry conditions are well below the pasture rooting zone. As a

comparison, in Waikato mineral soils 100% of the root mass (dry weight) of perennial ryegrass occurs within the top 30 cm of soil and 75% occurs within the top 7 cm of soil (Wedderburn et al., 2010).

Annual net methane emissions from the study site were calculated to be 44.72 kg CH<sub>4</sub> ha<sup>-1</sup> yr<sup>-1</sup>. It has been well established in the literature that methane emissions are highly variable both spatially and temporally and reported annual fluxes for drained peatlands are no exception. For example Kandel et al. (2018) found that for a drained temperate peat bog, annual methane emissions were negligible, while both Schrier-Uijl et al. (2010) and Teh et al. (2011) found significant methane emissions of 170.37 and 125.78 kg CH<sub>4</sub> ha<sup>-1</sup> yr<sup>-1</sup> in an intensive grassland on drained peat and drained temperate peatland under pasture respectively. This shows that our study site was a moderate source of methane when compared to the methane fluxes that others have reported from drained peatlands. In addition, the IPCC emission factor for shallow drained, nutrient rich peatlands is 39 kg CH<sub>4</sub> ha<sup>-1</sup> yr<sup>-1</sup>, which is very close to the measured value for our study site. This would lead us to conclude that the calculated annual net methane flux is for drained peatlands under dairy grazing. However, it should be noted that during the period January to June 2019 the study site had very dry conditions with only 55% of the normal amount of rainfall (Figure 4.5). Hence, it is surprising that even under the extremely dry conditions, the study site was still a net methane source. Furthermore, it would suggest that under normal rainfall conditions the measured net annual methane flux might be even higher due to the wetter soil conditions.

The net methane flux for our study site was calculated to be 44.72 kg CH<sub>4</sub> ha<sup>-1</sup> yr<sup>-1</sup>. Goodrich et al. (2015) measured methane emissions from a natural peatland in New Zealand at the Kopuatai wetland, an ombrotrophic raised bog, which is the largest remaining unaltered peatland in New Zealand (Goodrich et al., 2015). They measured net annual methane emissions of 292.5, 196.3, 199.0 and 189.7 kg CH<sub>4</sub> ha<sup>-1</sup> yr<sup>-1</sup> for 2012 – 2015 respectively (Goodrich et al., 2017). These methane fluxes are substantially higher than the methane fluxes that were measured at our study site. However, this is not unusual as methane emissions are significantly reduced when wetlands are drained (Hahn et al., 2018; Tiemeyer et al., 2016). If it is

assumed that the measured methane emissions from Kopuatai (189.7 – 292.5 kg CH<sub>4</sub> ha<sup>-1</sup> yr<sup>-1</sup>) are representative of pristine peatlands and our calculated value (44.72 kg CH<sub>4</sub> ha<sup>-1</sup> yr<sup>-1</sup>) is representative of drained peatlands under dairy grazing, then when drained, peatland methane emissions are reduced by 76 – 85%, which is in line with what is reported in the literature. Abdalla et al. (2016) reported that drainage results in a reduction of methane emissions by an average of 84%.

Methane fluxes from an undrained section of the Moanatuatua peat bog were measured over the 2016 – 2017 period (University of Waikato, Unpublished data). Methane fluxes measured from Moanatuatua were approximately 20 kg CH<sub>4</sub> ha<sup>-1</sup> yr<sup>-1</sup> over the 2016 – 2017 period (University of Waikato, Unpublished data). This is considerably lower than what was measured at the study site (44.72 kg CH<sub>4</sub> ha<sup>-1</sup> yr<sup>-1</sup>), which is located on a drained section of the Moanatuatua peat bog. This is unusual as methane fluxes from the undrained site should be higher than from the drained site. However, the low methane fluxes from Moanatuatua wetland could be caused by the extremely low water table compared to other natural wetland sites such as Kopuatai. For example over the 2015 – 2016 period the water table depth at Moanatuatua ranged from 0.24 – 0.94 m below the peat surface while Kopuatai ranged from 0.06 – 0.17 m below the peat surface (Ratcliffe et al., 2019). In addition, the higher methane fluxes measured at the study site could be due to the impacts of grazing as the water table depth at the study site was similar to that observed at Moanatuatua (Figure 4.11b). This is possibly because the addition of cow dung has been shown to increase methane fluxes and change the microbial community due to the addition of rumen-associated methanogens (Hahn et al., 2018).

Substantial methane emissions have recently been identified in pastures on mineral soils. For example, for a dairy farm site on a mineral soil, mean methane fluxes in February 2017 were 0.44 mg CH<sub>4</sub> m<sup>-2</sup> h<sup>-1</sup> (Campbell, personal communication, October 9, 2019). This site is located approximately 28 km from Gamma Farm and a site description can be found in Wecking et al. (2020). In addition, Laubach and Hunt (2018) measured annual methane fluxes of 49.41 kgCH<sub>4</sub>ha<sup>-1</sup>yr<sup>-1</sup> from a irrigated pasture in Canterbury, New Zealand. At our study



site mean daily methane fluxes were primarily in the 0 – 1.5 mg CH<sub>4</sub> m<sup>-2</sup> h<sup>-1</sup> range (Figure 4.16) and the net annual methane flux was 44.72 kg CH<sub>4</sub> ha<sup>-1</sup> yr<sup>-1</sup>. The fact that these two mineral soils have similar methane fluxes is unusual as mineral pasture soils are typically small methane sinks with fluxes >–1 kg CH<sub>4</sub> ha<sup>-1</sup> yr<sup>-1</sup> (Saggar et al., 2008). Laubach and Hunt (2018) found that the methane emissions from cow excreta (dung and urine) only accounted for a minor fraction of the methane fluxes, and therefore the majority of the methane fluxes must originate from other sources. They postulated three different possible methane sources. First, the application of nitrogen fertilisers could inhibit methane oxidation and / or stimulate methanogenesis (Laubach & Hunt, 2018). Second, plants have been shown to emit methane after physical injury (Bruhn et al., 2012; Laubach & Hunt, 2018). Hence after a grazing event, the grass itself may be a source of methane. Lastly, plants have been shown to emit methane at rates of 200 ng CH<sub>4</sub> g<sup>-1</sup>DM h<sup>-1</sup> when irradiated with UV light (Laubach & Hunt, 2018; Vigano et al., 2008). In addition, it is typically expected that peat soils would have a higher net methane flux due to high methane emissions from drainage ditches. This is because drainage ditches typically contribute up to 60 – 70% the total methane emissions (Schrier-Uijl et al., 2010).

#### **4.4.3.2 Eddy covariance versus chamber measurements**

There was a large discrepancy between the methane fluxes measured by chambers and the methane fluxes measured by eddy covariance. From the chamber measurements, the crown, slope and ditch edge landforms were found to be net methane sinks, while the drainage ditches were a net methane source, with the study site overall being a net methane sink (Figures 4.8 & 4.24). However, the eddy covariance data suggests the study site being a net methane source (Figures 4.16 & 4.24). The reason that there is a large discrepancy between the two methods is not entirely clear.

It is possible that the discrepancy between the chamber measurements and the eddy covariance measurements is largely caused by the different spatial and temporal scales of the two measurement techniques. For example, during each sampling campaign 12 chambers were deployed covering a total area of 0.54 m<sup>2</sup>

(0.045 m<sup>2</sup> individually), while eddy covariance measures fluxes over several hectares (as the flux footprint moves around). In addition, each chamber measurement only lasted 45 minutes, while eddy covariance provides continuous half-hourly measurements. Methane fluxes from drained peatlands are highly variable both spatially and temporally, this means that eddy covariance measurements are more suited to accurately capturing spatially averaged methane fluxes at fine-scale temporal resolution. This contrasts with the small spatial and temporal extent of the chamber measurements which means that the fluxes measured by the chambers may not be representative of what is occurring over the entire paddock. Hence, it is possible that all of the chamber measurements simply missed areas or times that had high methane fluxes. In addition, it should also be noted that there can be some bias introduced into the eddy covariance measurements due to the methodology that is used to calculate fluxes. The flux footprint of an eddy covariance tower is the area where the measured gas fluxes originate (i.e. fluxes generated in this area are registered by the instruments on the eddy covariance tower) (Burba, 2013). The fetch is the distance between the flux tower and the distant edge of the flux footprint (Burba, 2013). However, the footprint area does not contribute to the measured flux equally. The contribution of different areas of the footprint is shown in Figure 4.25.

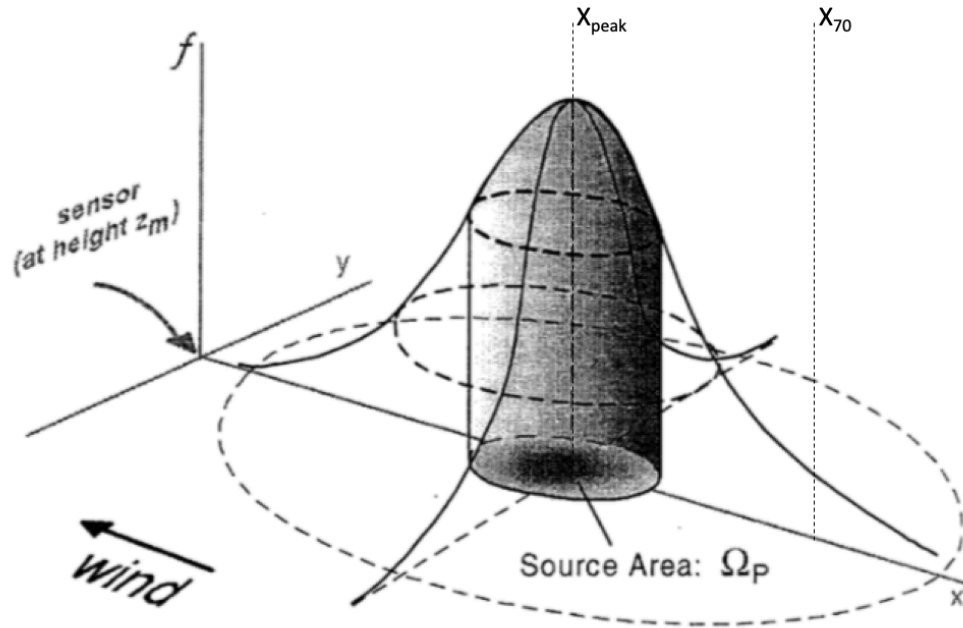


**Figure 4.25** Conceptual model showing the relative contribution to the measured flux of the footprint area of an eddy covariance flux tower. The eddy covariance flux tower is at an upwind distance of zero [Adapted from: Schmid (2002)].

$X_{\text{peak}}$  is the distance from the flux tower to the peak of the footprint flux probability distribution and  $X_{70}$  is the distance from the flux tower within which 70% of the measured flux is sourced (Burba, 2013). Hence, the measured methane flux can change based on the spatial variation of methane fluxes across the landscape, combined with the size and shape of the flux footprint (Teh et al., 2011). At our study site,  $X_{\text{peak}}$  was generally less than 25 m and  $X_{70}$  was generally less than 150 m (Figure 4.18). This means that the majority of the measured methane fluxes were sourced from within the two study paddocks. Examining the wind direction and the measured methane fluxes (Figure 4.19) there was a higher density of fluxes measured between 225 and 270°. Although the majority of the measured fluxes were below  $1 \text{ mg CH}_4 \text{ m}^{-2} \text{ h}^{-1}$ , when the wind was blowing from this direction there was a higher proportion of methane fluxes that were above  $1 \text{ mg CH}_4 \text{ m}^{-2} \text{ h}^{-1}$  (Figure 4.19). Combining the wind direction and footprint peak distance ( $X_{\text{peak}}$ ), when the wind is blowing from the southwest between 225 and 270°,  $X_{\text{peak}}$  was typically less than 18 m (Figure 4.20). This shows that there is a slight bias in the measured methane fluxes, with a higher proportion of high methane fluxes sourced from the southwest and within 18 m from the eddy covariance flux tower.

As there is a shallow drainage ditch (“spinner drain”) that is located to the south of and in close proximity to the flux tower, the cause of the higher measured fluxes could be due to a higher proportion of the measured methane fluxes being sourced from a drainage ditch. Hence, this could result in a higher measured net flux and explain some of the discrepancy between the chamber measurements and the eddy covariance measurements.

Another possibility is that there was a problem in the chamber design or use. It should be noted that linear regression was used to calculate the flux, which has some inherent errors associated with its use. It has been well established in the literature that due to the inherent non-linearity of chamber gas fluxes linear regression will tend to underestimate the gas flux (e.g. Pihlatie et al., 2013). For example Pihlatie et al. (2013) found that the use of linear regression underestimated the gas flux by up to 33%. Despite this, linear regression is still widely used when calculating gas fluxes. However, there was no evidence of any non-linear increases in the chamber headspace concentrations. In addition, this is unable to explain the discrepancy between the spatially weighted chamber-based methane fluxes for our study site and the corresponding methane fluxes measured by eddy covariance (Figure 4.24). This is because the flux underestimation acts to bring the measured flux closer to zero. Hence, the crown, slope and ditch edge landforms would have a higher rate of net methane oxidation and the drainage ditch would have a higher rate of net methane emission. When calculating the overall flux for the study site, as the underestimation occurs on all of the individual flux measurements equally, the net flux for the study site is also affected equally. Hence, when the study site was found to be a net sink, if the flux underestimation was corrected then the net sink strength would increase. Therefore, the discrepancy would actually increase for every sampling date except for 2 September when the study site was found to be a small methane source (Figure 4.24). It would also not explain the much smaller drainage ditch fluxes measured by the chambers compared to the literature (Table 4.5) as all but three studies used linear regression (Hendriks et al., 2007; Huttunen et al., 2003; Minkkinen & Laine, 2006; Schrier-Uijl et al., 2010). For the remaining three, two did not state

their method (Bubier et al., 1993; Waddington & Day, 2007) and one used a boundary layer methodology instead of flux chambers (Hamilton et al., 1994).

It is also possible that during chamber deployment ambient air could have entered the chambers either through a leaking seal or the vent tube, thereby lowering the measured flux. While this could explain why the measured methane fluxes in the drainage ditches were so low when compared to other studies, it still does not explain the variance between the chamber fluxes and the eddy covariance fluxes for the same reasons using linear regression does not. This is because ambient air entering the chamber also acts to bring the measured flux to zero. Hence, ambient air entering the chamber would result in lower measured rates of both methane oxidation and methane emissions. Therefore, the overall net flux for the study site is unlikely to change significantly.

Lastly, the net methane fluxes calculated for each sampling date from chamber measurements do not include any contribution to the methane flux that is sourced from cow dung patches. The effect of this is likely minor as methane fluxes from cow dung are typically only high when freshly deposited with methane fluxes quickly trending towards zero (Saggar et al., 2004). Methane fluxes typically return to normal levels 10 -35 days after the deposition of cow dung (Mori & Hojito, 2015). As there was only one sampling day with large methane fluxes from cow dung (days since grazing = 11), and due to the low spatial extent of the cow dung, it can be concluded that the methane flux contribution from cow dung is likely to be minor. The inclusion of the cow dung contribution would have increased the net flux measured by the chambers and hence decreased the discrepancy between the chamber data and the eddy covariance data to some degree. However, this reduction would be minor and would only occur immediately after a grazing event. In addition, there was no clear pattern of increased methane fluxes, following grazing events observable over the normal spatial and temporal variations in methane fluxes.

Thus, it is still unclear why there is a discrepancy between the chamber measurements and the eddy covariance measurements. But the most likely

explanation is the large spatial and temporal scale differences between the two measurement techniques.

Our approach could be improved by both using more chambers and increasing the number of sampling dates. During each sampling campaign 12 chambers were used. Three chambers measured methane fluxes from each of the crown and slope landforms and two chambers measured methane fluxes from each of the ditch edge and drainage ditch landform as well as cow dung patches. At least four chamber measurements per landform would be ideal as this would provide a higher confidence in measured fluxes. More frequent chamber measurements would also be ideal as this would provide much better insight into temporal variation of methane fluxes. Both of these improvements would act to reduce the spatial and temporal scale differences between chamber measurements and eddy covariance measurements.

#### **4.4.4 Impact of drained peatlands on New Zealand's greenhouse gas inventory**

Taking the measured net methane emissions ( $44.72 \text{ kg CH}_4 \text{ ha}^{-1} \text{ yr}^{-1}$ ) and the area of drained peatlands under agricultural use in New Zealand (154,108 ha), it can be calculated that drained peatlands under agricultural use in New Zealand might emit 6.89 kt  $\text{CH}_4$  (192.92 kt  $\text{CO}_2\text{-eq}$ ) per year. These emissions are relatively small when compared to the total annual emissions of methane in New Zealand (34,132 kt  $\text{CO}_2\text{-eq}$ ), the total annual agricultural emissions in New Zealand (38,881 kt  $\text{CO}_2\text{-eq}$ ) or the total annual greenhouse gas emissions from agricultural soils in New Zealand (8,566 kt  $\text{CO}_2\text{-eq}$ ) (Ministry for the Environment, 2019b). As New Zealand does not currently include drained peatland methane emissions in its greenhouse gas inventory, the inclusion of methane emissions from drained peatlands under agricultural use would only increase total annual methane and agricultural emissions by 0.6 and 0.5% respectively. Although, the methane emissions from drained peatlands seems small when comparing to total annual methane emissions for New Zealand, the 6.89 kt of methane (192.92 kt  $\text{CO}_2\text{-eq}$ ) emitted annually is still a significant contribution to net greenhouse gas emissions. To put

the emissions into perspective, these emissions are equivalent to CO<sub>2</sub> emissions from burning 85,436,344 kg of coal or the electricity use of 30,046 homes (United States Environmental Protection Agency, 2018). In addition, the spatial extent of drained peatlands in New Zealand is relatively low, especially when compared to European countries such as the UK. For example, annual methane emissions from UK peat grasslands are 6,300 kt CO<sub>2</sub>-eq.

New Zealand agricultural peatlands are typically drained using one of two main drainage ditch styles: shallow-drained and deep-drained. Shallow-drained peatlands such as our study site are drained by a series of shallow “spinner” drains within the paddocks that discharge into deeper “border” drains. Conversely, deep-drained peatlands are typically only drained by deep “border” drains at the paddock edges. Deep-drained peatlands typically have a deeper water table and therefore methane emissions are expected to be lower. This is shown by the IPCC emission factors of 39 kg CH<sub>4</sub> ha<sup>-1</sup> yr<sup>-1</sup> versus 16 kg CH<sub>4</sub> ha<sup>-1</sup> yr<sup>-1</sup> for shallow-drained and deep-drained, nutrient rich peatlands respectively. In addition, this study only comprises of one year of methane flux measurements. Hence, there are some limitations in the application of the calculated annual net flux to New Zealand drained peatlands. However, the overall management practices for drained peatlands in New Zealand are likely to be similar and as studies on methane fluxes from drained peatlands in New Zealand are limited, the net methane emission presented here (44.72 kg CH<sub>4</sub> ha<sup>-1</sup> yr<sup>-1</sup>) is the best estimate for methane emissions from drained New Zealand peatlands under agricultural use.

# Chapter Five

## Summary and conclusions

---

### 5.1 Review of thesis aims and objectives

The aim of this study was to determine the magnitude of methane emissions from drained peatland under dairy grazing and where and when do the emissions occur throughout the year. In order to achieve this aim, the objectives were to:

- Determine where the methane emission hotspots are and when are they active.
- Determine how much methane is emitted by scaling up small-scale chamber measurements.
- Determine total methane emissions as measured by eddy covariance and reconcile this with the small-scale chamber measurements.

The hypotheses were:

- That methane emissions will be elevated in close proximity to drains where the water table is elevated.
- That soil-based methane emissions from a drained peatland under dairy grazing will be elevated compared to a mineral soil.

### 5.2 Summary

The methane flux from our study site was found to be highly variable, both spatially and temporally, with maximum emissions of  $0.365 \text{ mg CH}_4 \text{ m}^{-2} \text{ h}^{-1}$  and maximum uptake of  $-0.101 \text{ mg CH}_4 \text{ m}^{-2} \text{ h}^{-1}$ . The crown, slope and ditch edge landforms were a net sink of methane averaging  $-0.019 \pm 0.005$ ,  $-0.019 \pm 0.008$  and  $-0.023 \pm 0.006 \text{ mg CH}_4 \text{ m}^{-2} \text{ h}^{-1}$  respectively. Interestingly, and in contrary to hypothesis 1, methane emissions in close proximity to the drainage ditches (i.e. the drain edges) were not elevated but were in fact the strongest sink of methane. The drainage ditches were a net source of methane averaging  $0.071 \pm 0.021 \text{ mg}$



$\text{CH}_4 \text{ m}^{-2} \text{ h}^{-1}$ . In addition to the drainage ditches, cow dung patches were also a source of methane. Cow dung emissions were initially very high (up to  $12.3 \text{ mg CH}_4 \text{ m}^{-2} \text{ h}^{-1}$ ) immediately after grazing and tended to decrease to zero as the days since grazing increased.

Methane fluxes from the drained peatland system were ultimately driven by the water table depth, with temperature becoming important at shallow water table depths when water was not limiting. In general, methane fluxes increased as temperature increased and depth to the water table decreased. However, when the water table was at its deepest, and the soil VMC dropped below 40%, methane fluxes tended towards zero, decreasing the rate of net methane oxidation. In addition, soil methane fluxes also tended to decrease as the concentration of ammonium increased. Within the drainage ditches the methane fluxes from the water surface did not have any apparent relationship with any water properties (pH, conductivity, dissolved oxygen, water temperature, water depth, nitrate concentration or dissolved phosphorus) that were measured. In addition, the highest methane fluxes that were measured in the drainage ditches occurred when there was no standing water present in the drainage ditch. However, the soil in the bottom of the drainage ditches was still relatively wet, with a VMC of 76 and 62% during the associated two sampling dates. The high emissions occurred because the maximum methane emission rate occurs when the soil is saturated, and the water table depth is close to the soils surface. In addition, due to variations in the water table depth and the temperature, a seasonal pattern in the methane flux was observed with higher fluxes in summer and lower fluxes in winter.

Chamber measurements showed that the crown, slope and ditch edge landforms were a net methane sink, while the drainage ditches were a net methane source. When the chamber measurements were weighted by the landform areas, they indicated that our study site was primarily a net methane sink. However, eddy covariance measurements over the same period showed that the study site was a net methane source with mean daily emission rates typically between 0 and  $1.5 \text{ mg CH}_4 \text{ m}^{-2} \text{ h}^{-1}$ . Hence, there is a large discrepancy between the two measurement techniques. Although the exact cause of this was not determined, it is likely due

to the large spatial and temporal scale differences between the two measurement techniques.

The annual net methane flux calculated from eddy covariance measurements to be  $44.72 \text{ kg CH}_4 \text{ ha}^{-1} \text{ yr}^{-1}$ . Currently, New Zealand does not include methane emissions from drained peatland soils or drains in its greenhouse gas inventory (Ministry for the Environment, 2019b). As New Zealand has 154,108 ha of drained peatlands under agricultural use, this represents 6.89 kt  $\text{CH}_4$  (192.92 kt  $\text{CO}_2\text{-eq}$ ) per year that are not accounted for. However, if these emissions were included in the greenhouse gas inventory, New Zealand's total annual methane (34,132 kt  $\text{CO}_2\text{-eq}$ ) and total annual agricultural (38,881  $\text{CO}_2\text{-eq}$ ) emissions would only be increased by 0.6 and 0.5% respectively.

### **5.3 Recommendations for future research**

Future research could focus on determining where methane emissions are sourced from in soils. This could apply not only to peat soils, but also to mineral soils as recent measurements such as those of Laubach and Hunt (2018) have shown significant methane emissions from pasture on mineral soils. Hence, drainage ditches and cow dung patches are not the only significant source of methane in soils.



## References

---

- 2 Degrees Institute. (n.d.). *Atmospheric CH<sub>4</sub> Levels Graph*. Retrieved from <https://www.methanelevels.org/#sources>
- Abdalla, M., Hastings, A., Truu, J., Espenberg, M., Mander, Ü., & Smith, P. (2016). Emissions of methane from northern peatlands: a review of management impacts and implications for future management options. *Ecol Evol*, *6*(19), 7080-7102. <https://doi.org/10.1002/ece3.2469>
- Adhya, T. K., Pattnaik, P., Satpathy, S. N., Kumaraswamy, S., & Sethunathan, N. (1998). Influence of phosphorus application on methane emission and production in flooded paddy soils. *Soil Biology & Biochemistry*, *30*, 177-181. [https://doi.org/10.1016/s0038-0717\(97\)00104-1](https://doi.org/10.1016/s0038-0717(97)00104-1)
- Allaby, M. (2013). *A Dictionary of Earth Sciences*. Oxford, UK: Oxford University Press.
- Alm, J., Shurpali, N., Minkinen, K., Aro, L., Hytönen, J., Laurila, T., . . . Laine, J. (2007). Emission factors and their uncertainty for the exchange of CO<sub>2</sub>, CH<sub>4</sub> and N<sub>2</sub>O in Finnish managed peatlands. *Boreal Environmental Research*, *12*, 191-209.
- Ausseil, A. G. E., Jamali, H., Clarkson, B. R., & Golubiewski, N. E. (2015). Soil carbon stocks in wetlands of New Zealand and impact of land conversion since European settlement. *Wetlands Ecology and Management*, *23*, 947-961. <https://doi.org/10.1007/s11273-015-9432-4>
- Baethgen, W. E., & Alley, M. M. (1989). A manual colorimetric procedure for measuring ammonium nitrogen in soil and plant Kjeldahl digests. *Communications in Soil Science and Plant Analysis*, *20*(9), 961-969. <https://doi.org/10.1080/00103628909368129>
- Baird, A. J., Green, S. M., Brown, E., & Dooling, G. (2019). Modelling time-integrated fluxes of CO<sub>2</sub> and CH<sub>4</sub> in peatlands: A review. *Mires and Peat*, *24*, 1-15. <https://doi.org/10.19189/MaP.2019.DW.395>
- Baldocchi, D., Detto, M., Sonnentag, O., Verfaillie, J., Teh, Y. A., Silver, W., & Kelly, N. M. (2012). The challenges of measuring methane fluxes and concentrations over a peatland pasture. *Agricultural and Forest Meteorology*, *153*, 177-187. <https://doi.org/10.1016/j.agrformet.2011.04.013>
- Barber, T., Burke, R., & Sackett, W. (1988). Diffusive flux of methane from warm wetlands. *Global Biogeochemical Cycles*, *2*(4), 411-425.
- Beetz, S., Liebersbach, H., Glatzel, S., Jurasinski, G., Buczko, U., & Höper, H. (2013). Effects of land use intensity on the full greenhouse gas balance in an

- Atlantic peat bog. *Biogeosciences*, 10, 1067-1082.  
<https://doi.org/10.5194/bg-10-1067-2013>
- Berglund, O. (2011). *Greenhouse gas emissions from cultivated peat soils in Sweden* (Doctoral thesis). Swedish University of Agricultural Sciences, Uppsala, Sweden.
- Bhullar, G. S., Edwards, P. J., & Olde Venterink, H. (2013). Variation in the plant-mediated methane transport and its importance for methane emission from intact wetland peat mesocosms. *Journal of Plant Ecology*, 6, 298-304.  
<https://doi.org/10.1093/jpe/rts045>
- Blakemore, L., Searle, P., & Daly, B. (1987). *Methods for chemical analysis of soils*. Lower Hutt, New Zealand: NZ Soil Bureau.
- Bodelier, P. L., Roslev, P., Henckel, T., & Frenzel, P. (2000). Stimulation by ammonium-based fertilizers of methane oxidation in soil around rice roots. *Nature*, 403, 421-424.
- Bodelier, P. L. E., & Laanbroek, H. J. (2004). Nitrogen as a regulatory factor of methane oxidation in soils and sediments. *Fems Microbiology Ecology*, 47, 265-277. [https://doi.org/10.1016/s0168-6496\(03\)00304-0](https://doi.org/10.1016/s0168-6496(03)00304-0)
- Boone, D. (1993). Biological Formation and Consumption of Methane. In M. Khalil (Ed.), *Atmospheric Methane: Sources, Sinks and Role in Global Change* (Vol. 13). Berlin Heidelberg, Germany: Springer-Verlag.
- Boyd, C. (1995). *Bottom Soils, Sediment, and Pond Aquaculture*. Boston, USA: Springer.
- Bridgham, S. D., Cadillo-Quiroz, H., Keller, J. K., & Zhuang, Q. (2013). Methane emissions from wetlands: biogeochemical, microbial, and modeling perspectives from local to global scales. *Global Change Biology*, 19, 1325-1346. <https://doi.org/10.1111/gcb.12131>
- Bridgham, S. D., Megonigal, J., Keller, J. K., Bliss, N., & Trettin, C. (2006). The carbon balance of North American wetlands. *Wetlands*, 26(4), 889-916.
- Bruhn, D., Moller, I. M., Mikkelsen, T. N., & Ambus, P. (2012). Terrestrial plant methane production and emission. *Physiologia Plantarum*, 144, 201-209.  
<https://doi.org/10.1111/j.1399-3054.2011.01551.x>
- Bubier, J. (1995). The relationship of vegetation to methane emission and hydrological gradients in northern peatlands. *Journal of Ecology*, 83(3), 403-420.
- Bubier, J., Costello, A., Moore, T., Roulet, N. T., & Savage, K. (1993). Microtopography and methane flux in boreal peatlands, northern Ontario, Canada. *Canadian Journal of Botany*, 71, 1056-1063.

- Burba, G. (2013). *Eddy Covariance Method for Scientific, Industrial, Agricultural, and Regulatory Applications: A Field Book on Measuring Ecosystem Gas Exchange and Areal Emission Rates*. Lincoln, NE, USA: LI-COR Biosciences.
- Bürgmann, H. (2011). Methane oxidation (aerobic). In J. Reitner & V. Thiel (Eds.), *Encyclopedia of Geobiology* (pp. 575-578). Dordrecht: Springer Netherlands.
- Cammack, R., Atwood, T., Campbell, P., Parish, H., Smith, A., Vella, F., & Stirling, J. (Eds.). (2008) *Oxford Dictionary of Biochemistry and Molecular Biology* (2 ed.). Oxford, UK: Oxford University Press. <https://doi.org/10.1093/acref/9780198529170.013.12306>
- Castro, M. S., Steudler, P. A., Melillo, J. M., Aber, J. D., & Bowden, R. D. (1995). Factors controlling atmospheric methane consumption by temperate forest soils. *Global Biogeochemical Cycles*, 9, 1-10. <https://doi.org/10.1029/94gb02651>
- Chaban, B., Ng, S. Y., & Jarrell, K. F. (2006). Archaeal habitats—from the extreme to the ordinary. *Canadian Journal of Microbiology*, 52, 73-116. <https://doi.org/10.1139/w05-147>
- Chin, K., Lukow, T., & Conrad, R. (1999). Effect of temperature on structure and function of the methanogenic archaeal community in an anoxic rice field soil. *Applied and Environmental Microbiology*, 65, 2341-2349.
- Christensen, J., Hewitson, B., Busuioc, A., Chen, A., Gao, X., Held, I., . . . Whetton, P. (2007). Regional Climate Projections. In S. Solomon, D. Qin, M. Manning, Z. Chen, M. Marquis, K. Averyt, . . . H. Miller (Eds.), *Climate Change 2007: The Physical Science Basis. Contribution of Working Group I to the Fourth Assessment Report of the Intergovernmental Panel on Climate Change*. Cambridge, United Kingdom and New York, NY, USA.: Cambridge University Press, Cambridge.
- Ciais, P., C. Sabine, G. Bala, L. Bopp, V. Brovkin, J. Canadell, A. Chhabra, R. DeFries, J. Galloway, M. Heimann, C. Jones, C. Le Quéré, R.B. Myneni, S. Piao and P. Thornton. (2013). Carbon and other biogeochemical cycles. In T. F. Stocker, D. Qin, G.-K. Plattner, M. Tignor, S.K. Allen, J. Boschung, A. Nauels, Y. Xia, V. Bex and P.M. Midgley (Ed.), *Climate Change 2013: The Physical Science Basis. Contribution of Working Group I to the Fifth Assessment Report of the Intergovernmental Panel on Climate Change*. United Kingdom and New York, NY, USA: Cambridge University Press.
- Cooper, M. D. A., Evans, C. D., Zielinski, P., Levy, P. E., Gray, A., Peacock, M., . . . Freeman, C. (2014). Infilled ditches are hotspots of landscape methane flux following peatland re-wetting. *Ecosystems*, 17(7), 1227-1241. <https://doi.org/10.1007/s10021-014-9791-3>
- Coulthard, T., Baird, A. J., Ramirez, J., & Waddington, J. M. (2009). Methane dynamics in peat: Importance of shallow peats and a novel reduced-complexity approach for modelling ebullition. In A. J. Baird, L. R. Belyea, X.

- Comas, A. S. Reeve & L. Slater (Eds.), *Carbon cycling in northern peatlands*. Washington, DC, USA: American Geophysical Union,,.
- Couwenberg, J. (2011). Greenhouse gas emissions from managed peat soils: is the IPCC reporting guidance realistic? *Mires and Peat*, *8*, 1-10.
- Couwenberg, J., & Fritz, C. (2012). Towards developing IPCC methane 'emission factors' for peatlands (organic soils). *Mires and Peat*, *10*, 1-17.
- Crill, P. M., Martikainen, P. J., Nykanen, H., & Silvola, J. (1994). Temperature and N fertilisation effects on methane oxidation in a drained peatland soil. *Soil Biology & Biochemistry*, *26*, 1331-1339. [https://doi.org/10.1016/0038-0717\(94\)90214-3](https://doi.org/10.1016/0038-0717(94)90214-3)
- Dalal, R., Allen, D., Livesley, S., & Richards, G. (2008). Magnitude and biophysical regulators of methane emission and consumption in the Australian agricultural, forest, and submerged landscapes: A review. *Plant and Soil*, *309*, 43-76. <https://doi.org/10.1007/s11104-007-9446-7>
- Davoren, A. (1978). *A survey of New Zealand peat resources*. Hamilton, New Zealand: The University of Waikato.
- de Klein, C., & Harvey, M. (2012). *Nitrous oxide chamber methodology guidelines*. Wellington, New Zealand: Ministry for Primary Industries.
- de Klein, C., & Harvey, M. (2015). *Nitrous Oxide Chamber Methodology Guidelines*. Wellington, New Zealand:
- Demarty, M., & Bastien, J. (2011). GHG emissions from hydroelectric reservoirs in tropical and equatorial regions: Review of 20 years of CH<sub>4</sub> emission measurements. *Energy policy*, *39*, 4197-4206. <https://doi.org/10.1016/j.enpol.2011.04.033>
- Denmead, O. T. (2008). Approaches to measuring fluxes of methane and nitrous oxide between landscapes and the atmosphere. *Plant and Soil*, *309*(1-2), 5-24. <https://doi.org/10.1007/s11104-008-9599-z>
- Dlugokencky, E. J. (2019). *Global CH<sub>4</sub> monthly means*. Retrieved from [https://www.esrl.noaa.gov/gmd/ccgg/trends\\_ch4/](https://www.esrl.noaa.gov/gmd/ccgg/trends_ch4/)
- Dlugokencky, E. J., Nisbet, E. G., Fisher, R., & Lowry, D. (2011). Global atmospheric methane: budget, changes and dangers. *Philosophical Transactions of the Royal Society A* *369*, 2058-2072. <https://doi.org/10.1098/rsta.2010.0341>
- Dooling, G. P., Chapman, P. J., Baird, A. J., Shepherd, M. J., & Kohler, T. (2018). Daytime-only measurements underestimate CH<sub>4</sub> emissions from a restored bog. *Écoscience*, *25*, 259-270. <https://doi.org/10.1080/11956860.2018.1449442>
- Duc, N. T., Silverstein, S., Lundmark, L., Reyier, H., Crill, P., & Bastviken, D. (2013). Automated flux chamber for investigating gas flux at water-air interfaces.

*Environmental Science & Technology*, 47, 968-975.  
<https://doi.org/10.1021/es303848x>

- Dunfield, P., Knowles, R., Dumont, R., & Moore, T. (1993). Methane production and consumption in temperate and subarctic peat soils: Response to temperature and pH. *Soil Biology and Biochemistry*, 25, 321-326.
- Eickenscheidt, T., Heinichen, J., & Drösler, M. (2015). The greenhouse gas balance of a drained fen peatland is mainly controlled by land-use rather than soil organic carbon content. *Biogeosciences*, 12, 5161-5184.  
<https://doi.org/10.5194/bg-12-5161-2015>
- Environment Waikato. (2006). *For Peat's Sake: Good management practices for Waikato peat farmers*. Hamilton, New Zealand: Environment Waikato.
- Evans, C. D., Renou-Wilson, F., & Strack, M. (2016). The role of waterborne carbon in the greenhouse gas balance of drained and re-wetted peatlands. *Aquatic Sciences*, 78, 573-590. <https://doi.org/10.1007/s00027-015-0447-y>
- Fang, C., & Moncrieff, J. (2001). The dependence of soil CO<sub>2</sub> efflux on temperature. *Soil Biology & Biochemistry*, 33, 155-165.
- Ferry, J. G. (2010). The chemical biology of methanogenesis. *Planetary and Space Science*, 58, 1775-1783.  
<https://doi.org/https://doi.org/10.1016/j.pss.2010.08.014>
- Flato, G., Marotzke, J., Abiodun, B., Braconnot, P., Chou, S., Collins, W., . . . Rummukainen, M. (2013). Evaluation of Climate Models. In T. Stocker, D. Qin, G. Plattner, M. Tignor, S. Allen, J. Boschung, . . . P. Midgley (Eds.), *Climate Change 2013: The Physical Science Basis. Contribution of Working Group I to the Fifth Assessment Report of the Intergovernmental Panel on Climate Change*. Cambridge, United Kingdom and New York, NY, USA: Cambridge University Press.
- Foken, T., Aubinet, M., & Leuning, R. (2012). The eddy covariance method. In M. Aubinet, T. Vesala & D. Papale (Eds.), *Eddy Covariance: A Practical Guide to Measurement and Data Analysis*. London, UK; New York, USA: Springer.
- Forbrich, I., Kutzbach, L., Hormann, A., & Wilmking, M. (2010). A comparison of linear and exponential regression for estimating diffusive CH<sub>4</sub> fluxes by closed-chambers in peatlands. *Soil Biology & Biochemistry*, 42  
<https://doi.org/10.1016/j.soilbio.2009.12.004>
- Frolking, S., Talbot, J., Jones, M. C., Treat, C. C., Kauffman, J. B., Tuittila, E.-S., & Roulet, N. (2011). Peatlands in the Earth's 21st century climate system. *Environmental Reviews*, 19, 371-396. <https://doi.org/10.1139/a11-014>
- Gao, C., Sander, M., Agethen, S., & Knorr, K.-H. (2019). Electron accepting capacity of dissolved and particulate organic matter control CO<sub>2</sub> and CH<sub>4</sub> formation in peat soils. *Geochimica et Cosmochimica Acta*, 245, 266-277.  
<https://doi.org/10.1016/j.gca.2018.11.004>



- Glaser, P. H., Siegel, D. I., Chanton, J. P., Reeve, A. S., Rosenberry, D. O., Corbett, J. E., . . . Levy, Z. (2016). Climatic drivers for multidecadal shifts in solute transport and methane production zones within a large peat basin. *Global Biogeochemical Cycles*, *30*, 1578-1598. <https://doi.org/10.1002/2016gb005397>
- Goodrich, J. P., Campbell, D. I., Roulet, N. T., Clearwater, M. J., & Schipper, L. A. (2015). Overriding control of methane flux temporal variability by water table dynamics in a Southern Hemisphere, raised bog. *Journal of Geophysical Research: Biogeosciences*, *120*, 819-831. <https://doi.org/10.1002/2014jg002844>
- Goodrich, J. P., Campbell, D. I., & Schipper, L. A. (2017). Southern Hemisphere bog persists as a strong carbon sink during droughts. *Biogeosciences*, *14*, 4563-4576. <https://doi.org/10.5194/bg-14-4563-2017>
- Goodrich, J. P., Varner, R. K., Frohking, S., Duncan, B. N., & Crill, P. M. (2011). High-frequency measurements of methane ebullition over a growing season at a temperate peatland site. *Geophysical Research Letters*, *38*(7), n/a-n/a. <https://doi.org/10.1029/2011gl046915>
- Google Earth. (2019). Google Earth Pro (Version 7.3.2.5776). Retrieved from <https://www.google.com/earth/versions/#earth-pro>
- Graham, D., Chaudhary, J., Hanson, R. S., & Arnold, R. (1993). Factors Affecting Competition between Type I and Type II Methanotrophs in Two-Organism, Continuous-Flow Reactors. *Microbial Ecology*, *25*, 1-17.
- Green, S. M., Baird, A. J., Evans, C. D., Peacock, M., Holden, J., Chapman, P. J., & Smart, R. P. (2018). Methane and carbon dioxide fluxes from open and blocked ditches in a blanket bog. *Plant and Soil*, *424*, 619-638. <https://doi.org/10.1007/s11104-017-3543-z>
- Hahn, J., Juottonen, H., Fritze, H., & Tuittila, E.-S. (2018). Dung application increases CH<sub>4</sub> production potential and alters the composition and abundance of methanogen community in restored peatland soils from Europe. *Biology and Fertility of Soils*, *54*, 533-547. <https://doi.org/10.1007/s00374-018-1279-4>
- Hamilton, J. D., Kelly, C., Rudd, J., Hesslein, R., & Roulet, N. T. (1994). Flux to the atmosphere of CH<sub>4</sub> and CO<sub>2</sub> from wetland ponds on the Hudson Bay lowlands (HBLs). *Journal of Geophysical Research*, *99*, 1495-1510.
- Hanson, R. S., & Hanson, T. E. (1996). Methanotrophic bacteria. *Microbiological Reviews*, *60*, 439-471.
- Hatala, J. A., Detto, M., Sonnentag, O., Deverel, S. J., Verfaillie, J., & Baldocchi, D. D. (2012). Greenhouse gas (CO<sub>2</sub>, CH<sub>4</sub>, H<sub>2</sub>O) fluxes from drained and flooded agricultural peatlands in the Sacramento-San Joaquin Delta. *Agriculture, Ecosystems & Environment*, *150*, 1-18. <https://doi.org/10.1016/j.agee.2012.01.009>

- Heinen, M. (2006). Simplified denitrification models: Overview and properties. *Geoderma*, 133, 444-463. <https://doi.org/10.1016/j.geoderma.2005.06.010>
- Heitmann, T., Goldhammer, T., Beer, J., & Blodau, C. (2007). Electron transfer of dissolved organic matter and its potential significance for anaerobic respiration in a northern bog. *Global Change Biology*, 13, 1771-1785. <https://doi.org/10.1111/j.1365-2486.2007.01382.x>
- Hendriks, D., Huissteden, J., Dolman, A., & van der Molen, M. (2007). The full greenhouse has balance of an abandoned peat meadow. *Biogeosciences*, 4, 411-424.
- Horz, H. P., Rich, V., Avrahami, S., & Bohannan, B. J. (2005). Methane-oxidizing bacteria in a California upland grassland soil: diversity and response to simulated global change. *Appl Environ Microbiol*, 71(5), 2642-2652. <https://doi.org/10.1128/AEM.71.5.2642-2652.2005>
- Hüppi, R., Felber, R., Krauss, M., Six, J., Leifeld, J., & Fuß, R. (2018). Restricting the nonlinearity parameter in soil greenhouse gas flux calculation for more reliable flux estimates. *PLoS ONE*, 13(7), e0200876. <https://doi.org/10.1371/journal.pone.0200876>
- Huttunen, J. T., Nykänen, H., Turunen, J., & Martikainen, P. J. (2003). Methane emissions from natural peatlands in the northern boreal zone in Finland, Fennoscandia. *Atmospheric Environment*, 37, 147-151.
- International Hydropower Association. (2010). *GHG Measurement Guidelines for Freshwater Reservoirs*. London, UK: International Hydropower Association (IHA).
- Inubushi, K., Otake, S., Furukawa, Y., Shibasaki, N., Ali, M., Itang, A. M., & Tsuruta, H. (2005). Factors influencing methane emission from peat soils: Comparison of tropical and temperate wetlands. *Nutrient Cycling in Agroecosystems*, 71, 93-99. <https://doi.org/10.1007/s10705-004-5283-8>
- IPCC. (2013). Summary for Policymakers. In T. F. Stocker, D. Qin, G.-K. Plattner, M. Tignor, S. K. Allen, J. Boschung, A. Nauels, Y. Xia, V. Bex and P.M. Midgley (Ed.), *Climate Change 2013: The Physical Science Basis. Contribution of Working Group I to the Fifth Assessment Report of the Intergovernmental Panel on Climate Change*. Cambridge, United Kingdom and New York, NY, USA: Cambridge University Press.
- IPCC. (2014a). *2013 Supplement to the 2006 IPCC Guidelines for National Greenhouse Gas Inventories: Wetlands*. Switzerland: IPCC.
- IPCC. (2014b). *Climate change 2014: Synthesis report. Contribution of Working Groups I, II and III to the Fifth Assessment Report of the Intergovernmental Panel on Climate Change*. Geneva, Switzerland: IPCC.

- Jacinthe, P. A., & Lal, R. (2006). Methane oxidation potential of reclaimed grassland soils as affected by management. *Soil Science*, 171, 772-783. <https://doi.org/10.1097/01.ss.0000209357.53536.43>
- Jarvis, S., Lovell, R., & Panayides, R. (1995). Patterns of Methane Emission from Excreta of Grazing Animals. *Soil Biology & Biochemistry*, 27(12), 1581-1588.
- Kammann, C., Grünhage, L., Jäger, H.-J., & Wachinger, G. (2001). Methane fluxes from differentially managed grassland study plots: the important role of CH<sub>4</sub> oxidation in grassland with a high potential for CH<sub>4</sub> production. *Environmental Pollution*, 115, 261-273.
- Kandel, T. P., Lærke, P. E., & Elsgaard, L. (2018). Annual emissions of CO<sub>2</sub>, CH<sub>4</sub> and N<sub>2</sub>O from a temperate peat bog: Comparison of an undrained and four drained sites under permanent grass and arable crop rotations with cereals and potato. *Agricultural and Forest Meteorology*, 256-257, 470-481. <https://doi.org/10.1016/j.agrformet.2018.03.021>
- Keller, J. K., Weisenhorn, P. B., & Megonigal, J. P. (2009). Humic acids as electron acceptors in wetland decomposition. *Soil Biology and Biochemistry*, 41, 1518-1522. <https://doi.org/10.1016/j.soilbio.2009.04.008>
- Kiese, R., Hewett, B., Graham, A., & Butterbach-Bahl, K. (2003). Seasonal variability of N<sub>2</sub>O emissions and CH<sub>4</sub> uptake by tropical rainforest soils of Queensland, Australia. *Global Biogeochemical Cycles*, 17, 1518-1522. <https://doi.org/10.1029/2002gb002014>
- Kirschke, S., Bousquet, P., Ciais, P., Saunoy, M., Canadell, J. G., Dlugokencky, E. J., . . . Zeng, G. (2013). Three decades of global methane sources and sinks. *Nature Geoscience*, 6(10), 813-823. <https://doi.org/10.1038/ngeo1955>
- Klüber, H. D., & Conrad, R. (1998). Effects of nitrate, nitrite, NO and N<sub>2</sub>O on methanogenesis and other redox processes in anoxic rice field soil. *Fems Microbiology Ecology*, 25(3), 301-318.
- Klüpfel, L., Piepenbrock, A., Kappler, A., & Sander, M. (2014). Humic substances as fully regenerable electron acceptors in recurrently anoxic environments. *Nature Geoscience*, 7, 195-200. <https://doi.org/10.1038/ngeo2084>
- Knorr, K.-H., Lischeid, G., & Blodau, C. (2009). Dynamics of redox processes in a minerotrophic fen exposed to a water table manipulation. *Geoderma*, 153(3-4), 379-392. <https://doi.org/10.1016/j.geoderma.2009.08.023>
- Kowalska, N., Chojnicki, B. H., Rinne, J., Haapanala, S., Siedlecki, P., Urbaniak, M., . . . Olejnik, J. (2013). Measurements of methane emission from a temperate wetland by the eddy covariance method. *International Agrophysics*, 27, 283-290. <https://doi.org/10.2478/v10247-012-0096-5>
- Kroon, P. S., Schrier-Uijl, A. P., Hensen, A., Veenendaal, E. M., & Jonker, H. J. J. (2010). Annual balances of CH<sub>4</sub> and N<sub>2</sub>O from a managed fen meadow

- using eddy covariance flux measurements. *European Journal of Soil Science*, 61, 773-784. <https://doi.org/10.1111/j.1365-2389.2010.01273.x>
- Kuzyakov, Y., & Blagodatskaya, E. (2015). Microbial hotspots and hot moments in soil: Concept & review. *Soil Biology and Biochemistry*, 83, 184-199. <https://doi.org/https://doi.org/10.1016/j.soilbio.2015.01.025>
- Landcare Research. (2015). Land Resource Inventory; Land Cover Database 4.1. New Zealand's Environment Reporting Series. Retrieved: from <https://iris.scinfo.org.nz/layer/48423-lcdb-v41-land-cover-database-version-41-mainland-new-zealand/>.
- Lau, M. P., Sander, M., Gelbrecht, J., & Hupfer, M. (2014). Solid phases as important electron acceptors in freshwater organic sediments. *Biogeochemistry*, 123, 49-61. <https://doi.org/10.1007/s10533-014-0052-5>
- Laubach, J., & Hunt, J. E. (2018). Greenhouse-gas budgets for irrigated dairy pasture and a winter-forage kale crop. *Agricultural and Forest Meteorology*, 258, 117-134. <https://doi.org/10.1016/j.agrformet.2017.04.013>
- Lazar, J. G., Addy, K., Welsh, M. K., Gold, A. J., & Groffman, P. M. (2014). Resurgent beaver ponds in the northeastern United States: implications for greenhouse gas emissions. *J Environ Qual*, 43, 1844-1852. <https://doi.org/10.2134/jeq2014.02.0065>
- Le Mer, J., & Roger, P. (2001). Production, oxidation, emission and consumption of methane by soils: A review. *European Journal of Soil Biology*, 37, 25-50. [https://doi.org/https://doi.org/10.1016/S1164-5563\(01\)01067-6](https://doi.org/https://doi.org/10.1016/S1164-5563(01)01067-6)
- Liang, L., Campbell, D. I., Wall, A. M., & Schipper, L. A. (2018). Nitrous oxide fluxes determined by continuous eddy covariance measurements from intensively grazed pastures: temporal patterns and environmental controls. *Agriculture, Ecosystems & Environment*, 268, 171-180. <https://doi.org/10.1016/j.agee.2018.09.010>
- Liu, X., Gao, Y., Zhang, Z., Luo, J., & Yan, S. (2017). Sediment-water methane flux in a eutrophic pond and primary influential factors at different time scales. *Water*, 9(8) <https://doi.org/10.3390/w9080601>
- Luan, J., & Wu, J. (2015). Long-term agricultural drainage stimulates CH<sub>4</sub> emissions from ditches through increased substrate availability in a boreal peatland. *Agriculture, Ecosystems & Environment*, 214, 68-77. <https://doi.org/10.1016/j.agee.2015.08.020>
- Maljanen, M., Virkajärvi, P., & Martikainen, P. J. (2012). Dairy cow excreta patches change the boreal grass swards from sink to source of methane. *Agricultural and Food Science*, 21, 91-99.
- Mancinelli, R. (1995). The regulation of methane oxidation in soil. *Annual Review of Microbiology*, 29, 581-605.

- Männistö, E., Korrensalo, A., Alekseychik, P., Mammarella, I., Peltola, O., Vesala, T., & Tuittila, E.-S. (2019). Multi-year methane ebullition measurements from water and bare peat surfaces of a patterned boreal bog. *Biogeosciences*, *16*(11), 2409-2421. <https://doi.org/10.5194/bg-16-2409-2019>
- Matthews, C., St. Louis, V., & Hesslein, R. (2003). Comparison of three techniques used to measure diffusive gas exchange from sheltered aquatic surfaces. *Environmental Science & Technology*, *37*, 772-780.
- McCraw, J. (2011). *The wandering river: Landforms and geological history of the Hamilton Basin*. New Zealand: Geoscience Society of New Zealand.
- McGinn, S. (2006). Measuring greenhouse gas emissions from point sources in agriculture. *Canadian Journal of Soil Science*, *86*, 355-371.
- Megonigal, J., Hines, M., & Visscher, P. (2004). Anaerobic metabolism: Linkages to trace gases and aerobic processes. In W. Schlesinger (Ed.), *Biogeochemistry* (pp. 317-424). Oxford, UK: Isevier-Pergamon.
- Meixner, F. X., & Yang, W. X. (2006). Biogenic Emissions of Nitric Oxide and Nitrous Oxide from Arid and Semi-Arid Land. In *Dryland Ecohydrology* (pp. 233-255).
- Mikkilä, C., Sundh, I., Svensson, B. H., & Nilsson, M. (1995). Diurnal variation in methane emission in relation to the water table, soil temperature, climate and vegetation cover in a Swedish acid mire. *Biogeochemistry*, *28*, 93-114.
- Ministry for the Environment. (2016). *New Zealand's Action on Climate Change*. Wellington: Ministry for the Environment.
- Ministry for the Environment. (2017a). *Map of regional climate impacts*. Retrieved from <http://www.mfe.govt.nz/publications/climate-change/map-regional-climate-impacts>
- Ministry for the Environment. (2017b). *New Zealand's Greenhouse Gas Inventory 1990-2015*. Wellington: Ministry for the Environment.
- Ministry for the Environment. (2018). *New Zealand's Greenhouse Gas Inventory 1990-2016*. Wellington, New Zealand: Ministry for the Environment.
- Ministry for the Environment. (2019a, 22/03/19). *Likely climate change impacts in New Zealand*. Retrieved from <http://www.mfe.govt.nz/climate-change/likely-impacts-of-climate-change/likely-climate-change-impacts-new-zealand>
- Ministry for the Environment. (2019b). *New Zealand's Greenhouse Gas Inventory: 1990-2017*. Wellington, New Zealand:
- Minkinen, K., & Laine, J. (2006). Vegetation heterogeneity and ditches create spatial variability in methane fluxes from peatlands drained for forestry. *Plant and Soil*, *285*, 289-304. <https://doi.org/10.1007/s11104-006-9016-4>

- Mohanty, S. R., Bodelier, P. L., Floris, V., & Conrad, R. (2006). Differential effects of nitrogenous fertilizers on methane-consuming microbes in rice field and forest soils. *Appl Environ Microbiol*, 72(2), 1346-1354. <https://doi.org/10.1128/AEM.72.2.1346-1354.2006>
- Monson, R., & Baldocchi, D. D. (2014). *Terrestrial Biosphere-Atmosphere Fluxes*. Cambridge, UK: Cambridge University Press.
- Moore, A., & Roulet, N. T. (1993). Methane flux water table relations in northern wetlands. *Geophysical Research Letters*, 20(7), 587-590.
- Mori, A., & Hojito, M. (2015). Methane and nitrous oxide emissions due to excreta returns from grazing cattle in Nasu, Japan. *Grassland Science*, 61(2), 109-120. <https://doi.org/10.1111/grs.12081>
- Munger, W., Loescher, H., & Luo, H. (2012). Measurement, tower, and site design considerations. In M. Aubinet, T. Vesala & D. Papale (Eds.), *Eddy Covariance: A Practical Guide to Measurement and Data Analysis*. London, UK; New York, USA: Springer.
- Murphy, J., & Riley, J. (1962). A modified single solution method for the determination of phosphate in natural waters. *Analytica Chimica Acta*, 27, 31-36.
- Naser, H., Nagata, O., Sultana, S., & Hatano, R. (2018). Impact of management practices on methane emissions from paddy grown on mineral soil over peat in central Hokkaido, Japan. *Atmosphere*, 9 <https://doi.org/10.3390/atmos9060212>
- National Academies of Sciences, E. a. M. (2018). *Improving Characterization of Anthropogenic Methane Emissions in the United States*. Washington, DC: The National Academies Press.
- National policy statement for freshwater management 2014 (2017). N. Z. Government.
- NIWA. (n.d.). CliFlo: NIWA's National Climate Database on the Web. National Institute of Water and Atmospheric Research (NIWA). Retrieved: 15-October-2019, from <http://cliflo.niwa.co.nz/>.
- Nungesser, M. K. (2003). Modelling microtopography in boreal peatlands: hummocks and hollows. *Ecological Modelling*, 165, 175-207. [https://doi.org/10.1016/s0304-3800\(03\)00067-x](https://doi.org/10.1016/s0304-3800(03)00067-x)
- Oertel, C., Matschullat, J., Zurba, K., Zimmermann, F., & Erasmi, S. (2016). Greenhouse gas emissions from soils—A review. *Chemie der Erde - Geochemistry*, 76, 327-352. <https://doi.org/https://doi.org/10.1016/j.chemer.2016.04.002>



- Olsen, S., Cole, C., Watanabe, F., & Dean, L. (1954). *Estimation of available phosphorus in soils by extraction with sodium bicarbonate* (Vol. 939). Washington, D.C.: U.S. Dept. of Agriculture.
- Parkin, T., & Venterea, R. (2010). Sampling Protocols. Chapter 3. Chamber-Based Trace Gas Flux Measurements. In R. F. Follet (Ed.), *Sampling Protocols*. USA: USDA-ARS.
- Paw, K., Baldocchi, D., Meyers, T., & Wilson, K. (2000). Correction of eddy-covariance measurements incorporating both advective effects and density fluxes. *Boundary-Layer Meteorology*, *97*, 487-511.
- Peltola, O., Hensen, A., Beileli Marchesini, L., Helfter, C., Bosveld, F. C., van den Bulk, W. C. M., . . . Mammarella, I. (2015). Studying the spatial variability of methane flux with five eddy covariance towers of varying height. *Agricultural and Forest Meteorology*, *214-215*, 456-472. <https://doi.org/10.1016/j.agrformet.2015.09.007>
- Petrescu, A. M., Lohila, A., Tuovinen, J. P., Baldocchi, D. D., Desai, A. R., Roulet, N. T., . . . Cescatti, A. (2015). The uncertain climate footprint of wetlands under human pressure. *Proceedings of the National Academy of Sciences of the United States of America*, *112*, 4594-4599. <https://doi.org/10.1073/pnas.1416267112>
- Pihlatie, M. K., Christiansen, J. R., Aaltonen, H., Korhonen, J. F. J., Nordbo, A., Rasilo, T., . . . Pumpanen, J. (2013). Comparison of static chambers to measure CH<sub>4</sub> emissions from soils. *Agricultural and Forest Meteorology*, *171-172*, 124-136. <https://doi.org/10.1016/j.agrformet.2012.11.008>
- Prather, M. J., & Holmes, C. D. (2017). Overexplaining or underexplaining methane's role in climate change. *Proc Natl Acad Sci U S A*, *114*(21), 5324-5326. <https://doi.org/10.1073/pnas.1704884114>
- Pronger, J., Schipper, L. A., Hill, R. B., Campbell, D. I., & McLeod, M. (2014). Subsidence Rates of Drained Agricultural Peatlands in New Zealand and the Relationship with Time since Drainage. *J Environ Qual*, *43*(4), 1442-1449. <https://doi.org/10.2134/jeq2013.12.0505>
- Ratcliffe, J. L., Campbell, D. I., Clarkson, B. R., Wall, A. M., & Schipper, L. A. (2019). Water table fluctuations control CO<sub>2</sub> exchange in wet and dry bogs through different mechanisms. *Sci Total Environ*, *655*, 1037-1046. <https://doi.org/10.1016/j.scitotenv.2018.11.151>
- Reay, D., Smith, P., & Amstel, v. (2010). Methane sources and the global methane budget. In D. Reay, P. Smith & A. van Amstel (Eds.), *Methane and Climate Change* (pp. 1-13). Washington DC, USA and London, UK: Earthscan.
- Rigby, M., Montzka, S. A., Prinn, R. G., White, J. W. C., Young, D., O'Doherty, S., . . . Park, S. (2017). Role of atmospheric oxidation in recent methane growth. *Proceedings of the National Academy of Sciences of the United States of America*, *114*(21), 5373-5377. <https://doi.org/10.1073/pnas.1616426114>

- Rochette, P. (2011). Towards a standard non-steady-state chamber methodology for measuring soil N<sub>2</sub>O emissions. *Animal Feed Science and Technology*, 166-167, 141-146. <https://doi.org/https://doi.org/10.1016/j.anifeedsci.2011.04.063>
- Saarnio, S., Alm, J., Silvola, J., Lohila, A., Nykänen, H., & Martikainen, P. J. (1997). Seasonal variation in CH<sub>4</sub> emissions and production and oxidation potentials at microsites on an oligotrophic pine fen. *Oecologia*, 110, 414-422.
- Saggar, S., Bolan, N. S., Bhandral, R., Hedley, C. B., & Luo, J. (2004). A review of emissions of methane, ammonia, and nitrous oxide from animal excreta deposition and farm effluent application in grazed pastures. *New Zealand Journal of Agricultural Research*, 47(4), 513-544. <https://doi.org/10.1080/00288233.2004.9513618>
- Saggar, S., Hedley, C. B., & Tate, K. (2003). Methane sources and sinks in New Zealand grazed pastures. *New Zealand Soil News*, 51, 6-7.
- Saggar, S., Tate, K., Giltrap, D., & Singh, J. (2008). Soil-atmosphere exchange of nitrous oxide and methane in New Zealand terrestrial ecosystems and their mitigation options: a review. *Plant and Soil*, 309, 25-42. <https://doi.org/10.1007/s11104-007-9421-3>
- Schmid, H. (2002). Footprint modeling for vegetation atmosphere exchange studies: a review and perspective. *Agricultural and Forest Meteorology*, 113, 159-183.
- Schrier-Uijl, A. (2010). *The influence of management alternatives on the greenhouse gas balance of fen meadow areas* (Doctoral thesis). Wageningen University, Netherlands.
- Schrier-Uijl, A., Kroon, P. S., Leffelaar, P. A., van Huissteden, J. C., Berendse, F., & Veenendaal, E. M. (2010). Methane emissions in two drained peat agroecosystems with high and low agricultural intensity. *Plant and Soil*, 329, 509-520. <https://doi.org/10.1007/s11104-009-0180-1>
- Schrier-Uijl, A., Veraart, A. J., Leffelaar, P. A., Berendse, F., & Veenendaal, E. M. (2011). Release of CO<sub>2</sub> and CH<sub>4</sub> from lakes and drainage ditches in temperate wetlands. *Biogeochemistry*, 102, 265-279. <https://doi.org/10.1007/s10533-010-9440-7>
- Segers, R. (1998). Methane production and methane consumption: A review of processes underlying wetland methane fluxes. *Biogeochemistry*, 41, 23-51.
- Serrano-Silva, N., Sarria-Guzmán, Y., Dendooven, L., & Luna-Guido, M. (2014). Methanogenesis and methanotrophy in soil: A review. *Pedosphere*, 24, 291-307. [https://doi.org/https://doi.org/10.1016/S1002-0160\(14\)60016-3](https://doi.org/https://doi.org/10.1016/S1002-0160(14)60016-3)



- Smemo, K., & Yavitt, J. (2006). A multi-year perspective on methane cycling in a shallow peat fen in central New York state, USA. *Wetlands*, 26, 20-29.
- Tate, K. R. (2015). Soil methane oxidation and land-use change – from process to mitigation. *Soil Biology and Biochemistry*, 80, 260-272. <https://doi.org/https://doi.org/10.1016/j.soilbio.2014.10.010>
- Tate, K. R., Ross, D. J., Scott, N. A., Rodda, N. J., Townsend, J. A., & Arnold, G. C. (2006). Post-harvest patterns of carbon dioxide production, methane uptake and nitrous oxide production in a *Pinus radiata* D. Don plantation. *Forest Ecology and Management*, 228, 40-50. <https://doi.org/10.1016/j.foreco.2006.02.023>
- Teh, Y. A., Silver, W. L., Sonnentag, O., Detto, M., Kelly, M., & Baldocchi, D. D. (2011). Large greenhouse gas emissions from a temperate peatland pasture. *Ecosystems*, 14, 311-325. <https://doi.org/10.1007/s10021-011-9411-4>
- Thomas, K. K. L., Benstead, J. J., Lloyd, S. S. H., & Lloyd, D. D. (2010). Diurnal Oscillations of Gas Production and Effluxes (CO<sub>2</sub> and CH<sub>4</sub>) in Cores from a Peat Bog. *Biological Rhythm Research*, 29, 247-259. <https://doi.org/10.1076/brhm.29.3.247.1442>
- Tiemeyer, B., Albiac Borraz, E., Augustin, J., Bechtold, M., Beetz, S., Beyer, C., . . . Zeitz, J. (2016). High emissions of greenhouse gases from grasslands on peat and other organic soils. *Global Change Biology*, 22, 4134-4149. <https://doi.org/10.1111/gcb.13303>
- Topp, E., & Pattey, E. (1997). Soils as sources and sinks for atmospheric methane. *Canadian Journal of Soil Science*, 77, 167-178.
- Turetsky, M. R., Kotowska, A., Bubier, J., Dise, N. B., Crill, P., Hornibrook, E. R. C., . . . Wilmking, M. (2014). A synthesis of methane emissions from 71 northern, temperate, and subtropical wetlands. *Global Change Biology*, 20(7), 2183-2197. <https://doi.org/10.1111/gcb.12580>
- Turner, A. J., Frankenberg, C., Wennberg, P. O., & Jacob, D. J. (2017). Ambiguity in the causes for decadal trends in atmospheric methane and hydroxyl. *Proceedings of the National Academy of Sciences of the United States of America*, 114(21), 5367-5372. <https://doi.org/10.1073/pnas.1616020114>
- United States Environmental Protection Agency. (2018). *Greenhouse Gas Equivalencies Calculator*. Retrieved from <https://www.epa.gov/energy/greenhouse-gas-equivalencies-calculator>
- University of Waikato. [Methane emissions from Moanatuatua peat bog]. *Unpublished data*. University of Waikato: Hamilton, New Zealand.
- Urbanová, Z., Pícek, T., & Tuttila, E. (2013). Sensitivity of carbon gas fluxes to weather variability on pristine, drained and rewetted temperate bogs. *Mires and Peat*, 11, 1-14.

- van Huissteden, J., van den Bos, R., & Marticorena Alvarez, I. (2016). Modelling the effect of water-table management on CO<sub>2</sub> and CH<sub>4</sub> fluxes from peat soils. *Netherlands Journal of Geosciences*, 85(01), 3-18. <https://doi.org/10.1017/s0016774600021399>
- Veraart, A. J., Steenbergh, A. K., Ho, A., Kim, S. Y., & Bodelier, P. L. E. (2015). Beyond nitrogen: The importance of phosphorus for CH<sub>4</sub> oxidation in soils and sediments. *Geoderma*, 259-260, 337-346. <https://doi.org/10.1016/j.geoderma.2015.03.025>
- Vigano, I., van Weelden, H., Holzinger, R., Keppler, F., McLeod, A., & Röckmann, T. (2008). Effect of UV radiation and temperature on the emission of methane from plant biomass and structural components. *Biogeosciences*, 5, 937-947.
- Waddington, J. M., & Day, S. (2007). Methane emissions from a peatland following restoration. *Journal of Geophysical Research*, 112, G03018. <https://doi.org/10.1029/2007JG000400>
- Wall, A. M., Campbell, D. I., Mudge, P. L., & Schipper, L. A. (2019). Temperate grazed grassland carbon balances for two adjacent paddocks determined separately from one eddy covariance system. *Unpublished work*.
- Wecking, A. R., Wall, A. M., Liang, L. L., Lindsey, S. B., Luo, J., Campbell, D. I., & Schipper, L. A. (2020). Reconciling annual nitrous oxide emissions of an intensively grazed dairy pasture determined by eddy covariance and emission factors. *Agriculture, Ecosystems & Environment*, 287 <https://doi.org/10.1016/j.agee.2019.106646>
- Wedderburn, M. E., Crush, J. R., Pengelly, W. J., & Walcroft, J. L. (2010). Root growth patterns of perennial ryegrasses under well-watered and drought conditions. *New Zealand Journal of Agricultural Research*, 53(4), 377-388. <https://doi.org/10.1080/00288233.2010.514927>
- Yang, W. H., McNicol, G., Teh, Y. A., Estera-Molina, K., Wood, T. E., & Silver, W. L. (2017). Evaluating the classical versus an emerging conceptual model of peatland methane dynamics. *Global Biogeochemical Cycles*, 31, 1435-1453. <https://doi.org/10.1002/2017gb005622>
- Zogorski, J. S., Carter, J. M., Ivahnenko, T., Lapham, W. W., Moran, M. J., Rowe, B. L., . . . Toccalino, P. L. (2006). *The quality of our nations waters: Volatile organic compounds in the nation's ground water and drinking-water supply wells*. Reston, Virginia: United States Geological Survey.